(1)

Amphibious Vehicle Propulsion System Final Report Volume I

For a Propulsion System Demonstrator (PSD) Vehicle

January 30, 1990

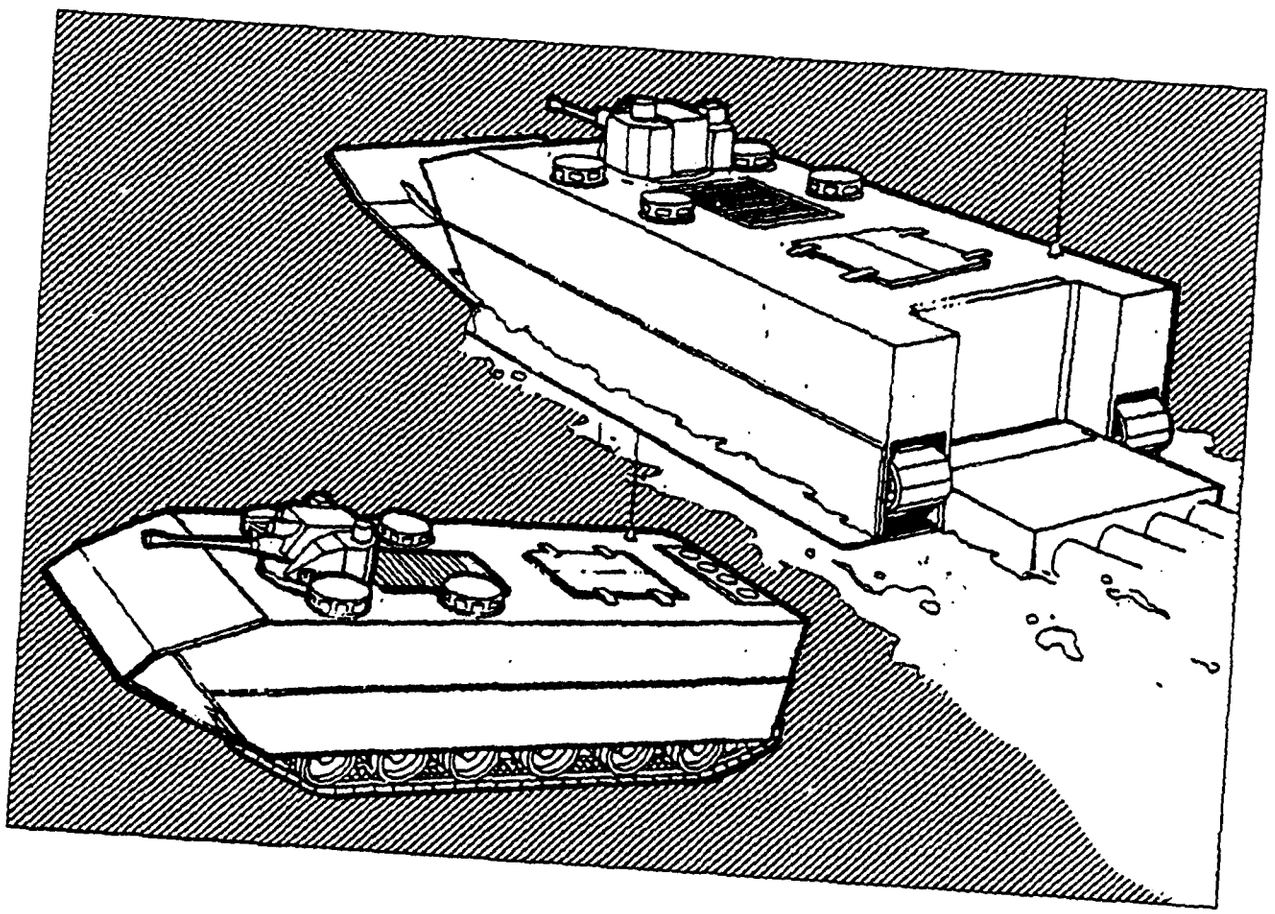

Prepared under
Contract No. N00167-86-C-0158
for David Taylor Research Center
Bethesda, Maryland

Westinghouse Electric Corporation
Naval Systems Division
18901 Euclid Avenue
Cleveland, Ohio 44117

UNCLASSIFIED
SECURITY CLASSIFICATION OF THIS PAGE

REPORT DOCUMENTATION PAGE

1a. REPORT SECURITY CLASSIFICATION UNCLASSIFIED	1b. RESTRICTIVE MARKINGS
2a. SECURITY CLASSIFICATION AUTHORITY	3 DISTRIBUTION / AVAILABILITY OF REPORT APPROVED FOR PUBLIC RELEASE DISTRIBUTION IS UNLIMITED
2b. DECLASSIFICATION / DOWNGRADING SCHEDULE	
4. PERFORMING ORGANIZATION REPORT NUMBER(S)	5. MONITORING ORGANIZATION REPORT NUMBER(S) DTRC-SD-CR-6-90 VOL I
6a. NAME OF PERFORMING ORGANIZATION WESTINGHOUSE ELECTRIC CORP. NAVAL SYSTEMS DIVISION 6b OFFICE SYMBOL (If applicable)	7a. NAME OF MONITORING ORGANIZATION DAVID TAYLOR RESEARCH CENTER
6c. ADDRESS (City, State, and ZIP Code) 18901 ELUCID AVENUE CLEVELAND, OHIO 44117	7b. ADDRESS (City, State, and ZIP Code) CODE 1240, (MCPO) BETHESDA, MD 20084-5000
8a. NAME OF FUNDING / SPONSORING ORGANIZATION DAVID TAYLOR RESEARCH CENTER 8b OFFICE SYMBOL (If applicable) MCPO	9. PROCUREMENT INSTRUMENT IDENTIFICATION NUMBER N0016786C0158
8c. ADDRESS (City, State, and ZIP Code) CODE 1240 BETHESDA, MD 20084-5000	10 SOURCE OF FUNDING NUMBERS PROGRAM ELEMENT NO: 26623M PROJECT NO: C0021 TASK NO: WORK UNIT ACCESSION NO: DN479001

11 TITLE (Include Security Classification)

AMPHIBIOUS VEHICLE PROPULSION SYSTEM - FINAL REPORT VOL I (U)

12 PERSONAL AUTHOR(S)

13a TYPE OF REPORT	13b TIME COVERED	14 DATE OF REPORT (Year, Month, Day)	15 PAGE COUNT
FINAL REPORT	FROM 9/86 TO 1/90	1990 JANUARY 30	190

16 SUPPLEMENTARY NOTATION

17 COSATI CODES			18 SUBJECT TERMS (Continue on reverse if necessary and identify by block number)
FIELD	GROUP	SUB-GROUP	ELECTRIC DRIVE MILITARY VEHICLE AMPHIBIOUS VEHICLE

19 ABSTRACT (Continue on reverse if necessary and identify by block number)

The David Taylor Research Center has funded the development of an electric drive train for waterjet propulsion system to demonstrate high water speed in a Marine Corps propulsion system demonstrator vehicle. In the water, this vehicle will be propelled by four waterjet each rated at 400hp, to provide the required thrust. The task was to design and develop a system that would be compact, lightweight, efficient and available to support vehicle demonstration testing.

A system trade-off study resulted in selection of an approach which uses four identical electric water propulsion modules, consisting of: an AC alternator and alternator control an AC induction motor with integral speed decreasing gearbox and a coupling that connects the motor/gearbox to the waterjet. This Report documents the hardware Design Effort, Fabrication and Testing completed.

20 DISTRIBUTION / AVAILABILITY OF ABSTRACT	21 ABSTRACT SECURITY CLASSIFICATION
☒ UNCLASSIFIED/UNLIMITED ☐ SAME AS RPT ☐ DTIC USERS	UNCLASSIFIED

22a NAME OF RESPONSIBLE INDIVIDUAL	22b TELEPHONE (Include Area Code)	22c. OFFICE SYMBOL
MICHAEL GALLAGHER	(301) 227-1852	1240

DD FORM 1473, 84 MAR 83 APR edition may be used until exhausted
All other editions are obsolete

SECURITY CLASSIFICATION OF THIS PAGE
UNCLASSIFIED

Westinghouse Electric Corporation
Electronic Systems Group

Naval Systems Division
476 Center Street
Chardon Ohio 44024

30 January, 1990

Department of the Navy
David Taylor Research Center
Code 1240
Bethesda, Maryland 20084

Subject: Contract N00167-86-C-0158

Enclosure: (1) Final Report

Gentlemen:

Pursuant to the requirements of the subject contract, Westinghouse Naval Systems Division is submitting this Final Report as documentation of the completion of the previous testing. This verifies the completion of this requirement in accordance with CDRL A005, Final Report Requirement.

If there are any questions please contact the undersigned at (216) 692-6994.

Cordially,

Westinghouse Electric Corporation
Naval Systems Division

Robert Bright

Robert Bright
Contracts Representative
BB75

Clin 0002

Amphibious Vehicle Propulsion System Final Report Volume I

January 30, 1990

Prepared under
Contract No. N00167-86-C-0158
for David Taylor Research Center
Bethesda, Maryland

Westinghouse Electric Corporation
Naval Systems Division
18901 Euclid Avenue
Cleveland, Ohio 44117

William Eastman, Technical Manager

Steven Specht, Program Manager

Table of Contents
Volume I and II

Volume I

Volume II

The design report is continued in volume two.

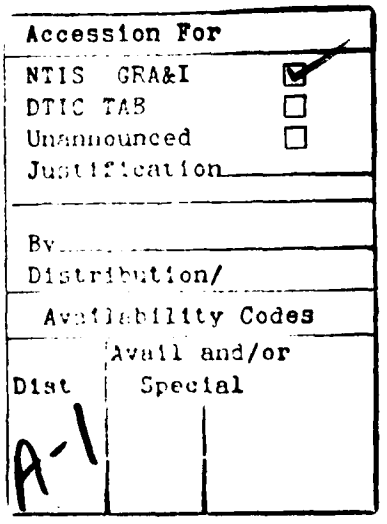

ABSTRACT

The Marine Corps Program Office at the David Taylor Research Center has funded the development of an electric drive train for a waterjet propulsion system to demonstrate high water speed in a Marine Corps propulsion system demonstrator (PSD) vehicle. In water, this vehicle will be propelled by four waterjets, each rated at 400 Hp, to provide the required thrust. The task was to design and develop a system that would be compact, lightweight, efficient and available to support vehicle demonstration testing in June of 1989.

Due to schedule and cost constraints the decision was made to design the propulsion motor to be compatible with an existing alternator (with minor modifications). After selection of the alternator was finalized design of an alternator controller, induction motor, speed decreasing gear (SDG) and coupling was begun.

After the design effort was completed fabrication was begun on all deliverable hardware. All non-critical parts and one complete system were completed. The remaining critical parts were stopped in their fabrication cycle at appropriate points to enable the incorporation of changes in design that might be indicated by testing of the first system.

After fabrication was completed component and system tests were conducted. Component testing was used to demonstrate, where possible, that components were ready for system testing. System testing was conducted to demonstrate all requirements that could be demonstrated in the laboratory.

The maximum rating demonstrated in the system testing was 161 Hp. Mechanical damage was observed at higher power levels. Testing for other requirements was not completed. Due to problems which developed during testing and schedule constraints the motor/SDG lubrication and cooling system was changed to have and external filter and heat exchanger.

Examination of the test data and the hardware indicated that the problems encountered in system testing could be solved with design changes to the stator, rotor and SDG. Additional design changes could produce a lubrication and cooling system completely contained in the motor/SDG unit as in the original design. The alternator, which was selected with cost and schedule drivers is not well suited to this application.

It is recommended that three phases of development should be pursued. The design changes to the stator, rotor and SDG should first be tested to verify that the design meets the requirements. At this point lubrication and cooling system changes should be developed along with other design improvements to the motor/SDG. Finally, a new alternator with higher efficiency, lower weight, lower noise, and no air flow (oil cooled) should be developed.

Section 1
EXECUTIVE SUMMARY

This report covers the design and development testing effort pertaining to the Electric Water Propulsion System (EWPS) which was intended for use in the Propulsion System Demonstrator (PSD) Vehicle. The results of the design effort are described in the "Amphibious Vehicle Propulsion System Design Report", Westinghouse Ind., Oceanic Division, July 8, 1988 (Appendix I). The fabrication and system testing programs are discussed on the the following pages. Component testing is described in the "Amphibious Vehicle Propulsion System Acceptance Test Report", Westinghouse Electric Corporation, Naval Systems Div., December 21, 1989 (Appendix II).

OBJECTIVES

The EWPS was designed to meet stringent size, weight and efficiency requirements. The motors were to include self contained lubrication and cooling and be totally submersible in seawater. Each EWPS was designed to deliver 400 Hp at 1250 RPM continuous and 520 Hp for 1 minute. The elements of the EWPS (alternator, controller and motor) were designed to be interchangeable with other EWPS units to minimize spares requirements.

ACCOMPLISHMENTS

After evaluation of several alternatives an alternator which met the design requirements with minor modifications was selected. One unit was fabricated and tested and four other units were fabricated. The controller was designed specifically for the application. One unit was fabricated and tested. The motor/SDG was also designed specifically for the application. One unit was fabricated and tested and a second unit was started and is 90% complete.

Component testing was conducted to verify that elements of the system were ready for system testing and to identify specific problems that were discovered during the program. System testing was started at low power levels to provide data to demonstrate that the system

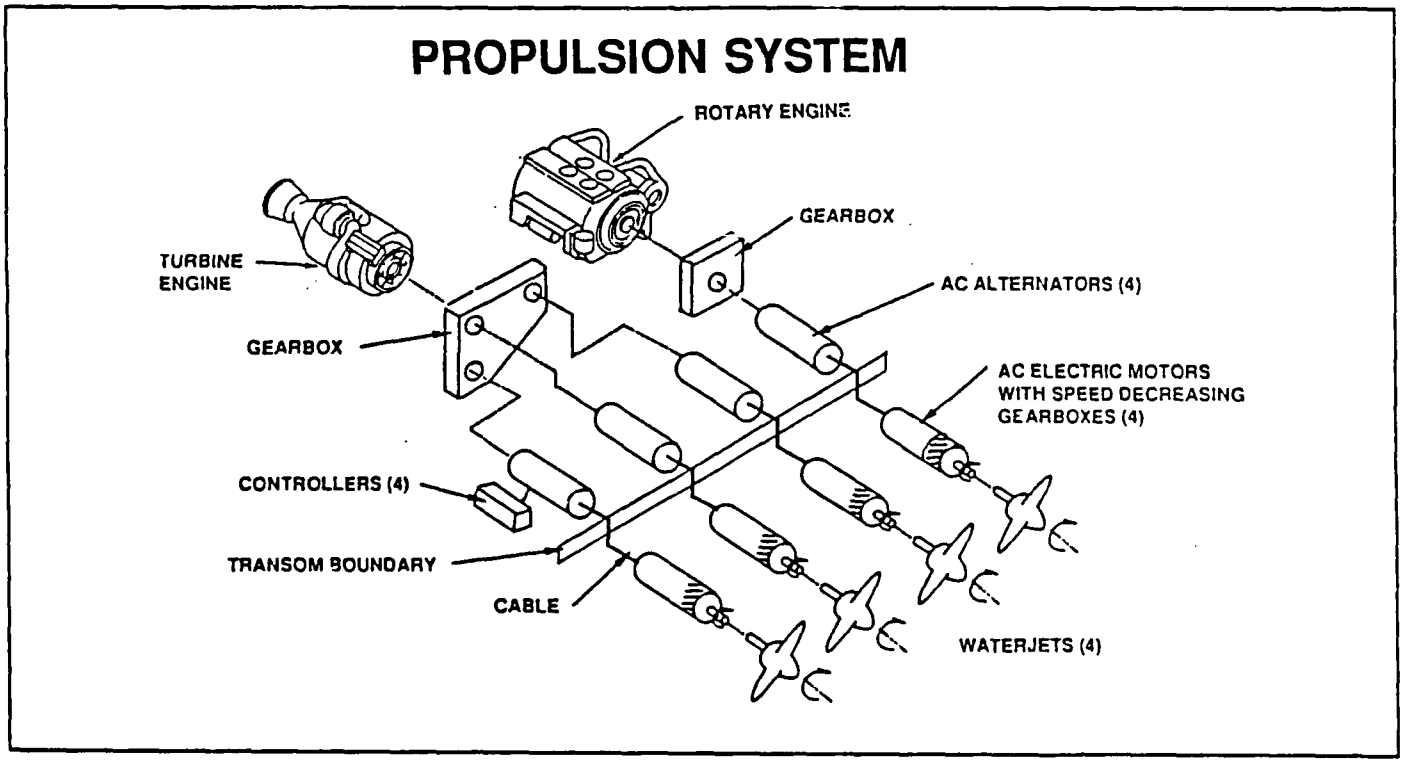

Section 1
EXECUTIVE SUMMARY

was ready for higher power levels. As higher power levels were tested problems developed in the motor/SDG and the system had to be derated to 161 Hp at 920 RPM. Further detail on the accomplishments will be found in the monthly reports.

REMAINING PROBLEMS

Design changes have been made to the rotor, stator, housing and SDG which are expected to result in achievement of the original design goals. Since the new hardware has not been tested, the problems which led to design changes are listed here as potential problems. The results of the system test program showed indicated excessive losses in the machine, overheating of the rotor and inadequate lubrication in the SDG.

RECOMMENDED SOLUTIONS

The losses are believed due to shorted laminations in the rotor and stator. Changes have been made in both designs to correct this problem. The rotor overheating is due to mechanical deformation in an element of the shorting ring centering device which cuts off the flow of cooling oil to the shorting ring. The new rotor design will eliminate this problem. The original lubrication system for the SDG did not provide adequate cooling to the gear train. The modified design is expected provide the best possible cooling.

RECOMMENDED SYSTEM IMPROVEMENTS

The most significant system improvement would be to develop a new oil cooled alternator with higher efficiency, lower weight, less noise and no air ducting needed. As will be discussed in section 2, the motor/SDG no longer has a completely self contained lubrication and cooling system. With further development the system could again be self contained.

Section 2
DESIGN REVIEW

OBJECTIVE OF DESIGN

The objectives of this design were low weight, high efficiency and high reliability. The design concept selected is represented schematically below. The weight requirements in the SOW were nearly met and with further development could be bettered. The effiency requirements were again nearly met and could also be bettered with further development. A reliability value has not been established for the design but reliability was considered carefully in the design effort. Since four independent systems are used on the vehicle, a failure in one system would not leave the vehicle without propulsion. The design concept selected also has the potential for integration with the traction drive since the alternators could be shared for the two propulsion requirements.

DESIGN STATUS

The design was completed in September, 87 and fabrication of the first system was completed in January, 89. Component testing was begun early in 88 and continued into the spring of 89. System testing was begun in March, 89 and continued until June, 89.

Various modifications to the design were made during the fabrication and test phases to solve problems as they were encountered. Further modifications were made to a second Motor/SDG unit which was partially fabricated after the test program was stopped.

Since the original design was documented in the "Amphibious Vehicle Propulsion System Design Report", Westinghouse Inc., Oceanic Div., July 8,1988 (Appendix !); this report will concentrate on the changes in the design since that report and on additional changes that are recommended.

Propulsion System Schematic

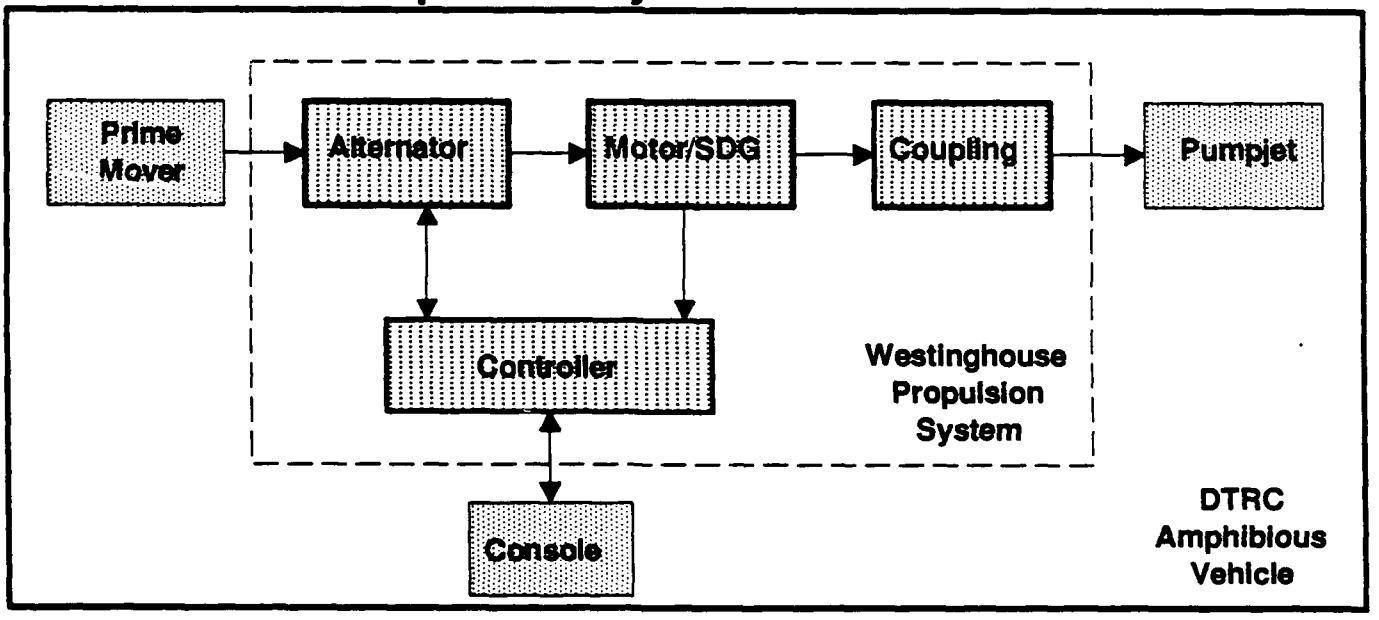

Section 2
DESIGN REVIEW

SYSTEM

The system is composed of an alternator, controller, motor/SDG and a coupling. The alternator is driven by the vehicle prime mover and supplies electrical power to the motor. The output speed of the motor is reduced in the SDG and the output power is transmitted to the vehicle pumpjet through the coupling. The controller regulates the voltage output of the alternator and monitors the alternator and motor.

The system is designed for an output power of 400 HP at 1250 RPM. A 1.3 overload (520 HP) is allowed for 1 Min. The system input speed is 9000 RPM. The controller is used to start and stop the motor and senses fault conditions in the system. The system requirements are summarized below. For additional details see the SOW.

There have been no system level design changes in the program and none are recommended.

Performance Requirements	
Output Rating Continuous	400 Hp (1250 RPM)
Output Rating Transient (1 Min.)	520 Hp (1250 RPM)
Output Speed	620 to 1250 RPM
Input Speed	4300 to 9000 RPM
Efficiency (target)	80%
Weight	800 Lb.

Control Functions	Monitor Functions
Start	Machine Temperature
Stop	Motor Oil Pressure
E-Stop	Current
Auto Shutdown (Fault)	Motor Slip
	Ground Fault

Section 2
DESIGN REVIEW

ALTERNATOR/PSB

The three phase brushless alternator is composed of three machines on a single shaft. The main machine has a rotating field which is energized by the exciter which has a stationary field. The final machine is a permanent magnet generator which is used to provide a shaft speed signal to the controller. Temperature sensors are mounted in the stator, and voltage and current transformers are mounted in the PSB box to provide signals to the controller. The machine is air cooled by an internal fan and lubricating oil for the bearings is supplied externally. A photograph of the machine appears on page 5A.

There have been no design changes to the alternator during the program. Recommended design changes are to develop a new alternator taylored to the application. The new machine would be oil cooled to eliminate the losses and noise in the fan cooled machine as well as eliminate the need for ducting in cooling air. The magnet iron in the new machine would be of higher quality which would reduce losses and weight. Provisions would also be made for sensors to support monitoring requirements.

ALTERNATOR SCHEMATIC

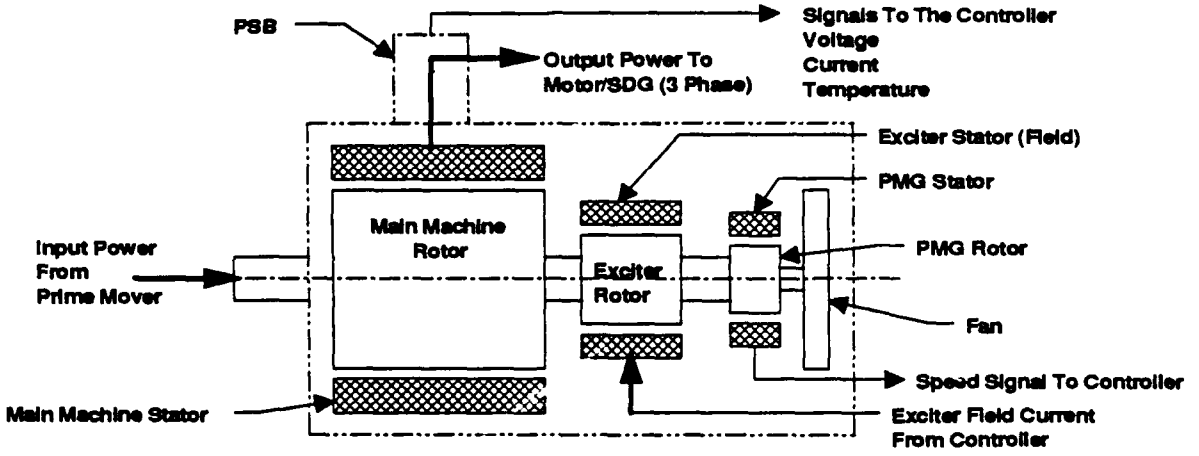

Summary of Alternator Specification

Cont. Rating	322 KW	Poles	6
Trans. Rating (1 Min.)	418 KW	Efficiency	88% Min.
Phase	3	Shaft Speed	9000 RPM
Voltage	520 VAC L-L	Weight	364 Lb.
Frequency	450 HZ	Cooling	Air- Internal Fan
		Dimensions	13.4 Dia. x 25.9 Lg

Section 2
DESIGN REVIEW

Figure 1. Alternator

Section 2
DESIGN REVIEW

CONTROLLER

The controller regulates the alternator output voltage to a constant volts/hertz value. The feedback control system varies the exciter field current to achieve the output voltage as a function of alternator speed. In addition to this function the controller also turns the motor on and off (as commanded), monitors all sensors in the alternator and motor, shuts the motor down in the event of a fault condition and sends data out through an RS-422 serial link. A photograph of the controller appears on page 6A.

Design changes to the controller were made in the boost converter, the field regulator and the software. In the original design the boost converter included included a current limit circuit to provide protection to the alternator and internal circuitry. Since the alternator was protected by a current limit circuit in the field regulator, this protection was redundant in that respect. In addition it was determined that internal circuit protection was not required and this circuit was eliminated to reduce cost.

The field requlator has three shutdown modes to provide redundancy for this critical function. The first level is an electronic mode in the field regulator. If this mode fails an electronic mode in the boost converter is commanded. In the original design, the third mode was a relay in the 150V field supply. During the component testing of the first unit it was determined that the stored energy in the field put an excessive load on capatitors in the circuit when this relay was opened. Therefore, the relay was relocated to the 28V input to the controller which served the same purpose and was easier to implement.

The controller was originally designed for a current limit value of 9 A to provide an adequate margin for starting the motor/SDG. During the fabrication phase it was determined that diodes in the alternator would be marginal at this current level. A value of 7 A was considered safe for the diodes and was expected to start the motor/SDG adequately. Therefore, the current limit was changed to this value and subsequent testing showed that it was adequate.

The software originally had three main programs (prestart, start and run) all of which set a 10 Ms timer as a first step, ran through their process and waited until the timer caused them to star over. During the development of the software it was found that the calculation of slip took longer than expected and caused the entire process time to exceed the 10 Ms. To overcome this the start and run programs were modified to alternate cycles such that slip was calculated in one cycle and all other functions were processed in alternate cycles.

CONTROLLER SCHEMATIC

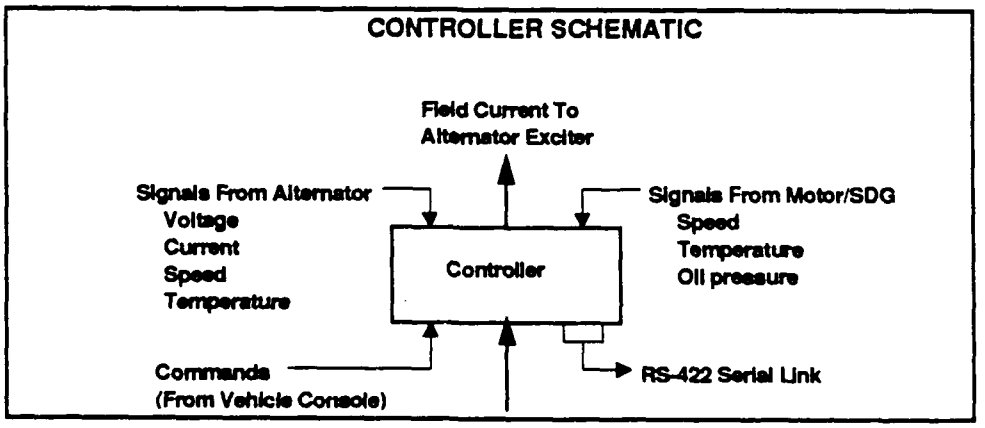

Section 2
DESIGN REVIEW

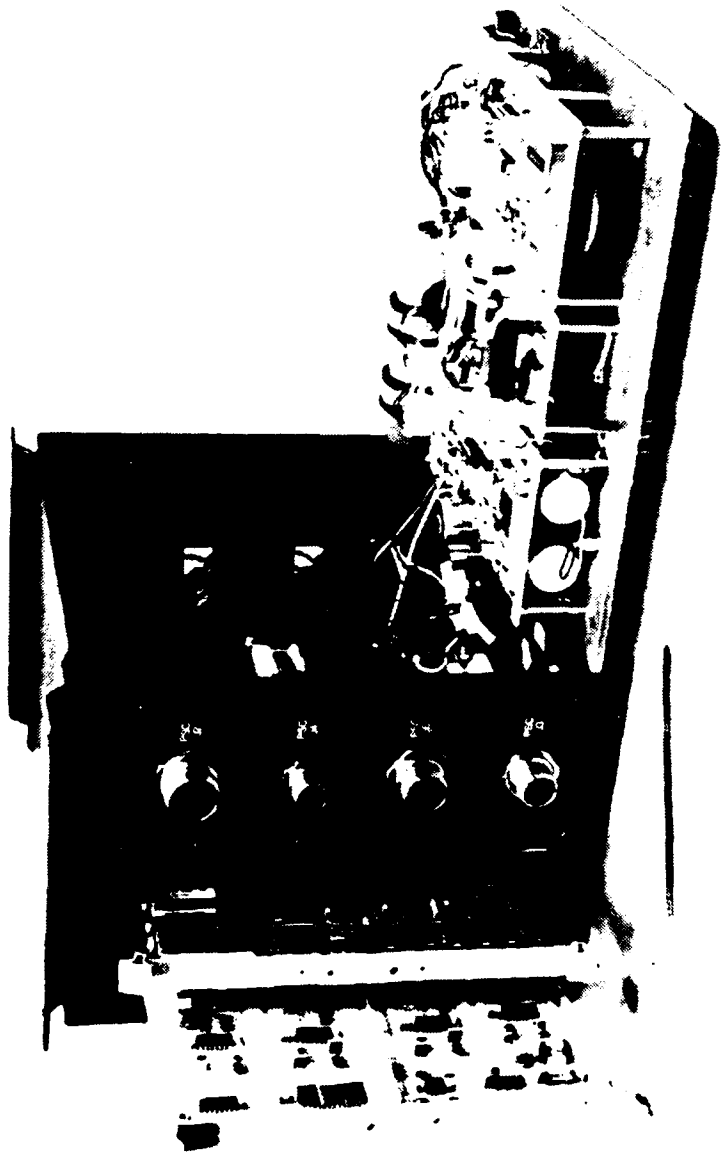

Figure 2. Controller

Section 2
DESIGN REVIEW

MOTOR/SDG

The motor/SDG is illustrated schematically below and consists of a three phase induction motor direct coupled to a planetary speed decreasing gear. It has a self contained lubrication system and has sensors for temperature, oil pressure and motor shaft speed which send signals to the controller. Details of the design will be discussed further under the individual subjects of the motor and SDG. A photograph of the machine appears on page 7A.

Design changes were made to the lubrication and cooling system, several components of the motor and the SDG. Under this topic the changes to the lubrication and cooling system which effected the motor/SDG as a unit will be discussed. The other changes will be discussed under the topics of motor and SDG which follow.

During the test programs for the motor/SDG and the system it was determined that the lubrication system was not delivering the design flow. Two problems were identified: the inlet filter created too much pressure drop and a vortex was forming in the sump causing air to be ingested by the lubrication pump.

In an attempt to preserve the schedule the internal filter was eliminated and replaced by an external filter positioned downstream of the pump. The vortex problem was solved by installing an inlet adaptor that drew oil from a large area and kept the inlet velocity low.

After test 203 (see section 4) it was determined that the motor/SDG cooling system was not performing adequately. Subsequent component tests on the stator

MOTOR/SDG SCHEMATIC

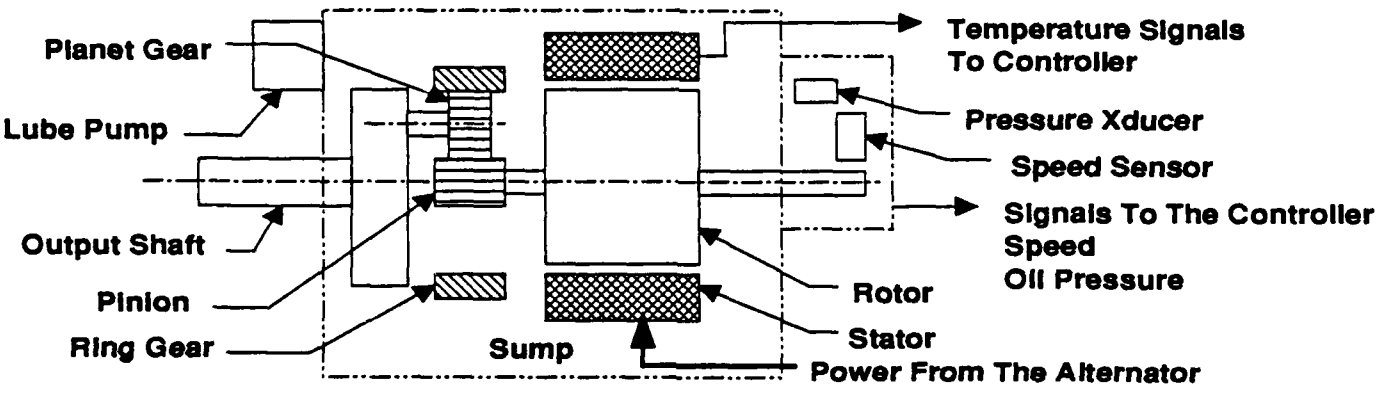

Summary of Motor/SDG Specification

Cont. Rating	400 Hp	Poles	6
Trans. Rating (1 Min.)	520 Hp	Efficiency	92% Goal
Phase	3	Shaft Speed	1250 RPM
Voltage	520 VAC L-L	Weight	301 Lb.
Frequency	450 HZ	Cooling	OIL
		Dimensions	

Section 2
DESIGN REVIEW

Figure 3. Induction Motor

Section 2
DESIGN REVIEW

showed that the heat transfer path from the stator to the outside of the motor housing was inadequate. The

cause of the high resistance was concluded to be the contact resistance between the inner and outer shells ofthe heat exchanger. For this reason the internal heat exchanger was eliminated and a water jacket was added to the outside of the new single shell housing design. An external heat exchanger was added to the lubrication and cooling system to replace the original heat exchanger.

Recommended design changes concern the lubrication and cooling system, the protective coatings, the mounting provisions and the output shaft. During the test program, as described above, the original concept of a self contained lubrication and cooling system was modified in an attempt to meet the schedule requirements. A self contained system is still possible but would require development. The original concept had a heat exchanger in the wall of the motor housing with water flooding the outside. Heat from the stator flowed through ribs in the heat exchanger to the water outside. The new concept would have water flowing through a water jacket inside the heat exchanger and outside the stator. This would improve the stator cooling path. The water jacket concept eliminates the need for flooding of the motor and reduces total vehicle weight.

The oil filter which was mounted externally during the test program to meet schedule requirements could be mounted on the SDG. This would restore the completely self contained lubrication system concept.

The present sump arrangement creates difficult tradeoffs: if the oil level is high the rotor may be partially submerged creating excessive drag and if the oil level is low the total amount of oil in the system is low (causing the oil to recirculate too often and degrade rapidly) and it becomes possible for the lubrication pump to ingest air and cut off oil flow to the system. It is therefore recommended that an oil reservoir be added and a scavange pump be used to deliver oil from the sump to the reservoir.

A water pump could be added to the SDG to supply water to the water jacket described above. This would make the water system completely self contained also.

The coating system originally selected for all external surfaces of aluminum parts was electroless nickel. During the test program it was found that the coating was very easily damaged. The coating itself is extremely hard and durable and has excellent corrosion resistance to seawater. However, the aluminum is soft and easily nicked. When this occurs the coating is disrupted and a flaw develops. In addition to this it was determined that nickel and aluminum have a high electro-potentail relative to each other and these flaws would result in severe corrosion in seawater or a seawater atmosphere. It is therefore recommended that a new protective coating be developed.

The present mounting provisions for the motor/SDG are two sets of bolt patterns; one in the forward bulkhead and the other in the SDG. This arrangement produces a need for load sharing between two brackets in the vehicle (and on the test stand) and results in unnecessarily sophisticated bracket designs. It is recommended that in a new design a single bolt pattern be placed in the SDG to carry the entire load.

The present output shaft design consists of a straight shaft with a keyway. This was the most desirable arrangement for use with a flexible coupling. However, if a reasonable amount of alignment can be maintained in the transom, a spline would seem more appropriate for this application. If the key is used the hub should be fixed to the shaft so the key does not wear out. This produces a possible problem with the development of axial forces on the shaft induced by temperature changes or mechanical deflections in the transom. A splined hub would not be fixed to the shaft and axial forces would be prevented. A small amount of misalignment can also be tolerated by a spline.

Section 2
DESIGN REVIEW

MOTOR

The three phase induction motor consists of a housing, stator, rotor, and forward bulkhead. The aft end of the rotor is supported by a bulkhead in the SDG. The motor is designed to direct couple to the SDG. A sump is attached to the housing for collection of oil and nozzles in the bulkhead spray oil on the rotor and end turns of the stator for cooling. Temperature sensors are embedded in the stator winding, a pressure transducer is connected to the oil supply passages and a speed sensor is mounted adjacent to the rotor shaft to provide signals to the controller.

Design changes have been made to the housing, stator, and rotor. The changes described below reflect the design which was partially fabricated at the end of the project and additional recommended design changes. Other design changes which occurred during the project will be discussed Section 3 Problems/Solutions.

Housing

The changes to the housing consisted of elimination of the internal heat exchanger, addition of a water jacket, replacement of the integral oil sump with bolt on version and enlargment of the oil suction passage. The new housing design is illustrated below. A new housing was fabricated in preparation for the assembly of a second

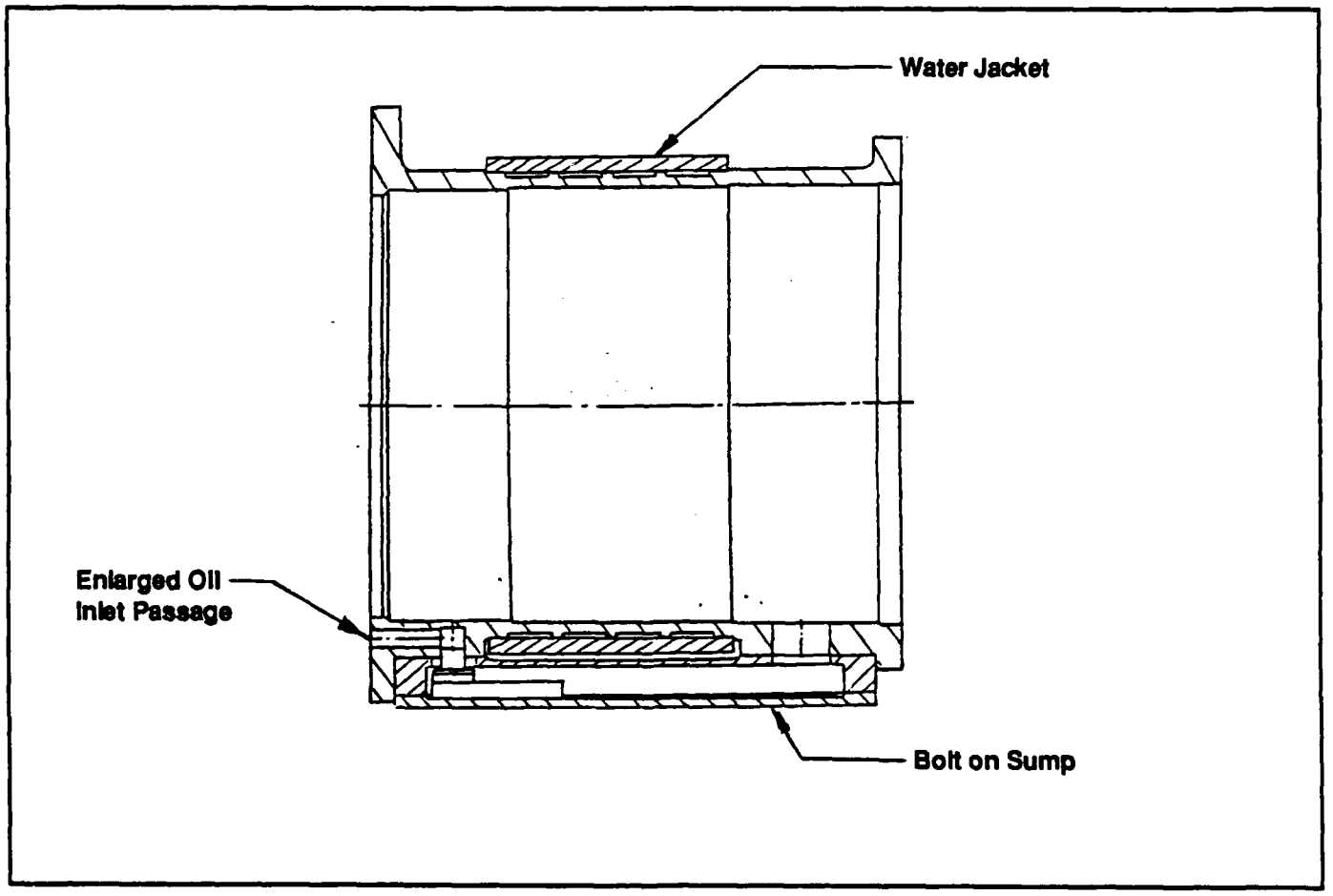

Section 2
DESIGN REVIEW

motor/SDG and is 95% complete. The heat exchanger and water jacket were discussed under subject of the motor/SDG.

The bolt on sump design was incorporated because of fabrication problems encountered with the first two housings produced. The first housing had a welded sump and had to be scrapped because of distortion produced by the welding process. The second housing had a brazed sump which had leaks in the braze joints. The new housing was therefore designed with a bolt on sump which is sealed by O-rings.

The enlarged oil inlet passage was the result of other changes in the lubrication and cooling system. After test 203 (see section 4) it was determined that the cooling system was inadequate. In subsequent component testing of the stator it was concluded that end turn cooling was required for the stator. This resulted in an increase in design flow from 3.5 to 4.5 GPM. The oil inlet passage was not adequate to handle this increased flow and was therefore enlarged in the new design.

Additional recommended design changes are described under the subject of the motor/SDG and are briefly to develop a new internal heat exchanger, add an oil reservoir and to develop a new protective coating process.

Stator

The changes to the stator were made to the insulation system, the stack and the top sticks. A photograph of the first stator appears on page 10A. During the fabrication of the first stator unit a short developed in the winding when a G-30 header strip (required to separate windings with a high potential relative to each other) was installed. The cause was traced to nicks in the winding insulation caused by the sharp edges of the header strip (which is a fiber glass laminate). To solve this problem, Nomex (a durable but soft paper) midsticks were designed with overlapping flaps which served the same function as the header strip. At the same time it was found that the Nomex-Kapton-Nomex slot liners did not hold up well to the bending operations on the winding. Therefore, since the winding had to be strippied for the above problem the slot liners were replaced with Nomex which is much more durable. Nomex will not withstand as high a potential as Nomex-Kapton-Nomex but is more than adequate for this application.

Modifications were made to the stack after test 519 (see section 4) when it was determined that every possible approach was required to reduce losses in the machine. At this time a second stator was fabricated in preparation for building a second motor/SDG. The original laminations were annealed to a condition which was a compromise between acceptable mechanical properties for the rotor stack and acceptable magnetic properties for the stator stack. At this time it was concluded that maximum properties in the stator laminations were worth the expense of reannealing.

When the first sample stacks were prepared for the first stator it was found that the laminations were shorted. After a great deal of investigation it was concluded that the shorting was limited to the edges of the laminations and would not have a serious impact on the machine performance. However, this could not be proved and it was decided after test 519 to change the process such that no shorts could be detected. Therefore the laminations in the second stator were given a double coat of epoxy which succeeded in eliminating all shorts.

The top stick design was modified as a result of component testing done shortly after test 203 (see section 4). After test 203 it was concluded that there were excessive losses in the motor/SDG and various tests were conducted to determine where the losses were occurring. In one of these tests it was determined that oil collecting at the end of the air gap was producing a significant loss (4.5 KW). To reduce this loss, drain passages were added to the top sticks to provide an escape path for the oil. In further component testing this design change was shown to have reduced the loss to 1.3 KW.

Section 2
DESIGN REVIEW

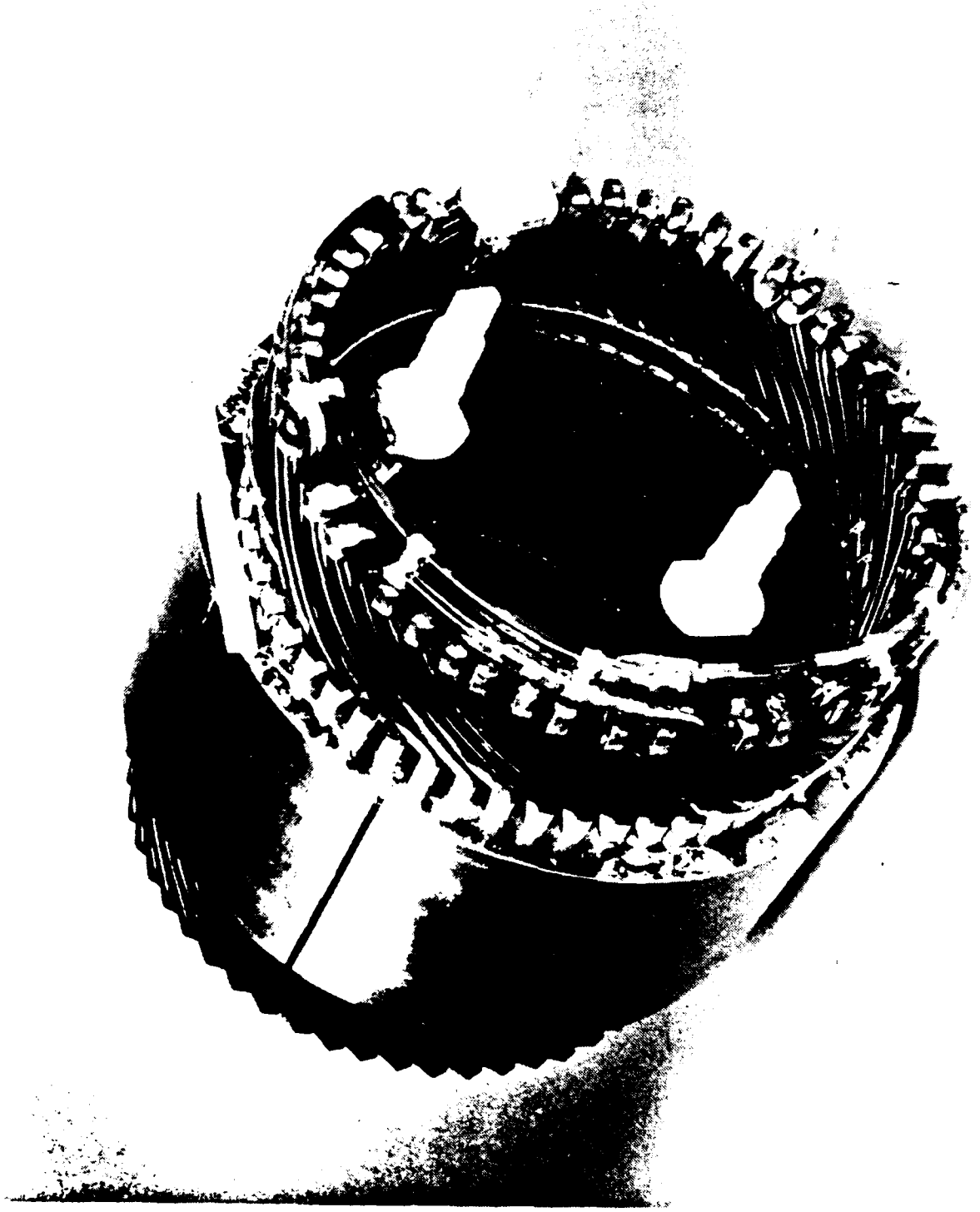

Figure 4. Stator

Section 2
DESIGN REVIEW

Rotor

Modifications to the rotor involved the lamination stack, the copper shorting rings and the rotor bars. After test 519 (see section 4) it was determined that every possible method must be employed to reduce losses in the rotor. A third rotor was fabricated in preparation for build a second motor/SDG and is 95% complete. The new rotor design is illustrated below.

Since the rotor operates at a very low frequency when it is up to speed the losses due to eddy currents are expected to be very small. Therefore, since the original design called for brazing of the bars (which would destroy any insulating material avalialble) the decision was made to use no insulation between the laminations.

Laminations for the new rotor were treated with a double coat of epoxy to eliminate eddy currents. Since this new stack was held together by the epoxy, the steel end plates in the original design (which were intended to support the stack) were no longer needed and since their presence in the machine magnetic field produces more losses, they were eliminated.

After the rotor is assembled the outside diameter of the stack is ground to obtain the desired size and concentricity. The grinding process smears metal between the laminations and creates new shorts between them. To eliminate this a final cut was taken with wire EDM which burns the material away and produces no smearing.

It was determined that an end ring centering mechanism was needed in the spin test of the second rotor.

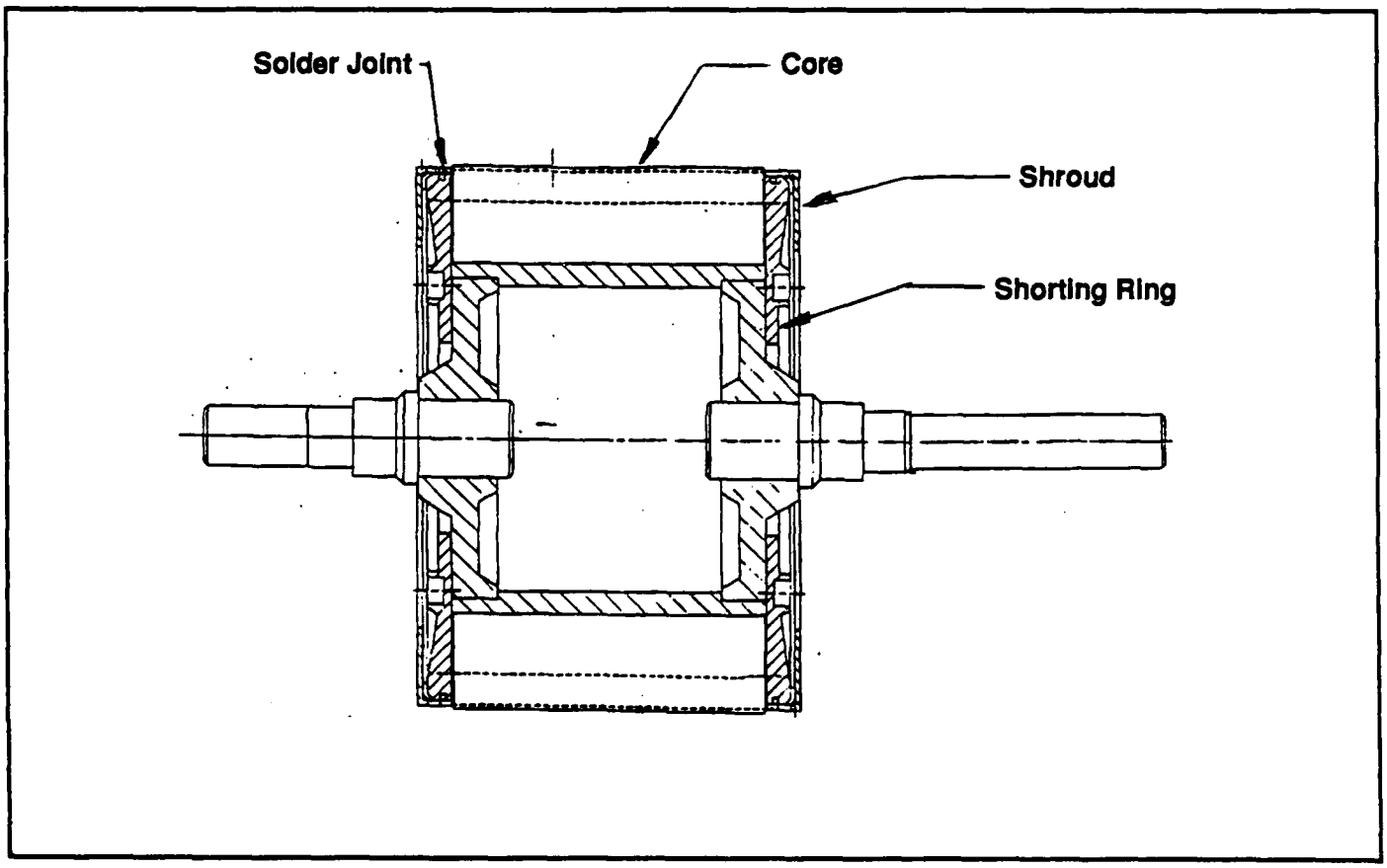

Section 2
DESIGN REVIEW

Two mechanisms were tried in an attempt to salvage this rotor but both failed. When a new rotor was built (after test 519) the end ring was redesigned to be pinned and screwed to the shaft.

After test 519 it was discovered that one of the elements of the centering mechanism had been slightly displaced and caused the rotor cooling oil to be thrown off without contacting the shorting ring. If they had been contoured (dished), the escaping oil would have been recaptured and at least some of the surface would have been cooled. The new shorting ring design does not have any elements which can be deformed but a contour has been added as protection against build up of foriegn material.

It is possible that when oil is sprayed on a rotating disc that some of it splashes off instead of flowing across the surface. For this reason a shroud was added to the new rotor design to collect any oil that may splash.

Since the stack design was changed to include epoxy insulation the brazing operation had to be eliminated. Therefore the bars are now soldered to the shorting rings. This resulted in the added benifit that the mechanical properties of the shorting rings were not effected by soldering and the shrink rings (which were needed in the original design to support the shorting rings) were eliminated.

Additional recommended design changes to the rotor are to enlarge the output shaft, make it out of 17-4 PH stainless steel and spline the end for coupling to the SDG. The present design requires the high strength PH 13-8 MO (which is expensive and not as readily available as 17-4 PH) due to the size. In the present design a coupling is keyed to the output shaft and drives the SDG pinion with a spline. If the end of the shaft were splined it could drive the pinion directly eliminating parts and taking less space.

Section 2
DESIGN REVIEW

SDG

The 7:1 reduction SDG consists of a housing, bulkhead (which is shared with the motor), a ring gear, an output shaft which carries the three planet gears, a sun pinion and a lubrication pump. The housing has lugs for mounting the motor/SDG in the vehicle. The lubrication pump is mounted on a manifold which connects the pump inlet to passages in the SDG housing and bulkhead leading to the oil inlet in the motor housing. The pump discharge is ported for connection to the external filter. Arelief valve in the manifold discharges oil to the SDG housing if system pressure becomes excessive.

Design changes have been made to the lubrication system in two areas: the pump discharge now flows to an external filtering system and heat exchanger and the original fixed sun pinion spray nozzles have been eliminated and replaced with nozzles mounted on the output shaft which spray the teeth of the sun pinion, planets and ring gear as they leave the mesh. The changes to external filter and heat exchanger were discussed under the previous topic of the motor/SDG.

The changes to the lubrication of the gearing were made after test 519 (see section 4). At this time it was concluded that the lubrication of the gears was inadequate and a new SDG was modified for use in the building of a second motor/SDG. The modifications were completed. The modified unit is illustrated below.

In the original design fixed nozzles directed a spray of oil onto the pinion teeth and the rest of the gears were lubricated by oil splashing off the pinion. Each time a planet gear went by a nozzle the flow to the pinion was

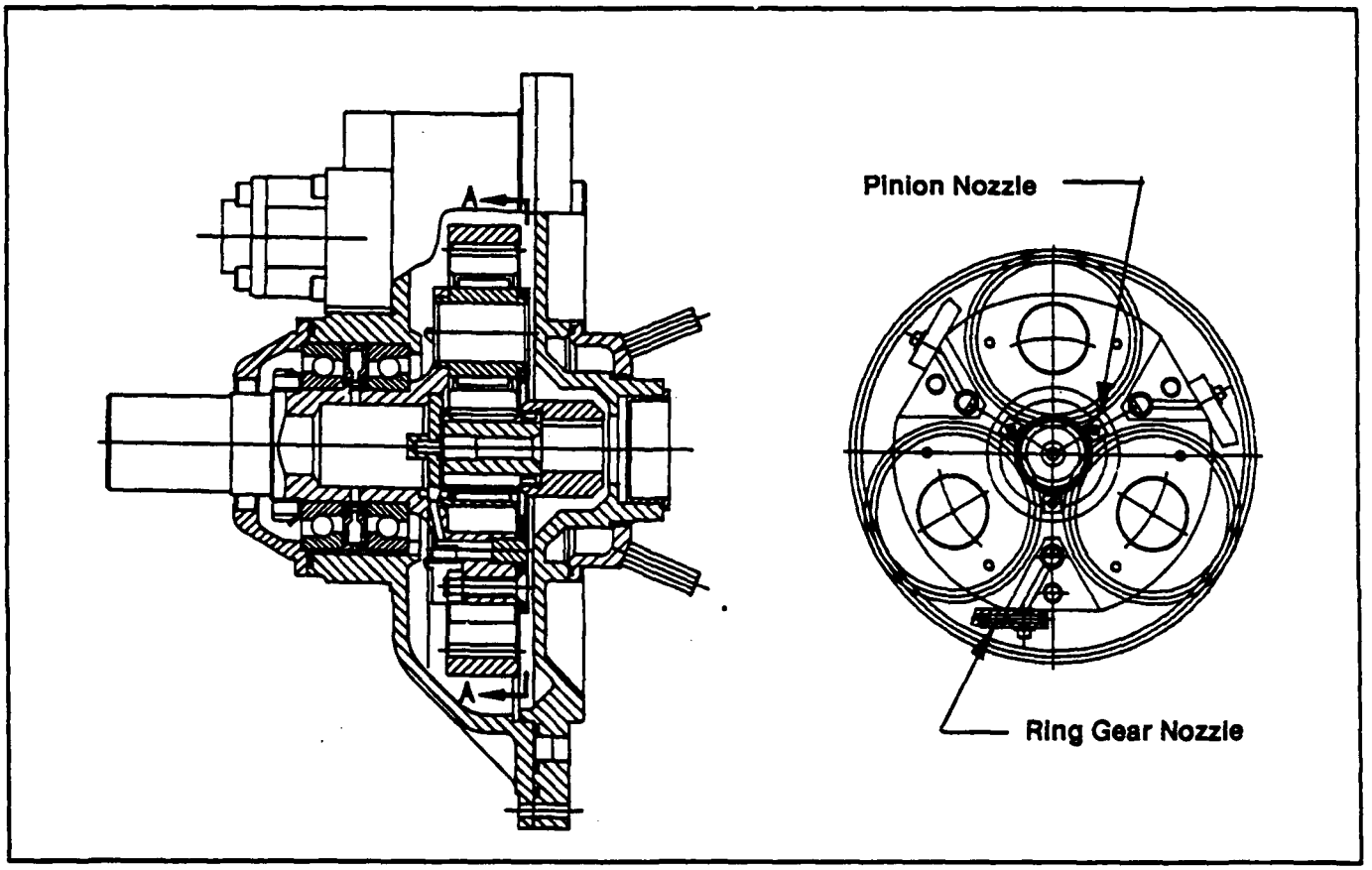

Section 2
DESIGN REVIEW

blocked with the result that a large portion of the time the pinion was getting no cooling.

Recommendations from several gear experts were considered prior making any changes. According to one of the experts the most critical function of the lubrication system is the removal of heat. He pointed out that as the gear teeth leave the mesh they have a high surface temperature. If the heat is removed at this time the heat transfer process is enhanced because there is a large temperature difference between the gear tooth and the oil. If it is not removed it soaks back into the tooth resulting in a higher average gear temperature. With a higher gear temperature the thin film of oil in the mesh is also higher and the viscosity becomes too low to support the load.

The amount of oil needed to provide a film in the mesh is extremely small and is adequately supplied by splash. It was also pointed out that in this design approximately the same amount of heat is generated in the ring gear mesh as in the the pinion mesh. Therefore spraying of the ring gear teeth as they leave the mesh is also recommended.

Based on these recommendations the fixed nozzles were eliminated and nozzles mere attached to the planet carrier to spray the pinion and ring gear as they leave the mesh.

The recommended design changes involve the housing, output shaft, lubrication system, and the addition of a water pump. Changes to the output shaft and lubrication system and the addition of a water pump were discussed under the topic of the motor/SDG. Changes to the housing include changing the mounting provisions, developing an improved coating system and changing the mounting for the ring gear. The mounting and coating system recommendations were also discussed under the topic of the motor/SDG.

The ring gear is presently kept in the proper plane by lugs on the bulkhead and housing and rotation is prevented by two pins in the bulkhead which engage lugs on the ring gear. The purpose of this arrangement is to allow the ring gear to float and enable the planet gears to share the load. In reality there is no evidence that this arrangement allows any float.

Since the pinion is allowed to float, load sharing is adequately provided for without this arrangement. Therefore, the ring gear could be fixed in the gear housing with no loss of function. This would simplify manufacturing as well as assembly.

Section 3
PROBLEMS/SOLUTIONS

INTRODUCTION

The project can be broken down into three phases: the design phase, fabrication phase and the testing phase. This section will describe the problems encountered in the last two phases, the design changes made and additional recommended design changes.

ALTERNATOR/PSB

During the fabrication phase of the alternator a ground developed between the exciter rotor winding and the shaft. The problem was traced to burrs on the edges of the laminations and a sandblasting operation was added to eliminate this problem.

A number of problems were encountered in the test phase. Due to the cantelever mounting of the alternator the machine vibrated excessively when it was first tested. To correct this problem a new stiffer mounting bracket was fabricated and installed.

The seal on the drive end bearing leaked oil into the machine. The oil was picked up by the cooling air and discharged into the laboratory. The cause of this leak has not been clearly identified. The seal function is dependent on air pressure and oil pressure to the bearing. This problem persisted through the entire test program.

The mounting for the PSB was inadequate and installation was difficult. Mounting provisions for the PSB consisted of four 8-32 tapped holes which were only about .156 inches deep located in the main power terminal block assembly. This prevented the incorportion of cable supports in the PSB. Since there were no temperature sensors embedded in the stator they had to be installed externally through holes in the housing. Jacketed RTD's were used to provide mechanical protection to the leads. However, the RTD's are not designed for mounting at both ends of the jacket and special provisions had to be made for this requirement.

Provisions for the external lubrication are complicated and requirements are difficult to establish. The supplies to each of the two bearings have to be independenly controlled because a parallel supply could result in one bearing being starved for oil. Oil in return lines was mixed with large quantities of air requiring large return lines and provisions for separating the air at the reservoir. Due to the leakage of one of the seals the oil in the reservoir had to be replaced frequently.

The air cooling system has to be restricted on the discharge side to provide the proper pressure environment for the seal discussed above. The machine has no provisions for connecting a duct for this purpose and attaching a duct was difficult.

No design changes have been made to the alternator/PSB. It is recommended that a new alternator/PSB would be developed with oil cooling, improved magnet iron and embedded sensors for sending signals to the controller. These recommendations are discussed in section 3.

ALTERNATOR/PSB PROBLEMS/SOLUTIONS

Component	Problem	Solution
Exciter Rotor	Winding Short	Remove Burrs
Drive Stand Bracket	Vibration	Replace Bracket
Drive End Seal	Leakage	None
PSB	Mounting & Ass'y	None
Lubrication	Control	None
Air Cooling System	Control	None

Section 3
PROBLEMS/SOLUTIONS

CONTROLLER

There were minor problems in two areas of the controller: the regulator and the software. The original design of the regulator called for a relay to interupt the field circuit in one shutdown mode. It was determined that this arrangement caused excessive load on capacitors in the circuit and the relay was relocated to the 28V input of the controller.

During the software development it was discovered that the slip calculation process took longer than expected. The total process time for slip and all other parameters exceeded the 10 Ms loop time in the main program. To solve this problem the main program was altered to alternate between sampling slip and sampling all other parameters.

These changes are discussed in section 2 Design Review.

CONTROLLER PROBLEMS/SOLUTIONS

Component	Problem	Solution
Relay	Excessive Load on Capatitors	Relocate Relay In Different Circuit
Software	Slip processing Time Greater Than Expected	Alter Main Program Cycle Time

Section 3
PROBLEMS/SOLUTIONS

MOTOR

Problems occurred in four areas during the fabrication and test phases: rotor, housing, lubrication system and stator.

Rotor

The stack laminations in the first rotor were welded together along three equally spaced axial tracks along the inside diameter. The purpose of these welds was to hold the stack together for the next assembly operation. The welds cracked prior to the assembly operation and a different method of assembly had to be used. The key was left out because it was considered a source of risk to the new assembly method. The steel end plates were welded to the shaft as a substitute for the key. Since a method of assembly had been worked out, the core for the second shaft was not welded.

The brazing operation on the rotor bars and shorting rings seriously reduced the material properties of the parts. It was determined that the material would still handle the loads and processing was continued.

The first rotor was placed into a fixture for spin testing and gradually brought up to the overspeed condition (10500 RPM). At 8600 RPM it came apart. The cause of the failure was concluded to be due to a loss in mechanical properties in the laminations caused by the welding process. Since the second rotor was not welded, no additional design changes were made at this time.

The second rotor was sucessfully spin tested but was out of balance after the test. The cause of this was concluded to be shifting of the shorting rings. A shorting ring centering mechanism was designed and installed and the rotor rebalanced. The second spin test produced no additional imbalance and the rotor was ready for assembly into the motor/SDG.

After test 203 (see section 4) the rotor was removed and found to have rubbed the stator. One of the elements of one of the end ring centering mechanisms had moved out of its proper location and was no longer serving to center the shorting ring. Although it was not clear at this time, in later tests it was concluded that axial motion of the shorting ring caused the movement of the centering element. Without a complete understanding of the problem it was concluded that a modification to the centering mechanism which prevented axial movement of the above element would solve the problem. It was also concluded that the rotor core was overheating due to shorted laminations (caused by smearing of metal in the grinding process) and a cut was made on the outside diameter of the stack with the wire EDM process (which burns the metal away) to minimize the shorting. After these changes were made testing continued.

ROTOR PROBLEMS/SOLUTIONS

Component	Problem	Solution
Rotor Core	Cracked Welds	Alter AssemblyMethod
Shorting Rings	Loss of Properties	Solder Instead of Braze
Rotor Core	Failed in Spin Test	Eliminate Welding of Core
Shorting Rings	Shifted in Spin Test	Add Centering Mechanism
Shorting Rings	Shifted in Motor Test	Modify Centering Mechanism
Shorting Rings	Shifted in Motor Test	Attach Shorting Rings to Shaft

Section 3
PROBLEMS/SOLUTIONS

After test 519 (see section 4) the rotor was again removed and found to have rubbed the stator again. This time the centering element was deformed by the axial motion of the shorting ring and the role of the axial movement became clear. The centering element was located in the path of the oil spray for cooling the rotor and before it was deformed the oil flowed from it across the face of the shorting rings. after it was deformed it threw the oil off without contacting the shorting ring and cut off the cooling to the rotor. This explains the overheating and rubbing of the rotor.

At this time a third rotor was fabricated for use in a second motor/SDG. The new design incorporates shorting rings which are contoured and attached to the shaft with pins and screws. The stack is insulated with epoxy and the outside diameter is cut with wire EDM. The bars are soldered to the shorting rings and shrouds have been added to the ends of the rotor. These design changes are discussed in section 2.

Additional recommended changes are to enlarge the output shaft and to spline the end of it. These changes are also discussed in section 2.

Housing

The original housing design consisted of an outer shell in which fins for the heat exchanger were brazed into grooves and an inner shell and sump which were welded to the outer shell. Welding deformation caused a separation to occur between the inner and outer shells resulting in an internal leak path for the heat exchanger which would severly impacted the function; therefore, the part was scrapped.

A second housing was fabricated in which the fins and sump were brazed to the outer shell and the inner shell was shrunk in place. After the unit was completed it was found that some of the braze joints leaked. This was not an optimum process since parts that were already in process for the other design were used and design freedom was limited. However, some of the leaks occurred in the joint between the sump and the housing. This joint, which would still be required in a completely new design is not suitable for the brazing process due to the complexity of the geometry and the rigidity of the parts. Therefore, the brazing process was abandoned for future designs.

The leaks in the second unit were plugged adequately to proceed with motor testing and it was used to assemble the first motor. After test 203 it was found that the heat exchanger removed heat from the oil adequately but the heat flow path from the stator to the outer shell was inadequate. The probable cause of this was a high thermal resistance between the inner and outer shells. To continue testing, the housing was modified to circulate water through the heat exchanger passages and the oil was redirected to an external heat exchanger. A new housing was designed and fabricated with a

HOUSING PROBLEMS/SOLUTIONS

Component	Problem	Solution
Heat Exchanger	Internal Leakage Due to Distortion	Replace Welding Operation With Brazing Operation
Sump	Leakage	Replace With Bolted Design
Heat Exchanger	Inadequate Stator Heat Flow	Eliminate Heat Exchanger and Add Water Passages to Housing

Section 3
PROBLEMS/SOLUTIONS

single shell design surrounded by a water jacket, an enlarged oil inlet passage and a bolt on sump. The new housing is discussed in section 2.

Additional recommended design changes ar to develop a new internal heat exchanger, add an oil reservoir and develop an improved coating system. These changes are discussed in section 2.

Lubrication System

The original lubrication/cooling system consisted of a pump which drew oil through a filter in the sump and forced it through the heat exchanger and into the nozzles. After the oil leaves the rotor it flows down to the sump. Early if the test program it was found that the filter caused too much pressure drop, caused the pump to cavitate and limited the flow to the system. At this time the internal filter was replaced with an external filter.

The flow rate continued to be less than expected and it was determined that air was being ingested in the pump suction line in the sump. This problem was solved by fabricating an oil inlet device which resisted the formation of a vortex in the sump.

After test 203 (see section 4) the total oil flow requirement was increased from 3.5 to 4.5 GPM. Since the lubrication pump had extra capacity this presented no problem for the pump. However, it was determined that the oil passage from the sump to the lubrication pump was inadequate. To maintain schedule an external suction line was added to the unit being tested and design efforts were begun on a new housing and modified SDG with enlarged passages. The new housing and SDG designs discribed in section 3 incorporate larger passages as well as the other design changes described above.

Additional recommended design changes are to add an oil reservoir, add a scavange pump and to alter the lubrication circuit. These changes are discussed in section3.

LUBRICATION SYSTEM PROBLEMS/SOLUTIONS

Component	Problem	Solution
Filter	Excessive Pressure Drop	Replace With External Filter
Oil Inlet	Air Ingestion	Alter Inlet to Prevent Vortex
Oil Inlet Passage	Excessive Pressure Drop	Enlarge Passage

Section 3
PROBLEMS/SOLUTIONS

Stator

Test samples for the first stator stack had a short circuit across the stack. Various methods were tried to eliminate the shorts without success. After extensive investigation it was concluded that the shorts were occurring at the edges of the laminations and would probably not create a serious loss in the machine. The lamination material was also tested at this time and found to have acceptable but less than desirable magnetic properties. The decision was made to continue with the build with the hardware unchanged.

During the winding process some insulation was scraped of one of the conductors by a header strip which was inserted to separate windings which have a high potential relative to each other. The material for the header strip was G-30 fibreglass laminate which has sharp edges. To eliminate this problem Nomex midsticks were designed with flaps on each end which overlapped adjacent flaps and formed an equivalent header strip. Since the winding had to be stripped for this change two other changes were made at the same time: the Nomex-Kapton-Nomex slot liners were replaced with Nomex which is more durable and the ends of the slots were deburred for added ensurance against insulation failure.

During the curing of the first unit (after VPI) the core developed cracks between some of the laminations. Clamps were added and the curing was completed without further problems. The clamps were permanently added to the process for future units.

The unit was assembled into the first motor and motor testing was begun. During the test program the total losses were found to be greater than expected. The exact contribution of each design element could not be determined. One specific problem identified after test 203 (see section 4) was oil drag caused by oil collecting at the edge of the air gap. This problem was solved by adding drain passages to the top sticks adjacent to the air gap in the rotor.

After test 519 a second unit was fabricated in preparation for building a second motor/SDG. At this time it was known that there were excessive losses in the machine but the specific sources could not be identified. It was therefore decided to make any changes to the stator which would possibly make an improvement. Thus, the laminations were reannealed to obtain the best possible magnetic properties and coated with two layers of epoxy to eliminate shorts in the next unit.

STATOR PROBLEMS/SOLUTIONS

Component	Problem	Solution
Stack	Lamination Shorts	Defferred
Header Strip	Cut Insulation on Winding	Replace With Nomex
Slot Liners	Not Durable	Replace With Nomex
Stack	Cracked During Cure	Clamp during Cure
Air Gap	Oil Drag	Add Drainage Passages

Section 3
PROBLEMS/SOLUTIONS

SDG

There were no significant problems in the fabrication of the SDG. After component testing was completed the first SDG was assembled to the motor and motor/SDG and system testing was begun. After test 203 (see section 4) it was observed that the pinion had developed severe scoring. The manufacturer identified the problem as due to insufficient lubrication. At this time it had been determined that the lubrication system had not been functioning correctly in previous testing and it was decided to correct the lubrication system problem, replace the SDG and continue testing.

After test 506 (after the lubrication system function had been established) a second pinion was found to have minor pitting and again the manufacturer indicated that the problem was insufficient lubrication. At this time the design was changed to cause partial flooding of the SDG. Further tests (515 and 519) showed that this method also did not work.

After test 519 a third SDG unit was modified to eliminate the fixed nozzles for the pinion and add nozzles to the planet carrier which direct flow to the pinion and ring gear teeth as they leave the mesh. These changes are discussed in section 2.

Additional recommended changes are to change the mounting of the ring gear, spline the output shaft, change the external mounting provisions and protective coating, and add pumps and a filter. These changes are also discussed in section 2.

SDG PROBLEMS/SOLUTIONS

Component	Problem	Solution
Pinion	Scoring	Correct Deficiencies in Lubrication System
Pinion	Minor Pitting	Modify SDG Lubrication System

Section 4
TEST OBJECTIVES/RESULTS

INTRODUCTION

The objective of the test program was in general to verify that the machine meets all specification requirements that can be demonstrated in the laboratory. Component testing was conducted to verify readiness of components for testing at higher assembly levels. System tests were begun at reduced power levels to provide assurance that performance at full power would be acceptable.

Since problems developed during the test program the full test program was not completed. In this section the objectives and results of the completed tests are described.

SYSTEM

At the system level there were 15 tests conducted. A schematic diagram of the test setup is shown below.

The DC drive motor was used to drive the alternator at the various required speeds and the dynamometer was used to apply the desired loads to the motor. The drive motor and dynamometer were controlled by the operator's console. Motor starting and stopping was controlled by the system console. Instrumentation readouts were located in the operator's console and a CRT connedted to the system console. Additional detail on the test setup and the instrumentation is contained in the "Ambpibious Vehicle Propulsion System Acceptance Test Report", Westinghouse Electric Corporation, Naval Systems Division, December 21, 1989 (Appendix II).

A brief description of each test appears on the following pages.

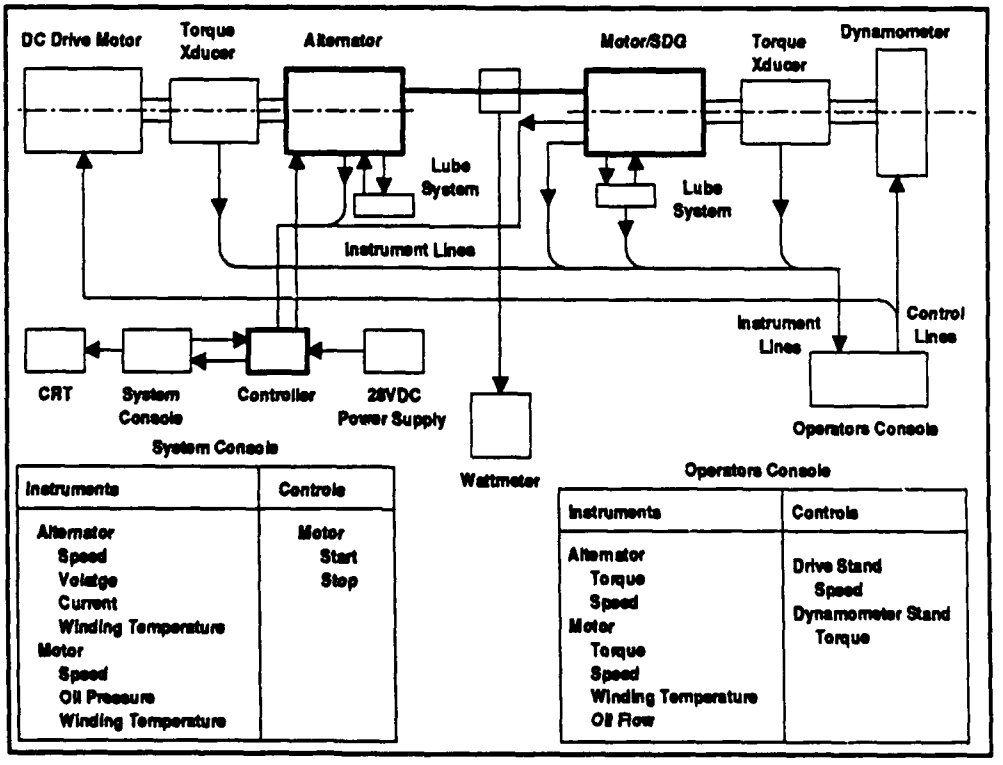

Section 4
TEST OBJECTIVES/RESULTS

Test 113

This test was run at the starting speed and 11% full power. The test was run until steady state temperature was achieved (50 Min.) to get an initial idea of the thermal behavior of the machine. Thermal performance was acceptable at this time.

Test 114

This test was run at 40% full power with the same objective as test 113. Due to difficulties with the test facility a torque surge occurred just as the operating point was reached. Rapid heating occurred in the motor winding and the controller shut the system down as it was designed to do. A maximum motor winding temperature of 162C was observed.

Test 115

This test was a repeat of test 114. After 10 minutes of operation one of the alternator RTD's failed and the controller shut the system down. The RTD was bypassed for further testing.

Test 116

This test was a repeat of test 114. After 2.5 minutes of operation another alternator RTD failure occurred and the controller shut the system down. This RTD was also bypassed.

Test 117

This test was a repeat of test 114. After 14 minutes of operation the controller shut the system down because one of the motor RTD's indicated excessive temperature. The RTD in question was not open circuited (indicating failure) but was reading much higher (200C) than the other RTD's in the machine.

Test 118

This test was a repeat of test 114. Testing continued after test 117 without change to see if the same result occurred again. After 19 minutes of operation an excessive winding temperature (120C) was indicated by a thermocouple. The unit was manually shut down. At this time it appeared that the RTD in test 117 was not behaving consistently.

Test 119

After test 118 it was hypothesized that the cooling system would function better at a higher speed. Therefore, this test was run at 75% full power. After 2 minutes of operation the controller shut the system down because of excessive temperature in the motor winding. It was concluded from this that there were other problems with the cooling system.

SYSTEM TEST RESULTS

Test	Date	Speed RPM	Power HP	Time MIN.	Comments
113	3/6/89	4300	46	50	Objective Met
114	3/6/89	6500	161	-	Aborted
115	3/7/89	6500	161	10	Aborted
116	3/7/89	6500	161	2.5	Aborted
117	3/7/89	6500	161	14.5	Aborted
118	3/7/89	6500	161	19	Aborted
119	3/7/89	8000	296	2	Aborted

Section 4
TEST OBJECTIVES/RESULTS

Test 201

After test 119 a flow meter was added to the cooling oil circuit. The flow rate (1.8 GPM) was found to be far below the design flow (3.5 GPM). It was found that increasing the oil level in the motor brought the flow rate up to design value and this test was therefore run at the 40% power level of 114 with an increased oil level. A steady state temperature was achieved in 60 minutes.

Test 202

This test was conducted at full power with the objective to demonstrate thermal steady state operation. After 2 minutes of operation an excessive winding temperature (130C) was indicated by a thermocouple. The system was shutdown manually. At this time it was concluded that the cooling system was inadequate.

Test 203

At this point it was desired to determine what power level the machine was capable of handling. Therefore this test was conducted at 70% full power. After 6 minutes of operation excessive motor winding temperature (180C) was indicated by a thermocouple. The system was manually shut down.

After this test it was determined that motor performance had deteriorated since the first test results were obtained. The machine was disassembled and damage was found on the rotor, stator and SDG pinion. Repairs were made to the rotor and a new end ring centering mechanism was designed and installed. The outside diameter was also cut with wire EDM in an effort to reduce edge shorts between the laminations produced by the grinding process.

Subsequent component testing showed that the friction and windage of the machine was excessive when oil was sprayed on the end of the rotor. The stator was modified at this time to include drainage passages in the top sticks adjacent to the end of the rotor. Further component testing showed a large improvement in performance.

The lubrication system was also modified at this time to include end turn cooling for the stator. This increased the requirement for total oil flow and subsequent component tests showed that the oil suction passage was restricted. Therefore, an external suction line was added as a temporary measure to continue the test program. No change was required for the lubrication pump since it already had adequate capacity to supply the new flow requirement.

Component testing was also done on the stator at this time and it was found that the heat flow from the stator through the housing was inadequate. At this time a new housing design with a water jacket was begun. To continue testing, the original housing was modified to flow water through existing heat exchanger.

The SDG had been used in all previous testing and it was known at this time that the lubrication system had not been functioning properly in some of those tests. Therefore, the SDG was replaced and no additional modifications made.

SYSTEM TEST RESULTS

Test	Date	Speed RPM	Power HP	Time MIN.	Comments
201	3/12/89	6500	161	60	Objective Met
202	3/12/89	9000	399	2	Aborted
203	3/12/89	8000	294	6	Aborted

Section 4
TEST OBJECTIVES/RESULTS

Test 505

This test was conducted at 11% full power to establish initial steady state thermal performance to be compared to previous data taken in test 113. Steady state was achieved in 10 minutes and temperatures ran substantially cooler than in previous tests.

Test 506

This test was conducted at 40% full power for comparison with data from test 201. Steady state was achieved in 10 minutes and again, temperatures ran substantially lower (120C) than in previous tests. Minor pinion damage was observed after this test which indicated inadequate lubrication in the SDG. At this time the SDG was modified to create a partially flooded gear train in an attempt to improve the lubrication performance.

Test 510

This test was conducted at 9000 RPM and 40% full power. The objective of this test was to compare the thermal performance of the machine at full speed and at the power of test 506 to the performance observed in test 506. Steady state was achieved in 10 minutes and temperatures continued to be lower than in previous tests. There was no additional damage observable on the SDG pinion.

Test 515

This test was conducted at 9000 RPM and 75% full power with the objective of demonstrating steady state at a higher power level. Steady state was achieved in 10 minutes. Additional SDG pinion damage was observed after this test (the pinion had suffered minor damage in test 506).

Test 519

This test was a repeat of test 515 except that the motor was reversed. In previous testing only one side of the pinion teeth were damaged. Therefore, reversing the motor was equivalent to starting with a new pinion. The purpose of this test was to determine if an undamaged pinion would perform better than the one used in test 515. Steady state was achieved in 10 minutes.

When the machine was torn down it was found that the SDG pinion sustained the same damage as before and that the rotor had rubbed the stator again. Testing was suspended until modifications could be made to the rotor and SDG lubrication system. The design changes are described in Section 3 Design Review.

SYSTEM TEST RESULTS

Test	Date	Speed RPM	Power HP	Time MIN.	Comments
505	5/18/89	4300	46	10	Objective Met
506	5/18/89	6500	161	10	Objective Met
510	5/30/89	9000	161	10	Objective Met
515	6/4/89	9000	300	10	Objective Met
519	6/7/89	9000	300	10	Objective Met

Section 4
TEST OBJECTIVES/RESULTS

COMPONENT TESTING

As mentioned at the beginning of this section component testing was conducted where practical to demonstrate that components were ready for testing at higher assembly levels. Results of this testing are given in the "Ambpibious Vehicle Propulsion System Acceptance Test Report", Westinghouse Electric Corporation, Naval Systems Division, December 21, 1989 (Appendix II). The table below summarizes the testing.

Component Test Results

Test Description	Test Objective
Alternator	
Dielectric	Verify insulation integrity/establish baseline
Vibration	Correct mounting bracket problem
Losses	Friction, windage, core losses
No Load Performance	Output voltage as a function of shaft speed and exciter current
Thermal performance	Steaty state temperature at full load
Efficiency	Electrical output / Mechanical input
Controller	
Current Limit	Verify maximum exciter current
Steady State Field Current	Verify regulation function
Heat Run	Steady state temperature at maximum load
Fault Protection	Verify all system functions
Alternator/Controller	
Main Field Frequency Response	Determine time constant
Closed Loop V/HZ Regulation	Verify controller function
Transient Response	Overshoot and recovery time
Motor/SDG	
Stator	Insulation integrity/verify design parameters
Rotor Bar Resistance	Verify joint resistance
Rotor spin	Verify deflection/strength
Spray Nozzle	Verify flow characteristics
Rotor Resonance	Verify critical speed
Locked Rotor	Determine resistance/leakage inductance
Stator AC resistance	Verify design parameters
Stator Heat Runs	Thermal resistance
Startup	Starting torque
Friction and Windage	Losses: friction, windage, oil drag
SDG	
Losses	Friction, windage, oil drag
Nozzle Performance	Verify Flow characteristics

Section 5
PRODUCTION COST ESTIMATE

The production cost estimate reflects the fact that no unusual, exotic or proprietary manufacturing processes are required to fabricate the propulsion system.

An estimate of the production cost of the amphibious propulsion system was performed. This estimate assumes the current design of all components. The production quantity was based on a production run of 1400 vehicles with 4 motor/alternator/controller sets per vehicle. The estimate includes tooling costs associated with this production quantity as well as all material and labor to deliver the propulsion units ready to install in vehicles.

The diagram below shows the work breakdown structure used to estimate and collect costs and represents the major hardware elements and tasks required to deliver an Amphibious Propulsion System. The table at the right corresponds to the diagram and shows the cost breakdown to the item or summary level indicated.

All costs were estimated in 1989 dollars and include all overheads and fees to represent an estimated unit production sell price to the NAVY.

Production Cost Estimate

WBS	Description	Estimated Cost for 1400 Vehicles	Estimated Cost per Vehicle
0.0	Amphibious Propulsion	$612,738,189	$437,670
1.0	Propulsion Drive	$310,019,117	$221,442
1.1	Motor	$168,432,551	$120,309
1.1.1	Housing	$13,765,920	$9,833
1.1.2	Rotor/Shaft	$47,158,676	$33,685
1.1.3	Stator	$94,299,976	$67,357
1.1.4	Forward Bulkhead	$13,116,552	$9,369
1.1.5	Pre-Amp PWB	$91,427	$65
1.2	Coupling	$6,672,124	$4,766
1.3	Speed Decreasing Gear	$114,566,144	$81,833
1.4	Power Cable	$5,214,149	$3,724
1.5	Propulsion Drive Integration	$13,771,316	$9,837
1.6	Propulsion Drive Test	$1,362,833	$973
2.0	Alternator System	$300,487,596	$214,634
2.1	Alternator	$220,458,592	$157,470
2.2	Controller	$79,565,495	$56,832
2.2.1	Power Sense Box	$9,065,592	$6,475
2.2.2	Main Control Box	$25,130,524	$17,950
2.2.3	Control Panel	$607,841	$434
2.2.4	Signal Sensors	$33,941,328	$24,244
2.2.5	External Interface Cables	$10,820,210	$7,729
2.3	Alternator/Controller Testing	$463,511	$331
3.0	Shipping	$1,067,968	$763
4.0	Program Management & Support	$1,163,506	$831

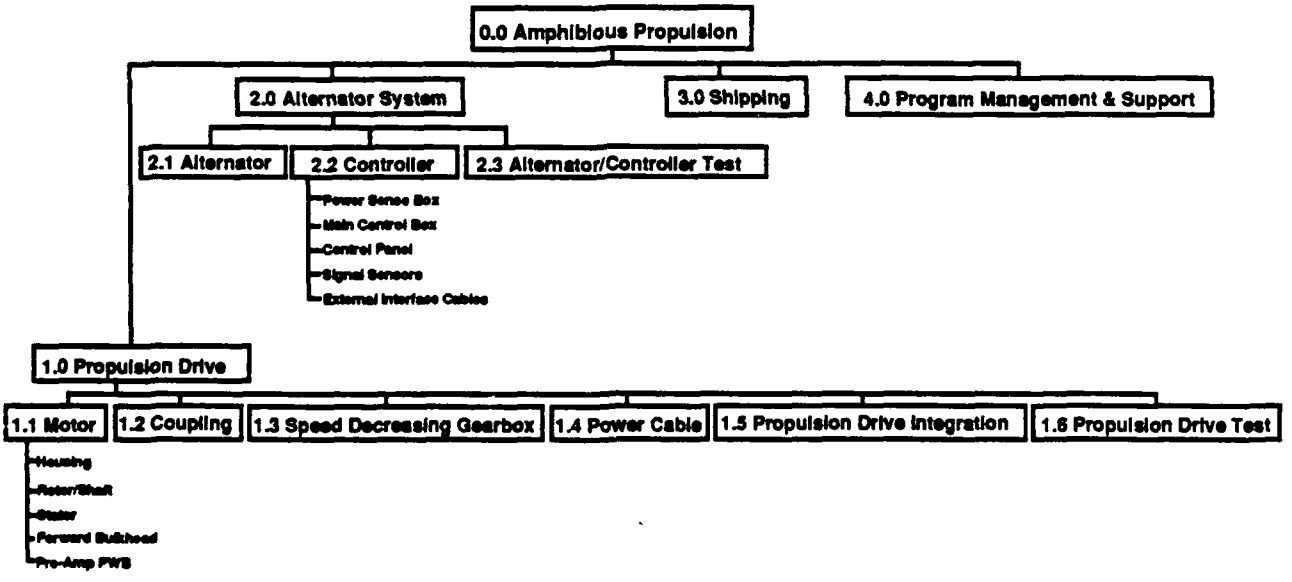

Production Cost Estimate Work Breakdown Structure

Amphibious Vehicle Propulsion System Design Report

For a Propulsion System
Demonstrator (PSD) Vehicle

July 8 , 1988

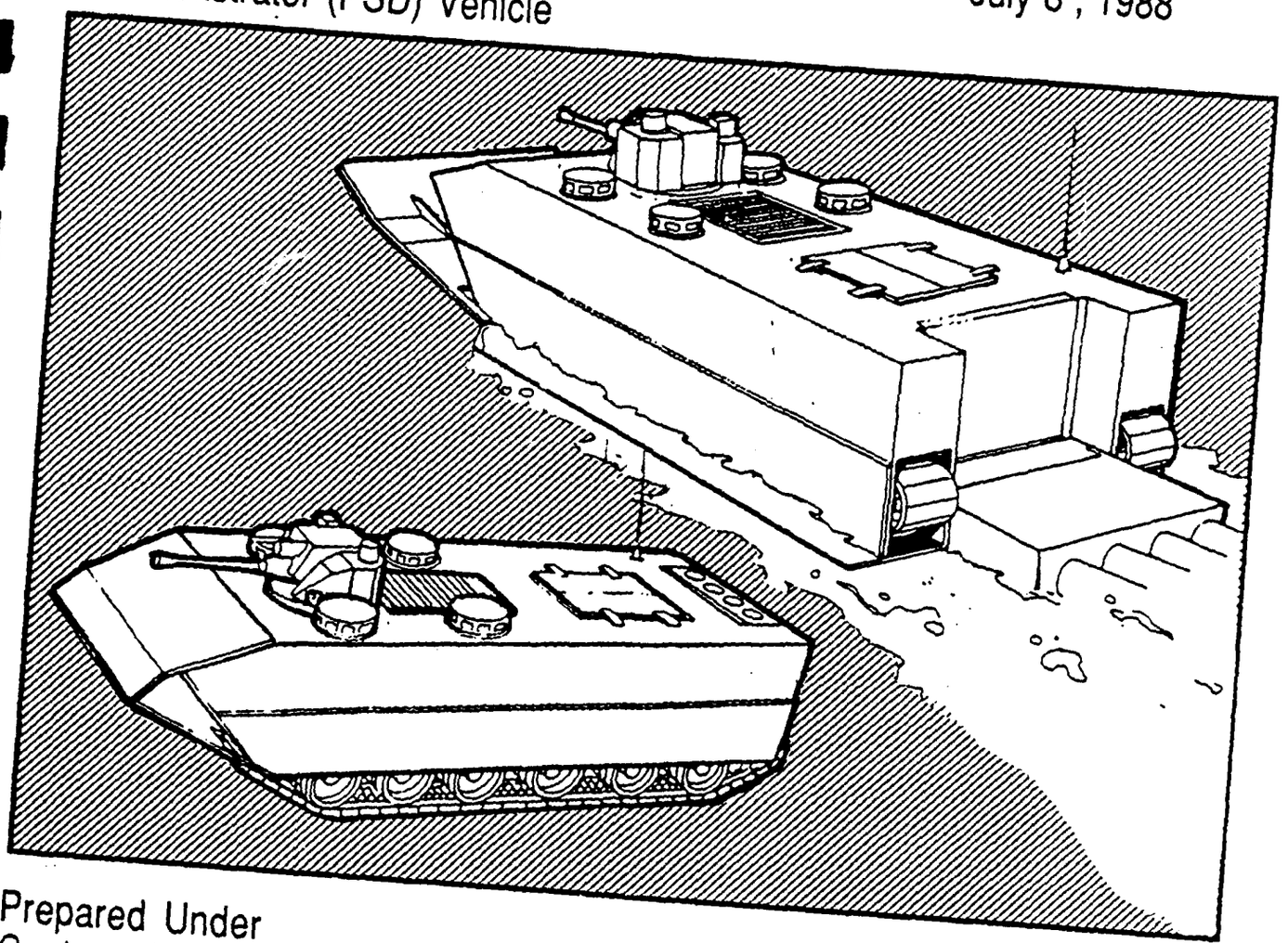

Prepared Under
Contract No. N00167-86-C-0158
for
David Taylor Research Center
Bethesda, Maryland

05/204/88/081-g

Westinghouse

Westinghoue Inc.
Oceanic Division - Cleveland Operation
18901 Euclid Avenue
Cleveland, Ohio 44117

CDRL A001

Amphibious Vehicle Propulsion System Design Report

July 8 1988

Prepared under
Contract No. N00167-86-C-0158
for David Taylor Research Center
Bethesda, Maryland

Westinghouse Inc.
Oceanic Division- Cleveland Operation
18901 Euclid Avenue
Cleveland Ohio 44117

John Witkowski, Technical Director

James Triner, Program Director

05/204/88/082-g

ABSTRACT

The Marine Corps Program Office at the David Taylor Research Center has funded the development of an electric drive train for a waterjet propulsion system to demonstrate high water speed in a Marine Corps propulsion system demonstrator (PSD) vehicle. In the water, this vehicle will be propelled by four waterjets, each rated at 400 hp, to provide the required thrust. The task was to design and develop a system that would be compact, lightweight, efficient and available to support vehicle demonstration testing in June of 1989.

Due to schedule and cost constraints a decision was made to design the propulsion motor around an existing alternator. A system trade-off study was embarked upon in October of 1986, to identify a system configuration. The study resulted in selection of an approach which uses four identical electric water propulsion modules, consisting of: an AC alternator and alternator controller, an AC induction motor with integral speed decreasing gearbox and a coupling that connects the motor/gearbox to the waterjet.

The alternator selected is a Westinghouse air cooled machine with the following output characteristics at nominal operating conditions:

322 kW nominal continuous power rating
520 volts line-to-line rms, 3-phase
450 Hz

Westinghouse has designed an AC induction motor to be compatible with the alternator and waterjet requirements. The motor has the following characteristics:

Water cooled exterior
Oil cooled/lubricated interior
7:1 single stage, speed decreasing gearbox (SDG)
Size: 16 inches O.D. X 24 inches long
Weight: 329 lb.
Efficiency (motor/SDG): 92%

DESIGN REPORT
FOR
ELECTRIC WATER PROPULSION SYSTEM
FOR A HIGH SPEED TRACKED AMPHIBIOUS VEHICLE

TABLE OF CONTENTS

TABLE OF CONTENTS (cont'd)

LIST OF FIGURES

LIST OF FIGURES (cont'd)

LIST OF FIGURES (cont'd)

LIST OF FIGURES (cont'd)

LIST OF TABLES

APPENDICES

1. Introduction

This report discusses the design of an Electric Water Propulsion System (EWPS) used to drive the primary waterjets of the Propulsion System Demonstrator (PSD) vehicle. The EWPS was designed to meet stringent size, weight and efficiency requirements that would demonstrate improved performance over an existing hydraulically operated propulsion system.

The EWPS is comprised of four parallel drives known as Electric Water Propulsion Modules (EWPM). Each EWPM has a continuous rated shaft horsepower of 400, for a total shaft horsepower rating of 1600 for the system. A dual primary power source is used to drive four alternators. A rotary engine/ gearbox is used to drive one alternator and a turbine will be used to drive the other three alternators from a splitter gearbox.

The EWPM consists of three main components; the first is an AC alternator which converts the mechanical energy available from the primary power sources to electrical energy; the second component is a Motor/Speed Decreasing Gearbox (M/SDG) which converts the electrical energy back to mechanical energy to drive a waterjet; and the last major component is the Propulsion System Controller (PSC) which regulates the power flow between the alternator and the M/SDG in response to the speed of the prime movers. A flexible coupling connects the M/SDG output shaft to the waterjet driveshaft.

A pictorial of the PSD vehicle electric high water speed powertrain is shown in Figure 1. Note that the waterjets which propel the vehicle have been shown simply as propellers in the figure.

1.1 Technical Requirements

The technical requirements for the EWPS were specified by DTRC. These requirements were derived from the goal of accelerating a 55,570 pound (28T) amphibious vehicle to a final speed greater than 20 knots. The key requirements are listed in Table 1.

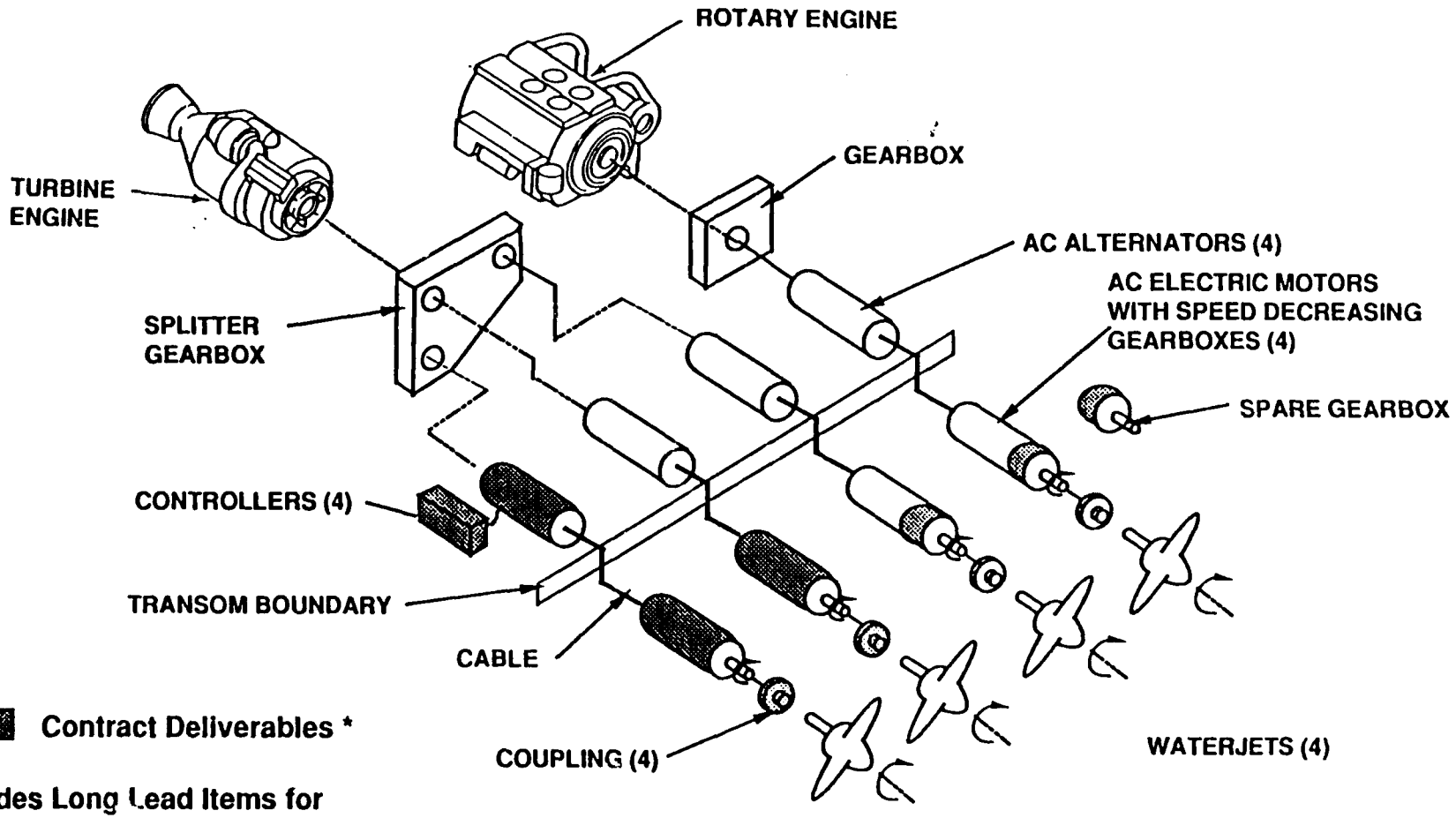

Figure 1. Electric Water Propulsion System

Table 1. EWPS Technical Requirements	
Weight	3200 lb.
Shaft Power (continuous)	1600 hp
Shaft Power (60s rating)	2080 hp
Shaft Speed Range, Operational	615-1,250 RPM
Power Source 1 Gearbox operational output speed range	Rotary Engine/Gearbox 4,306-9,000 rpm (±100 RPM)
Power Source 2 Gearbox operational output speed range	Turbine/Splitter Gearbox 4,306-9,000 rpm (±100 RPM)

As discussed Westinghouse's design features four identical parallel EWPM's. Each EWPM is one-fourth of the ratings in Table 1. The ratings for an individual EWPM are shown in Table 2.

Table 2. Individual EWPM Technical Requirements	
Weight	800 lb.
Shaft Power (continuous)	400 hp
Shaft Power (60 second rating)	520 hp
Shaft Speed Range, Operational	615-1,250 RPM

A detailed description of all system requirements is contained in Appendix I, Interface Specification.

1.2 System Study

After Westinghouse was contracted to design and fabricate the induction motors, DTRC requested Westinghouse assistance in determining an appropriate EWPS configuration for the PSD vehicle. A study was performed to identify an EWPS configuration that would preferably use an existing alternator design. Three system concepts, outlined in Figure 2, were examined. In addition to technical trade-offs, program issues including hardware availability, schedule, and cost were considered for each concept.

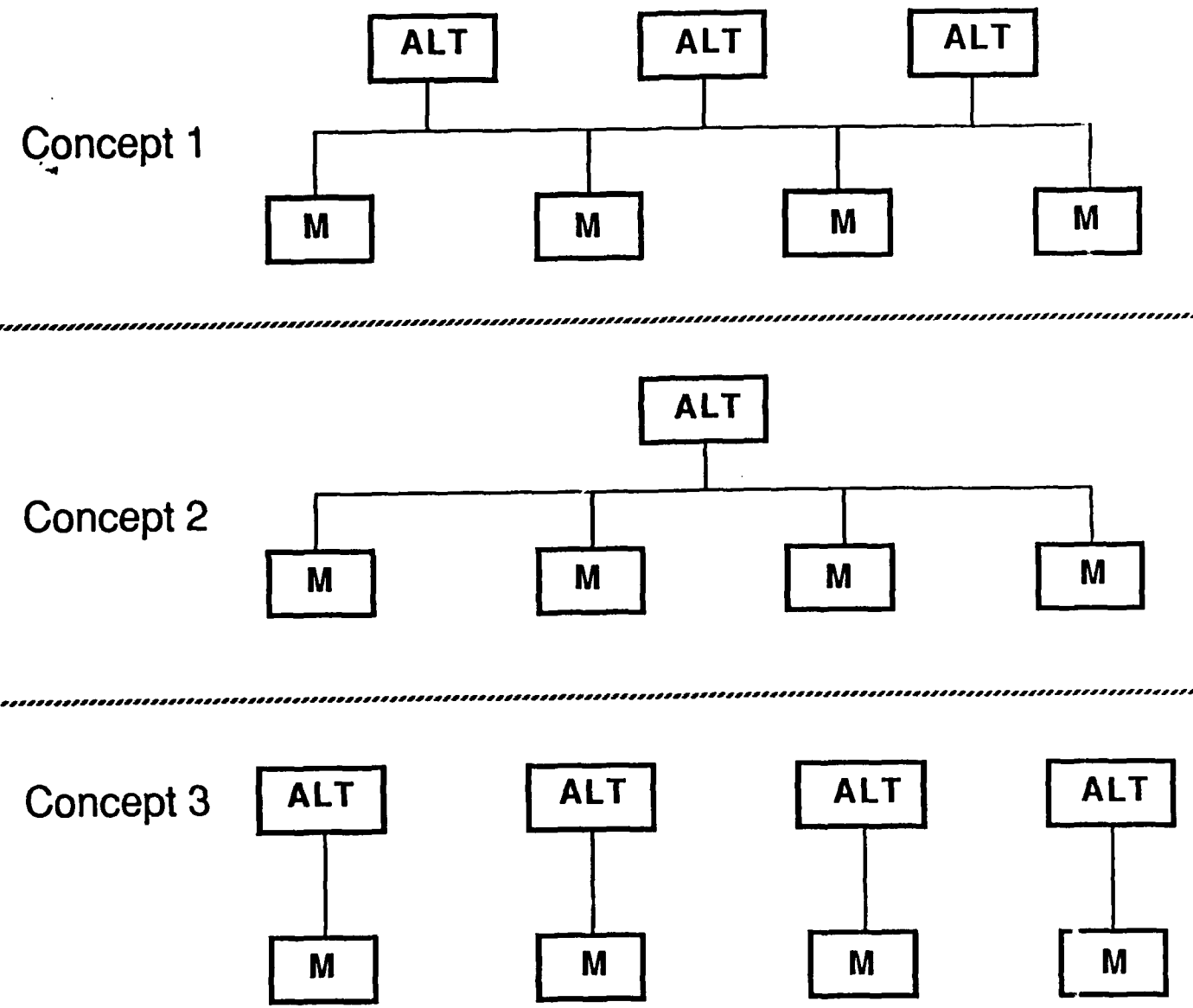

Figure 2. Electric Water Propulsion System Configurations.

Design Concept 1 uses multiple alternators, and motors on a common bus. This was an extension of the electric propulsion design concept for the High Water Speed Technology Demonstrator (HWSTD) vehicle. The advantage of using this approach is having multiple electrical power sources. Should one alternator go offline for any reason, the vehicle could still operate at reduced power.

However, there are several disadvantages to this concept: 1) There is a severe switchgear penalty (size and weight) imposed on the system; 2) The motors are operating from a common bus, therefore, each alternator must have the same phase sequence and exact voltage (magnitude and phase) for parallel operation and load sharing. Any difference of voltage between the alternators will cause large circulating currents to flow and overheat the alternators; 3) The alternators must be mechanically indexed so that the poles are oriented exactly; and 4) Each alternator must have a power rating of approximately 430kW for which an existing design of that rating could not be identified.

Design Concept 2 uses a single Government Furnished Equipment (GFE) alternator rated at 1.193 MW (1600 hp). The alternator would supply power directly, or through switchgear, to four parallel M/SDG units, each rated at 298.3 kW (400 hp). The alternator powering the M/SDG units directly, as shown in Figure 2, has the advantage of simplicity; however, in the event of a M/SDG failure, the entire system could fail. A variation to this approach is shown in Figure 3. This system is similar to the one shown in Figure 2, with the exception that switchgear has been added between the alternator and each M/SDG. The weight and volume of the switchgear and high current requirements for the alternator and cabling are major disadvantages with this design approach.

Since the weight and volume of the switchgear is a function of the system voltage, two classes of switchgear were investigated for the above applications. The impact of including motor starters was also examined. The typical weights and volumes are shown in Table 3.

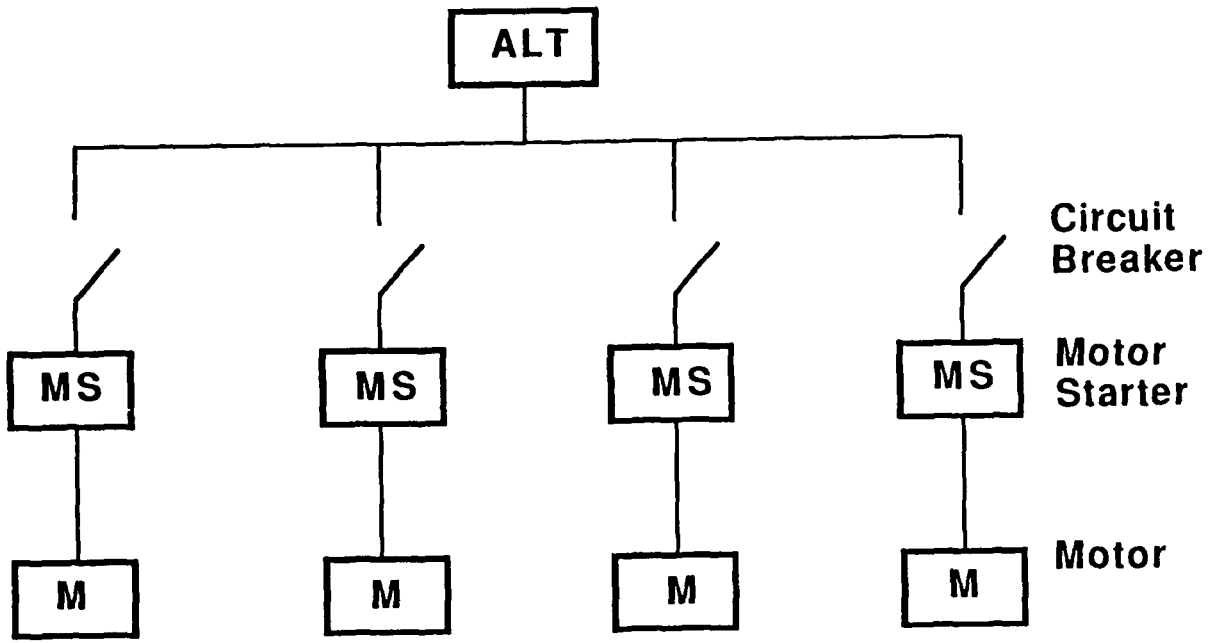

Figure 3. Typical Electric Water Propulsion System with Switchgear

Table 3. Physical Characteristics, Off-The-Shelf Switchgear

Item	Low Voltage 600 V	High Voltage 5 kV
Circuit Breakers		
Weight	75 lb.	2850 lb.
Volume	0.42 ft^3	188 ft^3
Motor Starters		
Weight	3160 lb.	4800 lb.
Volume	120 ft^3	135 ft^3

The significant weights and volumes of off-the-shelf switchgear were determined to be unacceptable. The development of custom switchgear was beyond the schedule constraints of this contract.

Design Concept 3 depicts four identical, independent, drives. Each drive has an alternator which powers an AC induction motor. The vehicle prime movers provide variable speed input power to the four alternators. Each alternator has a voltage controller which maintains the appropriate field excitation to the alternator to produce a required volts/hertz output to the motor. The voltage and frequency of the alternator varies proportionally with the prime mover speed which results in varying the speed of the motor accordingly. The controllers provide the ability to start and stop each motor independently, thereby eliminating the need for switchgear. The disadvantages of this approach are: 1) four power takeoffs must be provided to drive the alternators; 2) the available alternator is air cooled and requires intake/discharge ducting which adds vehicle complexity; and 3) the available alternator exceeds noise goals.

The system study concluded that design Concepts 1 and 2, and their described variations, were rejected for the following disadvantages:

1. Switchgear weight and volume penalties
2. Alternator unavailability; an alternator having desired ratings and an acceptable delivery schedule could not be identified
3. Lower mission reliability than could be achieved with four independent drives

The study concluded that Concept 3 should be pursued as a result of the following advantages:

1. Lowest overall system weight and volume
2. Alternator availability; an existing design of a Westinghouse 322 kW, air cooled alternator would provide the required output power and could be procured in time to support program schedules
3. Mission reliability is improved; the vehicle can operate at reduced power if a drive component failure does occur.

2. EWPS Description

The design approach resulted from the system study described above. The goal of maximizing overall system efficiency while staying within the propulsion system weight budget influenced the design of the hardware. The design intent was to minimize both technical and developmental risks. The three major EWPS components are 1) Alternator; 2) Motor/SDG; and 3) Propulsion System Controller. A brief description follows. A more detailed discussion of each of the above components is described later in this report.

The power source is a three phase, brushless alternator. The specification weight requirements dictated a high power density design. This led to the selection of a military type (400 Hz) alternator. The alternator was modified to maximize the induction motor starting and steady state performance. The alternator full load speed was increased to 9000 rpm and the exciter field pole and armature material was changed to a Cobalt-Iron alloy to enhance starting performance. The performance compatibility of the air cooled alternator and the availability guided the selection process.

Each EWPM consists of an AC induction motor, a speed decreasing gear box, and a shaft coupling to connect to the waterjet. In order to fit within the envelope of the transom, an integrated motor/SDG assembly was designed. A single stage speed decreaser was selected minimizing the axial length of the SDG. The coupling connecting the motor/SDG to the waterjet is designed to take angular and parallel misalignment. The waterjet thrust is not absorbed by the EWPM.

The propulsion system controller (PSC) provides start/run/off control for the vehicle and provides the required power conditioning and excitation to the alternator during starting and full power operation. The PSC provides the interface to the vehicle controller via an RS-232 serial link. The microprocessor monitors the motor and alternator warning and fault conditions. The PSC has software programmable setpoints for motor start limits, motor run limits, and motor voltage limits.

The weight of each of the major components was a key consideration in the design process. The selected alternator satisfies the weight goal. The integrated motor/SDG assembly is oil cooled to minimize both its size and weight. The motor also uses high magnetic permeability steel for its stator and rotor cores to minimize its weight.

2.1 Operational Requirements

The operational requirements of the vehicle establish the operational requirements of the EWPS. The detailed Interface Specification is included in Appendix I. The shaft horsepower (HP_{shaft}) requirements are illustrated in Figure 4 as a function of shaft speed. The actual shaft speed based on the design of record speed decreasing gear is discussed in Section 2.3.1. The shaft horsepower varies as a cube function of shaft speed and is approximated by the following equation, where $k = 2.048 \times 10^{-7}$:

$$HP_{shaft} = k \times RPM^3$$

The overload capability of the propulsion system is defined as 1.3 times HP_{shaft}, at 1,250 RPM for 60 seconds maximum. The propulsion system overload condition is to be demonstrated once during acceptance testing. Currently, there are no operating requirements for the overload condition after the initial demonstration.

Efficient delivery of the required shaft horsepower is an important goal of the EWPS. The system efficiency goal is 80%. The efficiency goal allocated to each of the components is shown in Table 4.

Table 4 Propulsion System Efficiency

Component	Efficiency Goal, %
Alternator	88
Alternator-M/SDG Cable	99
M/SDG Motor 96 Speed Reducing Gear 96	92
System Efficiency	80

Note: Efficiencies are only expressed at the full load operating point of 400 HP_{shaft} at 1,250 rpm.

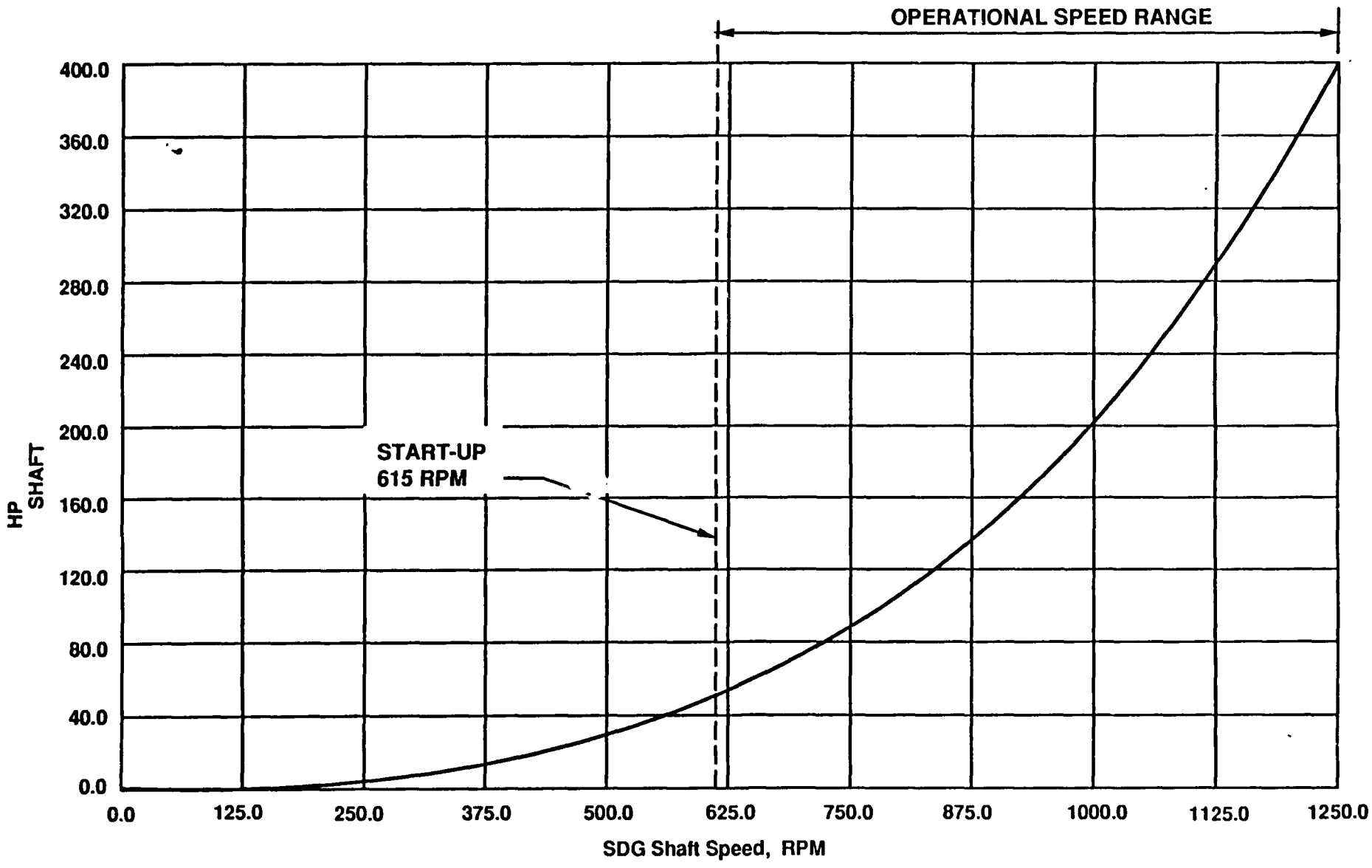

Figure 4. Motor/SDG Power/Speed Requirements

2.2 Alternator

Program constraints dictated the selection of an existing alternator. An industry wide survey of military style alternators was conducted and is summarized in Appendix II. This study resulted in the selection of the Westinghouse alternator, shown in Figure 5. This machine was designed to deliver 250 kW at 8,000 RPM. The original application of this machine required a conservative design. Consequently, the alternator is capable of producing the required rating of 322 kW by increasing the RPM to 9,000. A summary of the machine rating is contained in Table 5.

Table 5. Alternator Summary

Design Type	Separately-Excited Rotating Rectifier
Continuous Rating	322 kW (432 hp)
Transient Rating (1 minute)	418 kW (561 hp)
Phases	3
Voltage	520 Vac Line to Line
Frequency	450 Hz
Number of Poles	6
Efficiency	0.88 Minimum
Min. Starting Current @215.3 Hz (4306 rpm)	900 amps for 3 sec.
Weight	373 lb
Cooling Method	Air cooled (Integral Fan)
Cooling Flow	1,100 CFM at 9,000 RPM
Shaft Speed @ 322 KW	9,000 RPM
Shock/Vibration	10 G (all axes)
Dimensions	See Interface Control Dwg., Alternator (E77497)

The alternator subsystem consists of a main alternator, an exciter, permanent magnetic generator (PMG) and a power system controller (PSC).

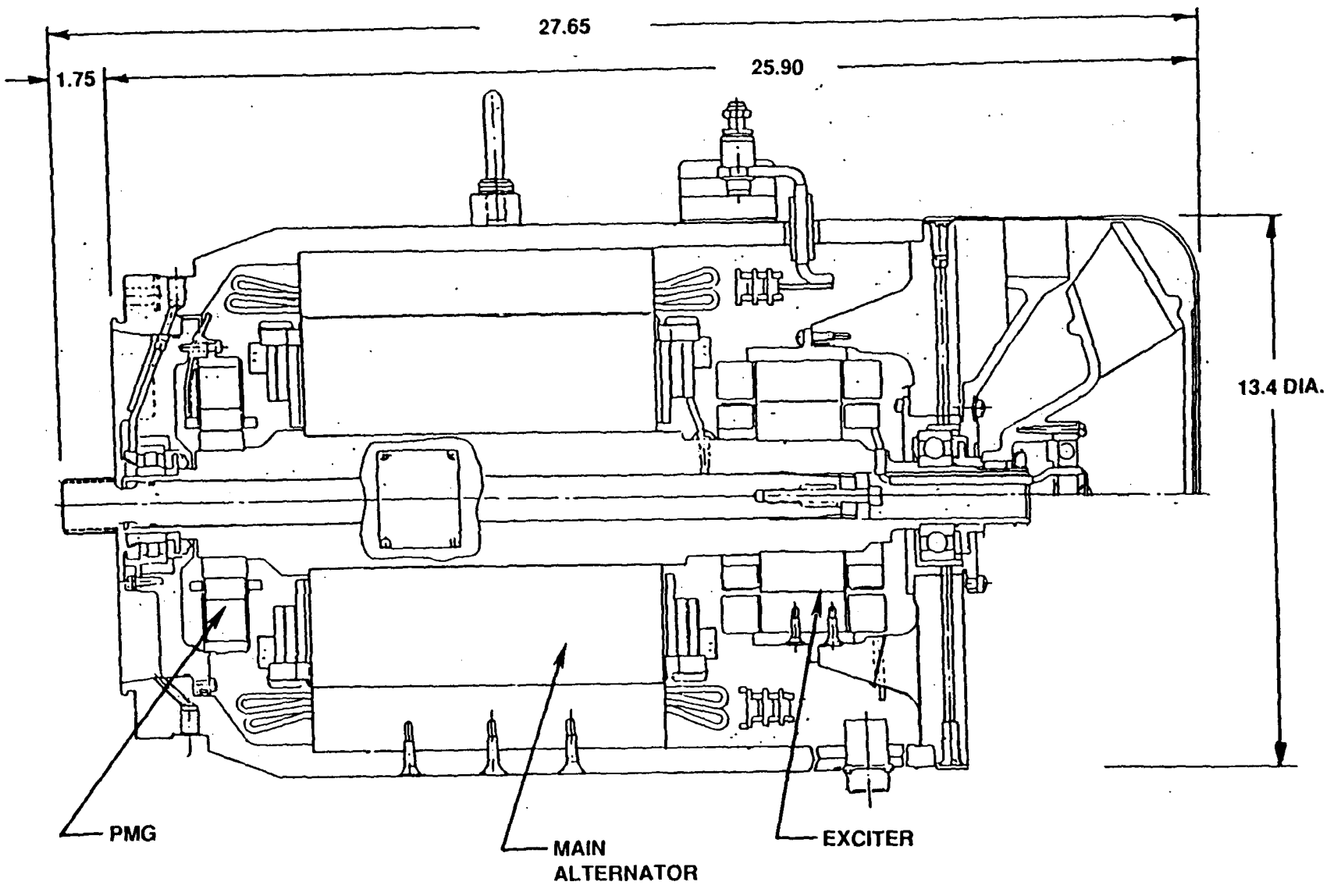

05/204/88/022

Figure 5. Alternator, Westinghouse Model 977J031-6

The alternator has demonstrated an overspeed condition of 10,500 RPM. Based upon the design margin continuous operation at 9000 rpm is reasonable. The conservative thermal design of the machine permits operation at continuous power levels exceeding the original design specification.

One minor design modification was performed on the alternator. The M-15 magnetic steel originally used to construct the exciter, was upgraded to Permendur V to enhance exciter performance. This change will enable the main machine to deliver starting currents in excess of 900 A_{rms}. The Westinghouse part number for this modified alternator is Model 977J031-6. A detailed description of the alternator is contained in Appendix III.

The turbine and rotary engines, through the appropriate gearboxes, will drive each of four identical alternators. The induction motor has been designed to operate with the three phase alternator voltage and frequency values shown in Table 5.

The turbine and rotary engine will be brought up to an idle speed of approximately 4300 RPM with no exciter field excitation applied. (The alternators are producing no electrical power.)

The PMG provides a voltage reference to the exciter field regulator. The PSC initiates the field excitation (during vehicle starting) providing an induction motor starting current in excess of 900 amperes. Later, the PSC provides the necessary field excitation to maintain constant volts/hertz to the induction motor as the alternator loading reaches steady state conditions. The design of the exciter field regulator and PSC is described in Section 2.5 of this report. The Power Sensing Box, which will mount on top of the alternator power terminal block, is described in Section 2.5.12 of this report.

In order to cool the alternator 1100 cfm of air is required at 9000 RPM. It is brought in at the anti-drive end through an expanded metal screen by a unidirectional fan. The air flows axially through the alternator and is exhausted at the drive end.

The schematic diagram of the alternator is shown in Figure 6. The electrical power flow through the alternator is as follows:

The single phase ac output of the PMG to the exciter field regulator is brought out at connector pins B and C. The output of the voltage regulator is brought into the exciter field through connector pins A and F. The three phases of the alternator are terminals T1, T2, and T3. Terminals T4, T5, and T6 together form the neutral connections.

The installation requirements for the alternator are shown in Figure 7, 322 kW Alternator Installation Requirements and are as follows:

a. Bearing Lubrication
b. Cooling Air
c. Mechanical Interface Data

The bearings require 230 cc/minute (.061 GPM) at .5 to 1.5 psi of MIL-L-7808 oil. The drive end oil outlet line only needs to be evacuated to 1.0 +/-.5 PSIG vacuum to prevent oil from flowing into the drive end bearing cavity. The oil flow through the anti-drive end is by gravity.

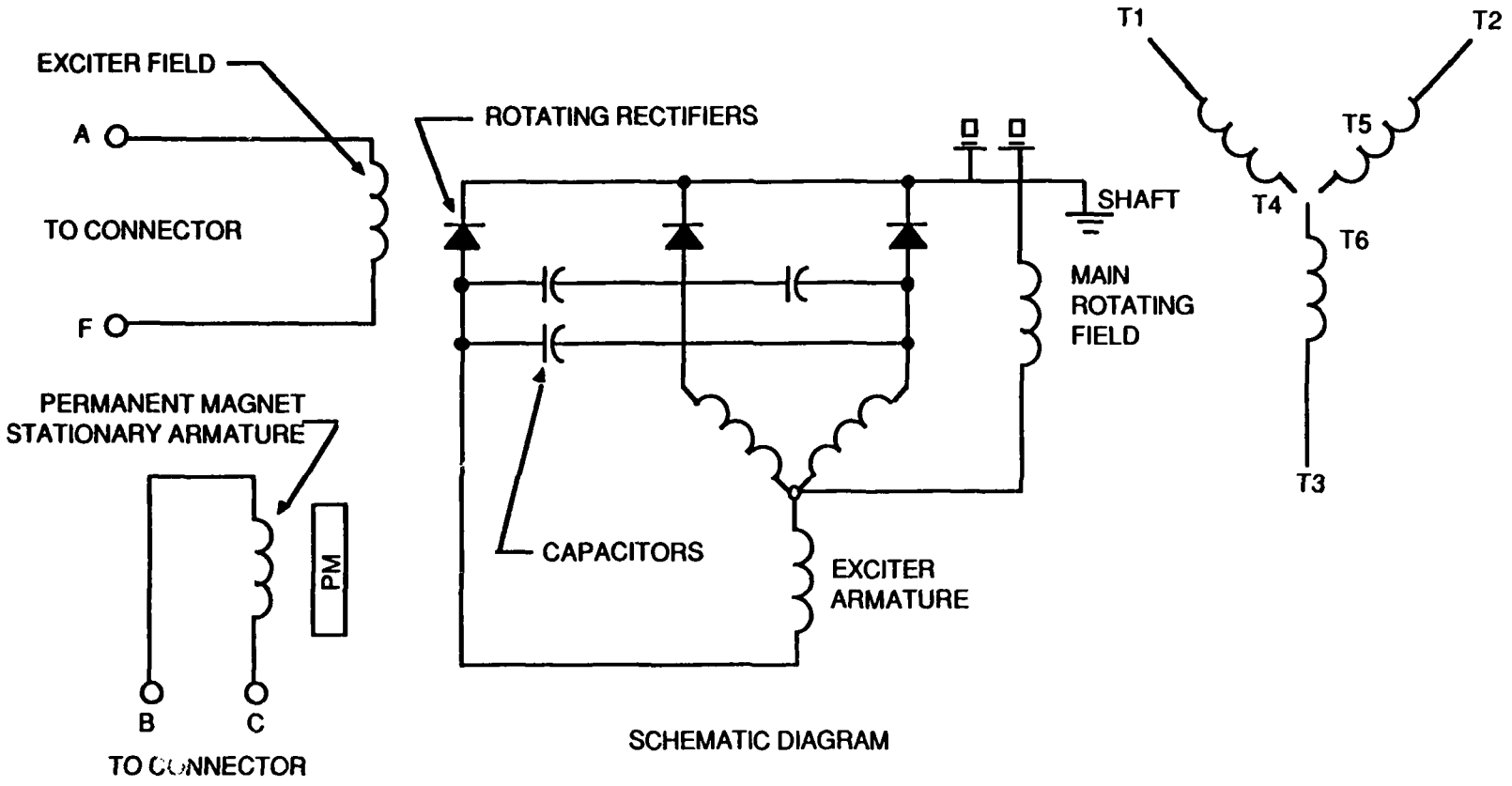

05/204/88/023-K

Figure 6. 322 kW Alternator-Electrical Interface

o BEARING OIL	
TYPE	MIL-L-7808
FLOW RATE @ 1.0 ±.5	.0615 GAL/MIN.
TEMPERATURE (MAX)	212°F
SPECIAL INSTRUCTIONS: DRIVE END OIL OUTLET LINE TO BE EVACUATED TO 1.0 ±.5 PSIG VACUUM MEASURED AT THE BEARING CAVITY OUTLET	
o COOLING AIR SUPPLY	
VOLUME	1100 CFM
SPECIAL AIR SUPPLY INSTRUCTIONS: COMBINED AIR INLET DROP AND EXHAUST BACK PRESSURE MUST NOT EXCEED 6.0" H_2O	
o SPLINE DATA	
NUMBER OF TEETH	24
PITCH	20/30 PITCH
PRESSURE ANGLE	30°
MAJOR DIAMETER	1.262"/1.267"
SPLINE LENGTH	1.250"
o MOUNTING FLANGE	
BOLT CIRCLE	10" DIAMETER

Figure 7. 322 KW Alternator Installation Requirements

The alternator cooling fan draws 1100 CFM at 9000 RPM. The combined air inlet drop and exhaust back pressure must not exceed 6.0" H_2O. A shroud must be provided at the drive end of the alternator frame to create a negative pressure drop in the bearing cavity of at least 3.0 inches H_2O below the exhaust back pressure measured at air outlet.

The alternator will mate to the appropriate gear box via the 10" bolt circle and spline on the drive shaft end. The alternator interface information is described on Westinghouse ICD, Dwg. No. E77497.

2.3 Motor/Speed Decreasing Gear/Coupling Design Overview

The motor/SDG is an integral design to minimize weight and volume. The design is totally enclosed with a self contained oil system for lubrication and cooling. Heat from the oil is transferred through an integral heat exchanger to water which flows over the exterior of the motor. The coupling provides for angular and parallel misalignment between the motor and pump jet. All surfaces which are exposed to seawater are corrosion resistant. All parts fabricated from aluminum are electroless nickel plated. All other parts are either corrosion resistant stainless steel or bronze. The overall dimensions of the motor/SDG and coupling are given in Figure 8 and additional detail is found on the ICD drawing number J77496. The weights of the various components are given in Figure 9.

The coupling is illustrated in Figure 10. A double flex gear type has been selected to provide for parallel and angular misalignment and to minimize size and weight. The coupling is constructed of stainless steel and sealed to retain the lubricant.

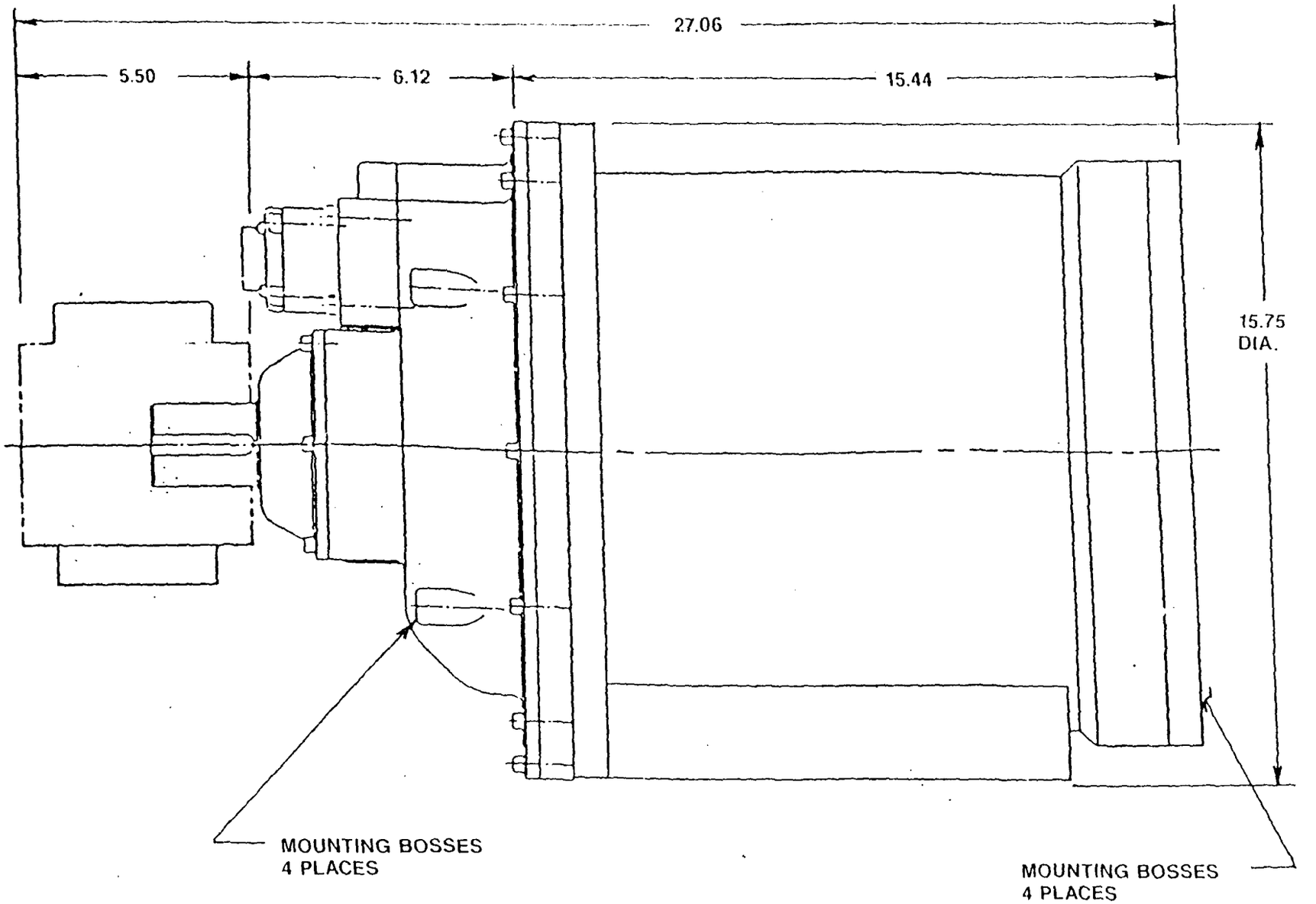

Figure 8. Waterjet Propulsion System - Transom Mounting Dimensions

Item	Weight, LBM
Motor Assembly	224
Gearbox	67
Coupling	33
Oil	5
Total	**329**

Figure 9. Weights Summary

Sier Bath
Size C-3

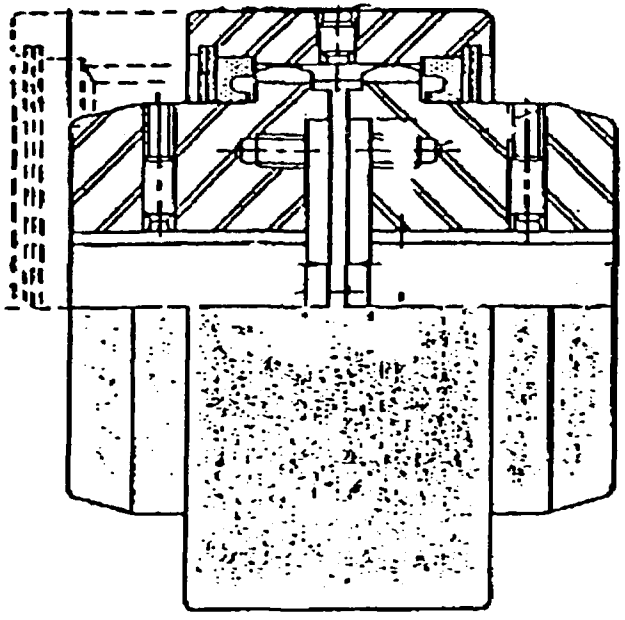

Weight	33 lbm
Size (inches)	6.625 dia. x 6.875 lg.
Misalignment	
Parallel	.010 in.
Angular	.2°
Torque	5180 ft-lbf Max
Material	316 SS

Figure 10 Coupling

2.3.1 Motor/Speed Decreasing Gear Constraints

The design of the motor was driven by the power and speed requirements of the waterjet and the need to be compatible with an existing 400 Hz alternator. An initial electromagnetic design sensitivity study indicated maximum frequency with the above constraints to be 600 Hz. In order to keep the size of the SDG at a minimum, a single stage reducer was desired. A single stage planetary gear reducer has a gear ratio upper limit of approximately 10:1. With a waterjet speed of 1250 RPM and a gear ratio of 10:1, the maximum motor speed is 12,500 RPM. During the design iterations a motor frequency of 500 hertz was selected to minimize the stator core losses and mechanical stresses in the rotor. The laminated rotor core and fabricated copper bar and end ring structure set an upper bound relative to the maximum operating speed that could be obtained. The maximum number of poles was determined to be six resulting in a motor speed of 10,000 RPM while still staying within the SDG constraints. Any lower number of poles (4 or 2) at 500 Hz results in increased weight of the motor and/or exceeds the available envelope.

Discussions with the alternator vendor established the upper speed limit for continuous operation at 9,000 RPM. Therefore the resulting design of record frequency is 450 hertz, which provides a motor synchronous speed of 9,000 RPM.

The full load operating point of 3,000 RPM prime mover/9,000 RPM alternator speeds and 1,250 RPM waterjet speed results in a 7.2:1 motor/SDG speed reduction ratio. The ideal ratio of 7.2:1 was used to perform initial design calculations. Based upon calculated motor slip (8,919 motor RPM), and a practical, achievable SDG ratio of 7:1, the resulting waterjet speed is 1,274 RPM. By adjusting prime mover speed the system will operate at the desired 1,250 RPM waterjet speed. The alternator and motor/SDG will provide the required 400 HP at the adjusted speed without incurring additional losses, as the efficiency is constant over minor speed variations around the full load operating point.

2.3.2 Induction Motor

The motor consists of the motor housing and stator assembly, forward bulkhead assembly, and shaft assembly. The motor housing, stator assembly and forward bulkhead assembly are shown in Figure 11.

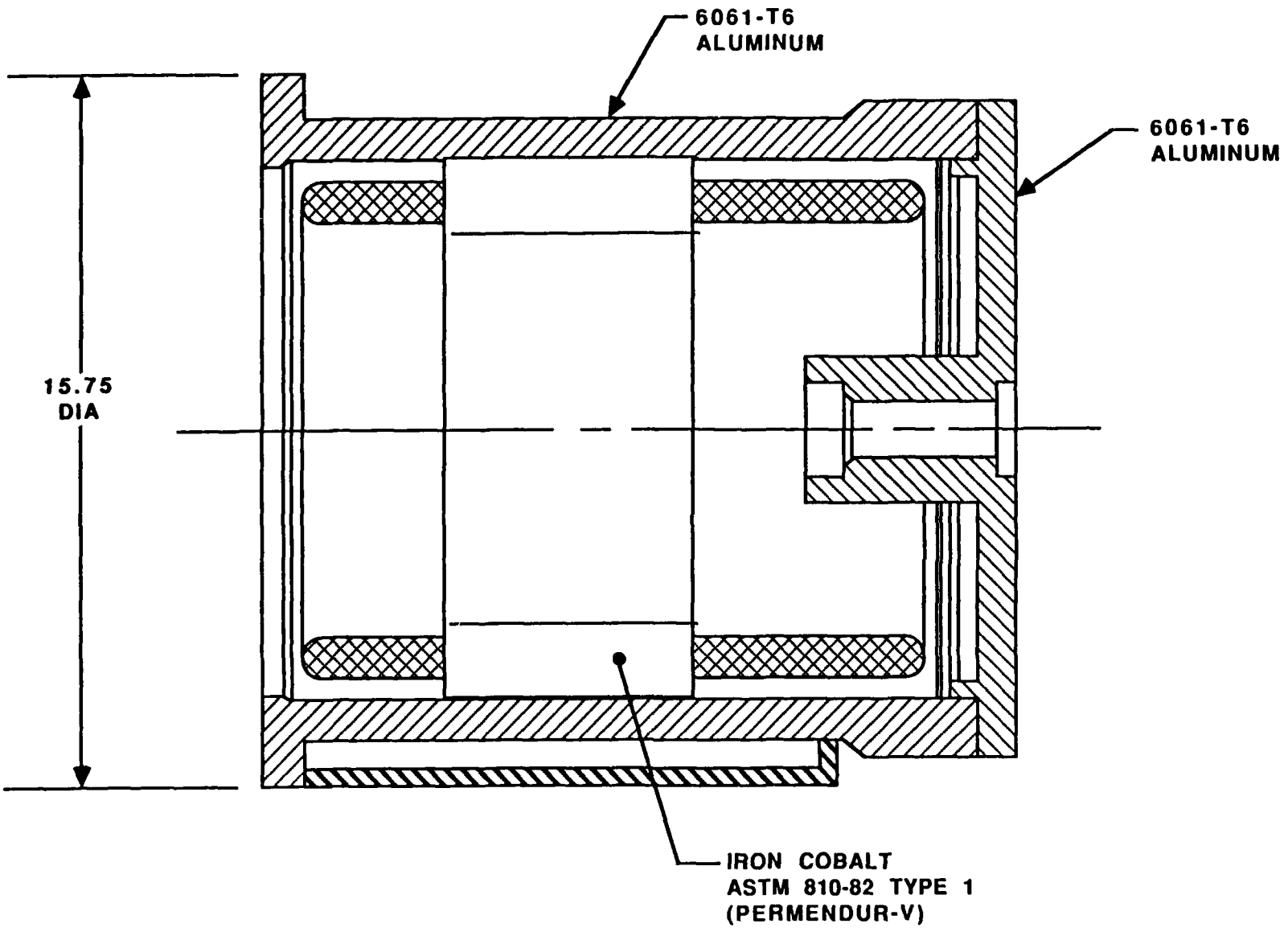

Figure 11. Motor Housing, Stator Assembly and Forward Bulkhead Assembly

2.3.2.1 Construction

The motor housing consists of 6061 aluminum inner and outer shells and sump which are welded together to function as a heat exchanger and oil reservoir. After the oil lubricates/cools the gearbox/motor it gravity drains into the sump. Fins made of 3003 aluminum are brazed into the outer shell to provide adequate heat transfer from the oil to the outer shell. The motor housing mounts the stator, which is shrunk into the bore, and mates up with the SDG and the forward bulkhead.

The stator assembly consists of 50% cobalt iron laminations which are bonded together with epoxy resin. The slots are lined with nomex-kapton-nomex insulation and the stator is wound with rectangular cross section oxygen free copper wire with ml insulation. The top and bottom turns in each slot are insulated from each other with G-30 mid sticks. Windings are retained in the slots with injection molded Torlon top sticks. End turns, jumpers, neutrals and feedthroughs are copper brazed. After brazing the stator assembly is vacuum pressure impregnated with an epoxy varnish.

The forward bulkhead assembly includes the forward bulkhead, the oil spray manifold and nozzles, and the speed pickup housing. The nozzles are made of brass and the bearing insert is made of 17-4PH stainless steel; the remaining parts are made from 6061-T6 aluminum.

The rotor assembly, Figure 12, can be further broken down into the shaft subassembly and the rotor. The shaft subassembly is illustrated in Figure 13. The stub shafts are rough machined, shrunk into the end plates and welded. These units are then shrunk into the drum which has been rough machined and the final welding is completed. The shaft subassembly is then rough turned and ground. At this point the first balancing operation is completed. The material selected for use in the stub shafts is PH13-8MO stainless steel which has the strength necessary to carry the torsional load and can be readily welded to the end plates. The drum and end plates are made of high strength ANSI 4130 alloy steel which combines high strength with availability and low cost.

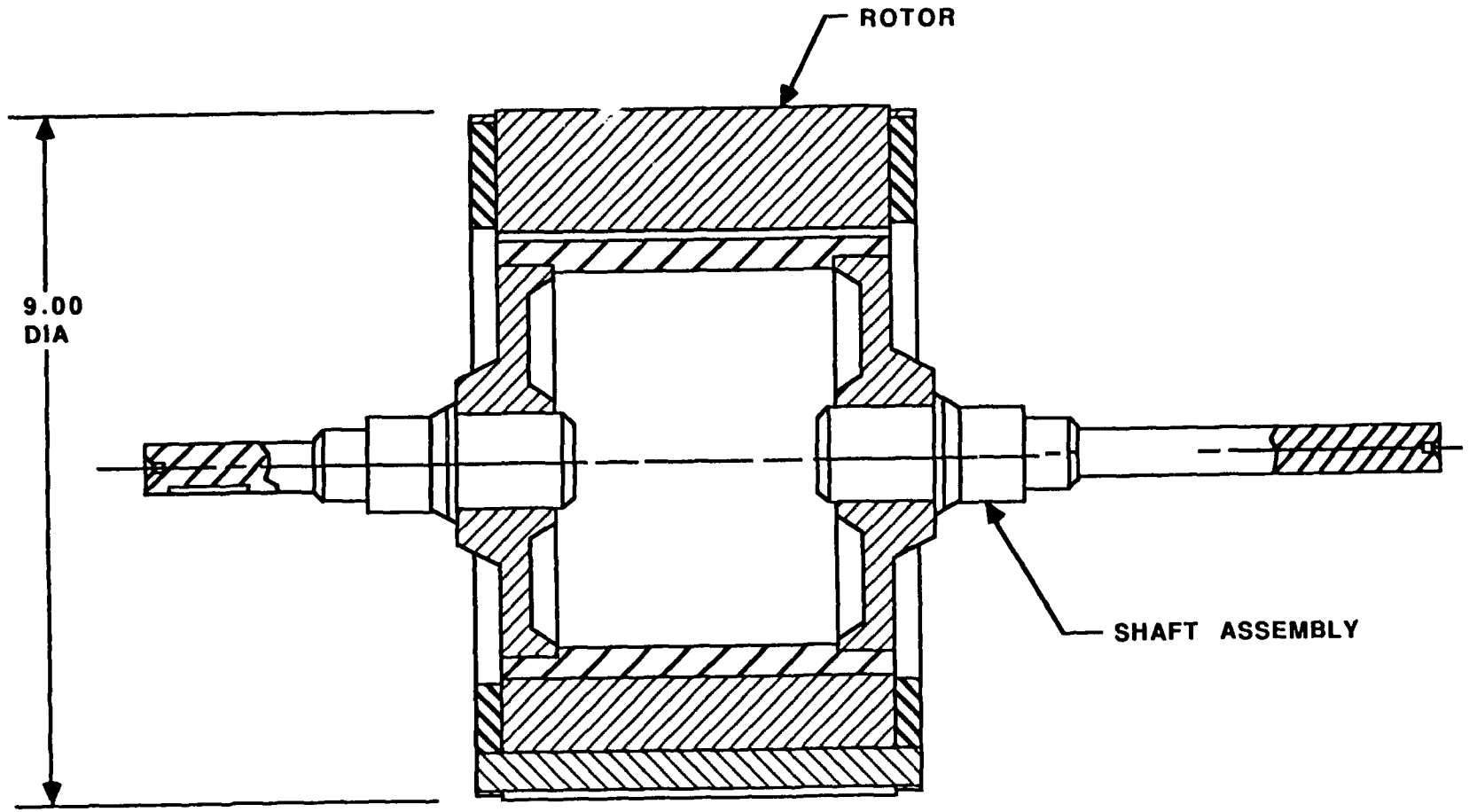

Figure 12. Rotor Assembly

05/204/88/068-F

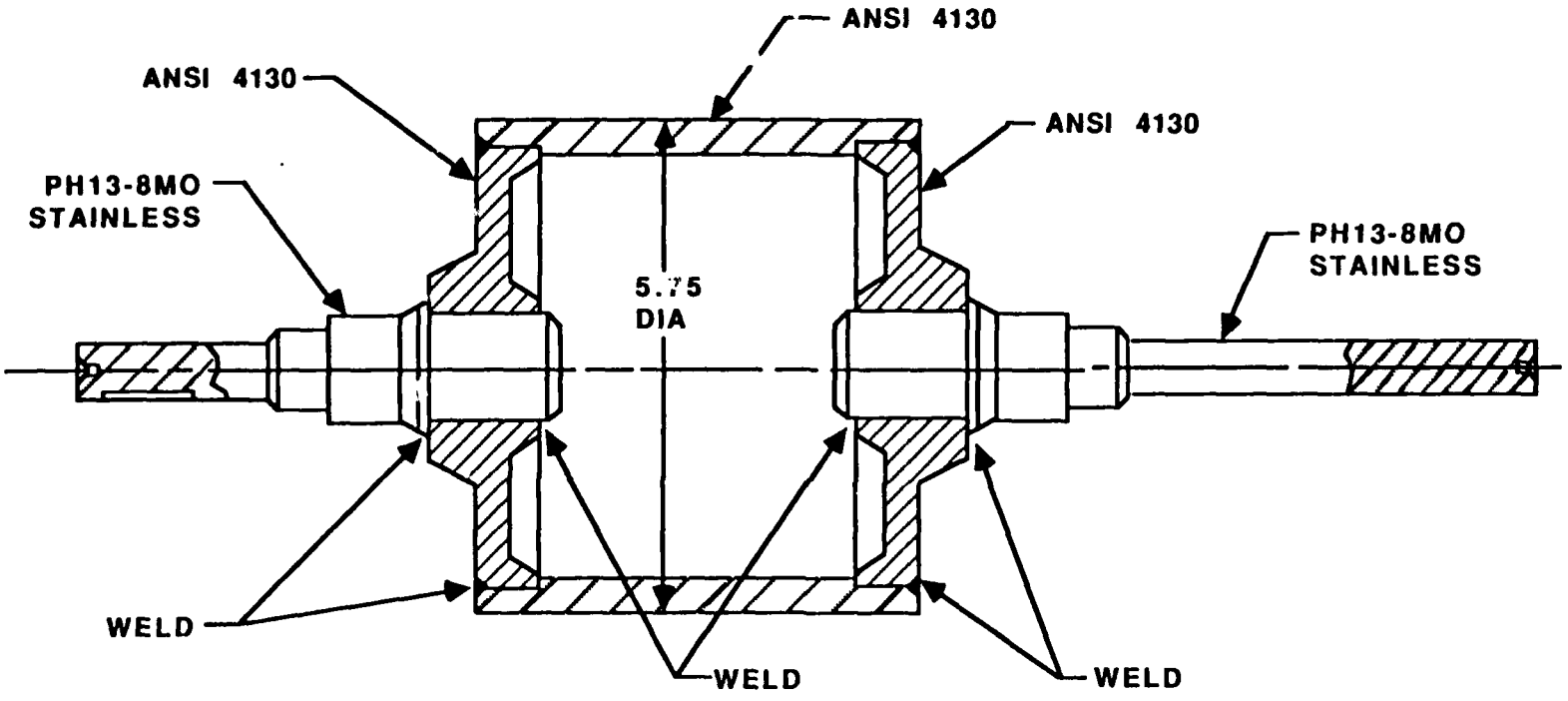

Figure 13. Shaft Subassembly

The rotor is shown in Figure 14. It consists of iron cobalt ASTM 801-82 Type 1 steel laminations, zirconium copper CDA 15000 bars and end rings, and Inconel 625 shrink rings. The laminations are stacked and clamped in an alignment fixture. The inside diameter is then ground and the shaft subassembly shrunk in place. The end plates are then welded to the shaft subassembly and the entire unit removed from the fixture. The rotor bars and end rings are then installed and brazed. The shaft is then finish ground and the end rings are machined for assembly of the shrink rings. Final balancing of the rotor assembly is done at this time. The lamination steel is selected for its magnetic properties and the zirconium copper for its combination of electrical and mechanical properties. The shrink ring provides support for the end rings and bars when they are subjected to centrifugal force.

All parts which are subjected to the salt water environment are either electroless nickel plated or made from stainless steel to protect from corrosion. Insulation materials have been selected to meet the life requirements over the range of operating temperatures and to be compatible with the MIL-L-7808 lubricating and cooling oil.

Many features of this design were incorporated to minimize weight. Among these are the hollow shaft construction, the selection of cobalt iron for the laminations which allows the use of higher flux densities and the selection of high strength aluminum alloys for the housing and bulkhead. A breakdown of the motor weights is given in Figure 15.

The oil system for the motor and SDG is shown in Figure 16. The oil is collected in the sump and after passing through a filter, flows through passages in the motor housing and SDG assembly to the oil pump which is driven by a gear on the planet carrier. A relief valve limits the pump discharge pressure to 200 psi during a cold start when the resistance to flow in the heat exchanger is high. At steady state operating temperature the oil pressure drops to about 50 psi. From the pump the oil flows into the heat exchanger which is built into the motor housing. Here the heat in the oil is transferred into the fins in the outer shell and conducted out to the surrounding water.

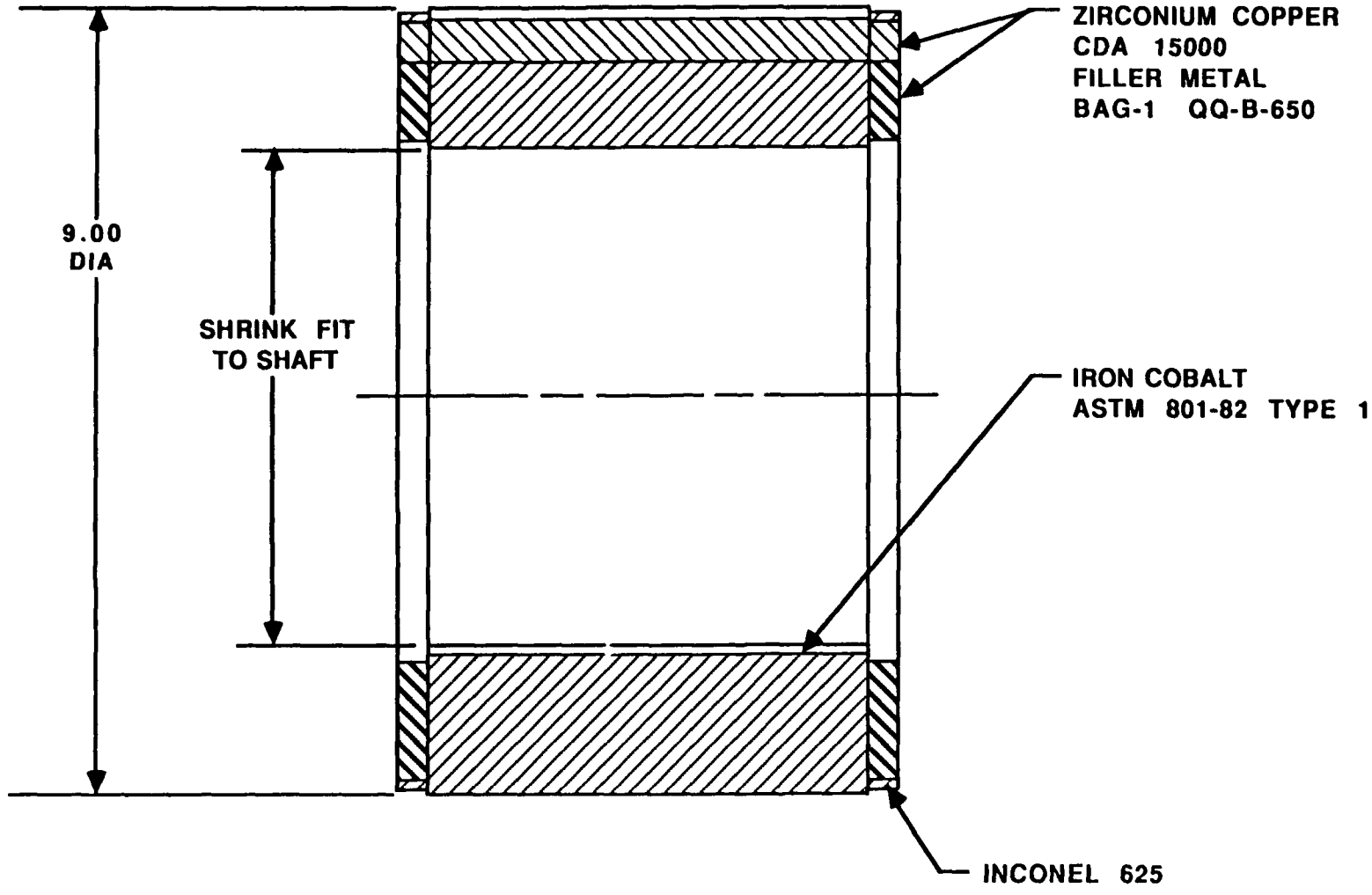

Figure 14. Rotor

Housing Assembly		**76.36**
Housing	(52.4)	
Fwd Bracket	(14.8)	
Misc.	(9.16)	
Stator		**71.53**
Laminations	(47.24)	
Copper	(24.29)	
Rotor		**76.21**
Shaft	(18.39)	
Laminations	(46.10)	
Copper	(11.72)	
TOTAL		**224.15**

Figure 15. Motor Weights (LBM)

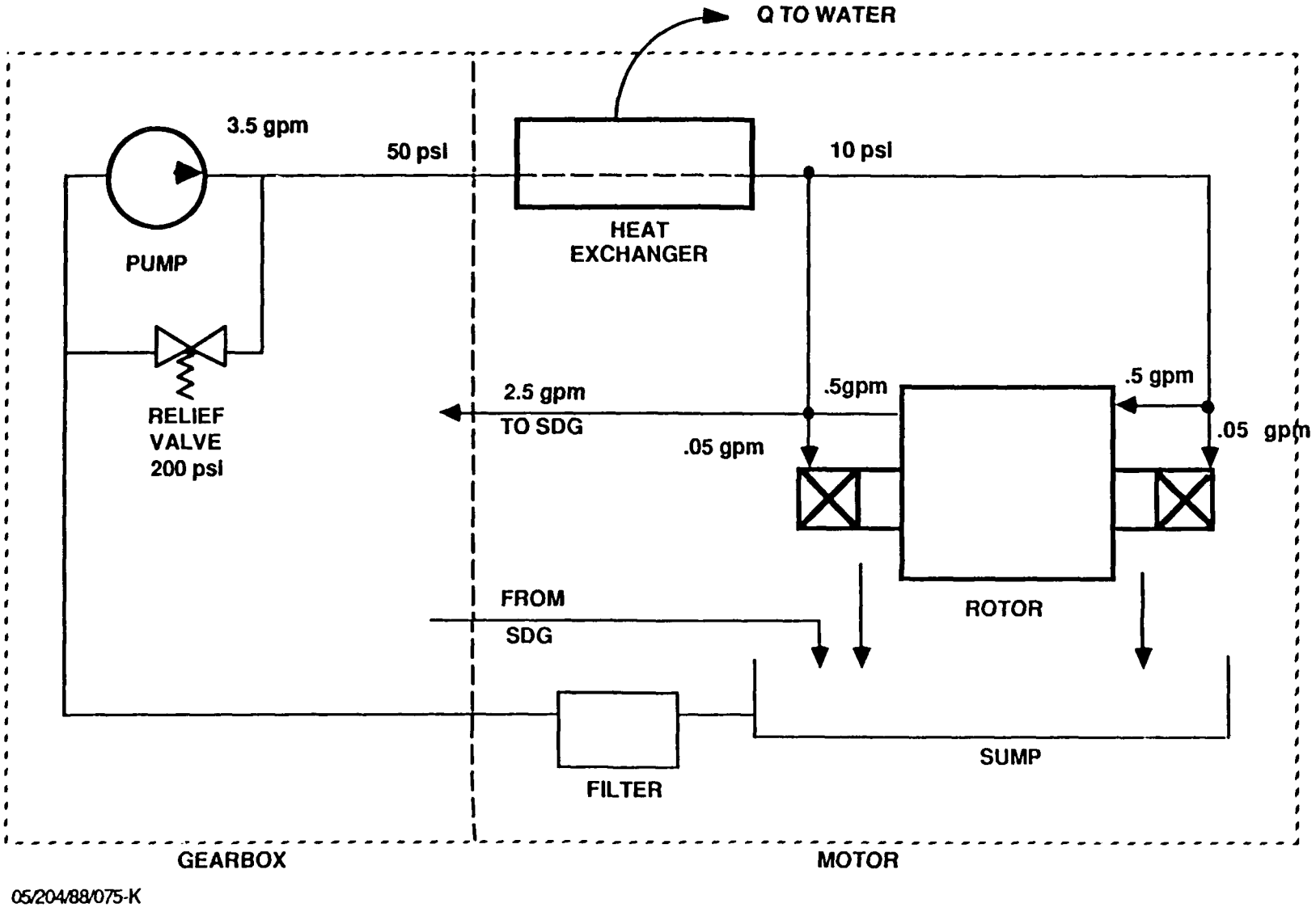

Figure 16. Oil Coolant and Lubrication System.

After leaving the heat exchanger the flow is split between the motor bearings and rotor and the SDG. A pressure transducer monitors the pressure at the discharge of the heat exchanger to ensure that oil flow is maintained.

The motor has been designed so that when the maximum combined vehicle/transom pitch angle of 18.5 degrees is established the oil continues to cover the oil inlet and does not flow into the air gap between the rotor and stator. The drain from the SDG has been designed to deliver the oil directly to the sump so that it is filtered prior to entering the motor.

2.3.2.2 Electrical Performance

The nominal load condition: (400 HP) is dictated by the single operating vehicle point that corresponds to the highest drag/power value that the vehicle may see when it reaches hydroplanning speed. The motor electrical performance was bounded by: steady state operation under nominal load conditions and starting behavior. A design compromise was achieved to meet the required efficiency level and still provide for satisfactory starting performance. Specification requirements call for a combined motor-SDG efficiency of 92% which dictates a high efficiency motor design at nominal conditions. The final motor size, weight and material selections are dominated primarily by the required motor design efficiency. The motor design must provide adequate starting torque with manageable starting phase currents. This was accomplished by utilizing rotor cage "deep bar" effect to enhance motor starting torque. This approach uses the skin effect phenomena present in the rotor bars during starting conditions to achieve increased rotor cage resistance and therefore increased torque during the starting interval. In addition to the above requirements the drive system must be capable of a 30% overload for 60 seconds. Sufficient thermal storage capability exists in the stator and rotor to meet this requirement.

A comparison of the nominal, overload and starting performance parameters is shown in Figure 17. The motor nominal HP is based on the assumption that the SDG efficiency will be 96% and the power delivered to the waterjet is 400 HP. The motor electromagnetic weight consists of those components that carry either electrical current or magnetic flux. The calculated starting time for these conditions is approximately three seconds based upon steady state performance data. More refined data is shown by the systems simulation model (see Section 2.5, Propulsion System Controller).

Parameter	Nominal Condition	Overload Condition	Starting (15°C)
Motor Terminal Voltage	300.22 Vrms (L-N)	300.22 Vrms (L-N)	87 Vrms (L-N)
System Frequency	450 Hz	450 Hz	215.3 Hz
Motor Horsepower Out	416.67	541.67	–
SDG Output Horsepower	400	520	–
Motor Phase Current	391 Amp	531 Amp	940 Amp
Motor Input Power	322 kW	424 kW	42 kW
Motor Speed	8919 rpm	8885 rpm	0 rpm
Motor Input P.F.	.914	.886	.169
Motor Efficiency	.962	.953	–
Motor Torque	245.2 Lb•ft	320 Lb•ft	40.6 Lb•ft
Breakdown Torque	444.8 Lb•ft	444.8 Lb•ft	148.4 Lb•ft
Acceleration Time	–	–	3 sec
Electromagnetic Weight	129 Lb		

Figure 17. Motor Electrical Design Summary

Figure 18 shows how the motor HP and predicted efficiency vary as a function of motor speed. Figure 19 illustrates the predicted motor power factor and phase current as a function of motor speed. These figures show that maximum efficiency is obtained near nominal conditions and that it is relatively insensitive to load up to the overload point.

2.3.2.3 Equivalent Circuit

The per phase equivalent circuit model of the induction motor is shown in Figure 20. The parameters shown are given at nominal conditions (322 kW, 8919 RPM, 450 Hz). The saturation factor used in the determination of the motor's magnetizing inductance is 1.054. The value of the stator winding phase resistance was evaluated at 150°C and includes the effect of stator coil cross slot eddy losses.

2.3.2.4 Electromagnetic Design

The stator and rotor cores are fabricated from .010 inch thick 50% cobalt-iron alloy laminations. This material was selected to minimize stator core losses and provide high permeability for the magnetic flux path. The stator laminations will be bonded together using an epoxy based adhesive. The adhesive serves to both electrically insulate the laminations from each other and to bond the core mechanically. This process reduces core losses. Figure 21 shows the details of the stator lamination design. The lamination has 54 partially closed slots which contain the stator winding. Both rotor and stator cores are 5.05 inches in axial (air gap) length.

The rotor lamination slot detail is shown in Figure 21. The rotor lamination has 63 partially closed slots within which the rotor bars will be placed. No bonding adhesive will be used between the rotor core laminations. The rotor will be constrained mechanically by axial welds in three circumferential positions on the rotor core I.D.. The welding procedure is used instead of epoxy adhesive since the rotor has low slip and does require insulation between laminations.

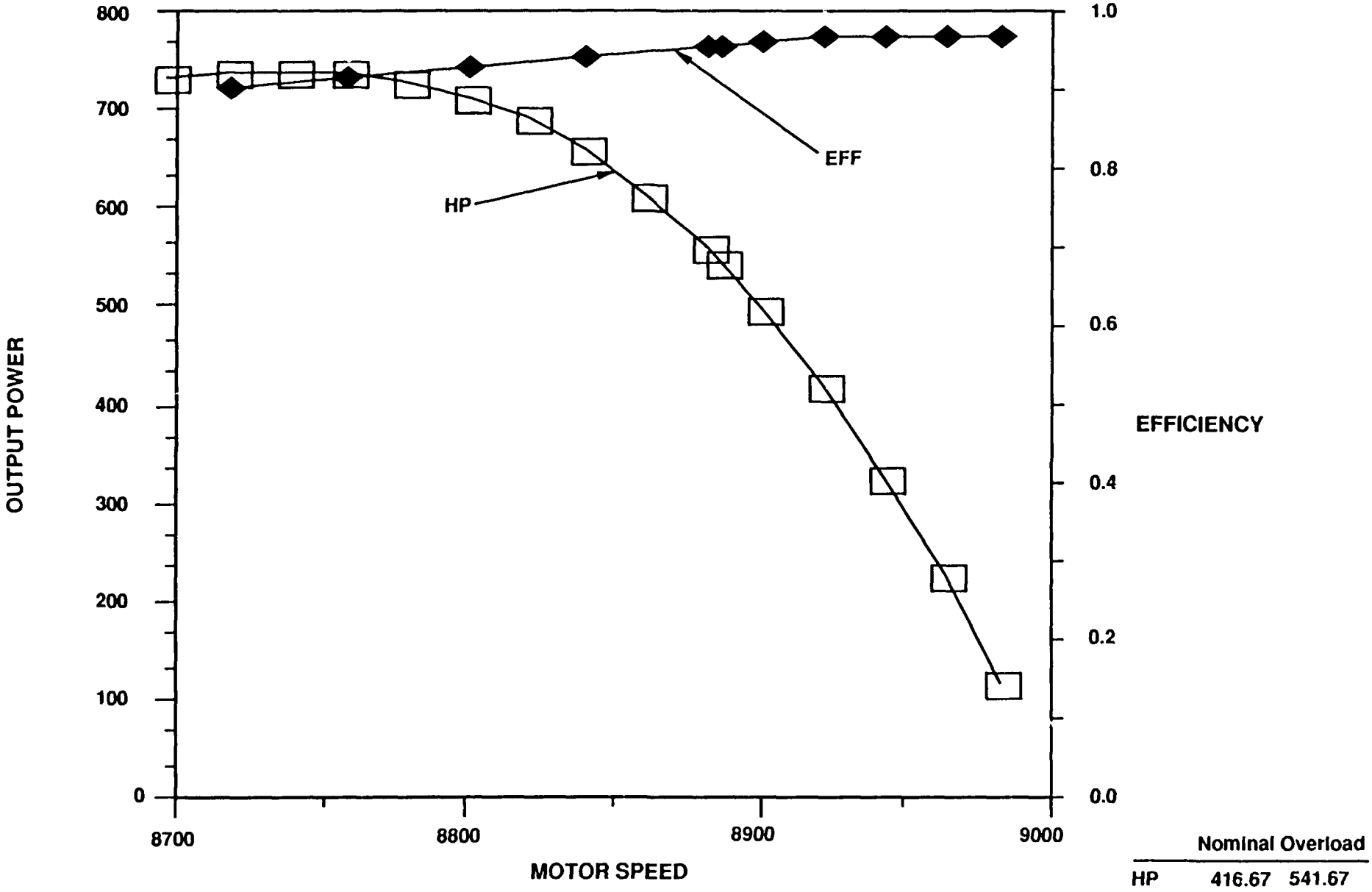

	Nominal	Overload
HP	416.67	541.67
EFF	.962	.953
PF	.914	.886
RPM	8919	8885
AMP	392	531

Figure 18. Predicted Induction Motor Performance - Power/Efficiency

05/204/88/007-A

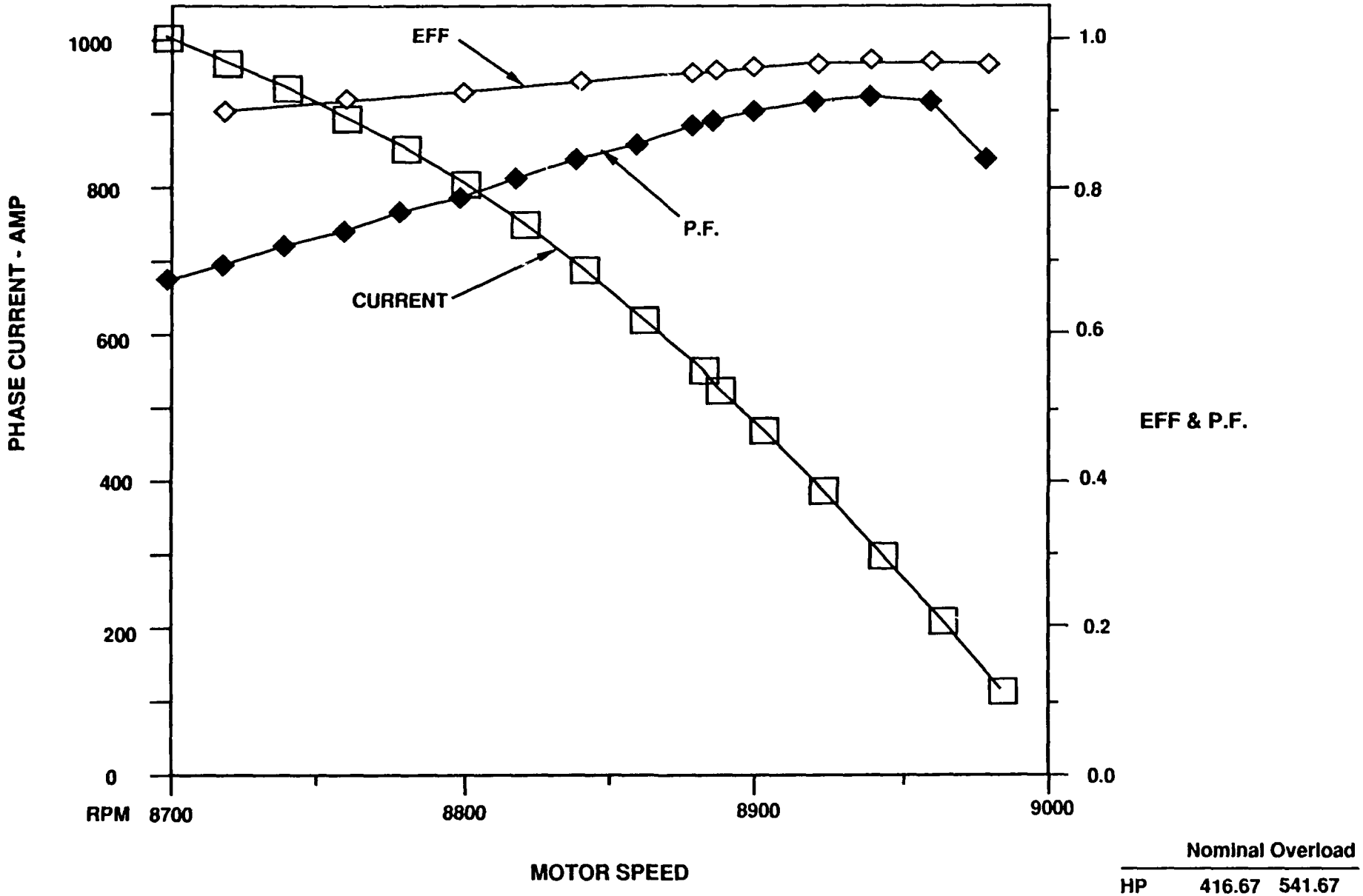

	Nominal Overload	
HP	416.67	541.67
EFF	.962	.953
PF	.914	.886
RPM	8919	8885
AMP	392	531

Figure 19. Predicted Induction Motor Performance - 450 Hz (Line Current/Power Factor)

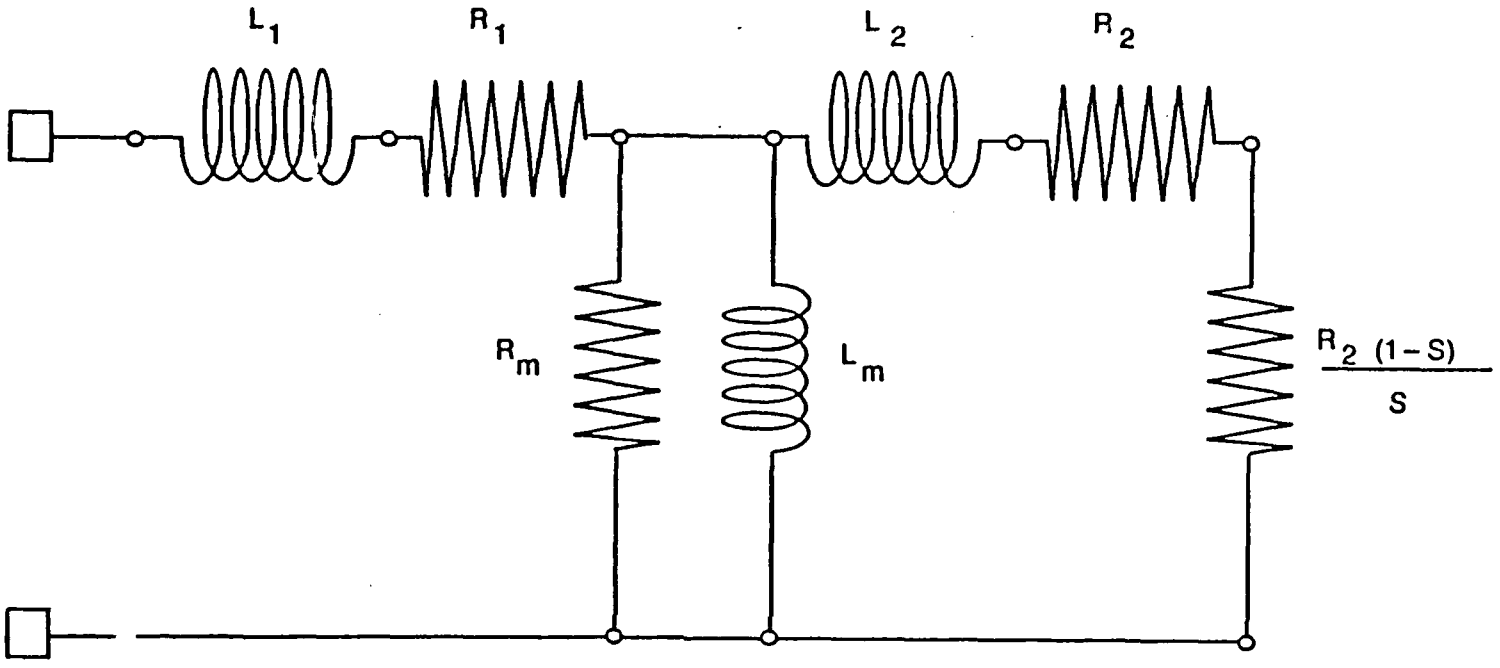

$L_1 = 4.35 \times 10^{-5}$ H

$R_1 = 1.27 \times 10^{-2}\ \Omega$

$R_m = 211.9\ \Omega$

$L_m = 1.79 \times 10^{-3}$ H

$L_2 = 3.27 \times 10^{-5}$ H

$R_2 = 6.53 \times 10^{-3}\ \Omega$

S = Per Unit Slip

Figure 20. Induction Motor Per Phase Equivalent Circuit

05/204/88/082

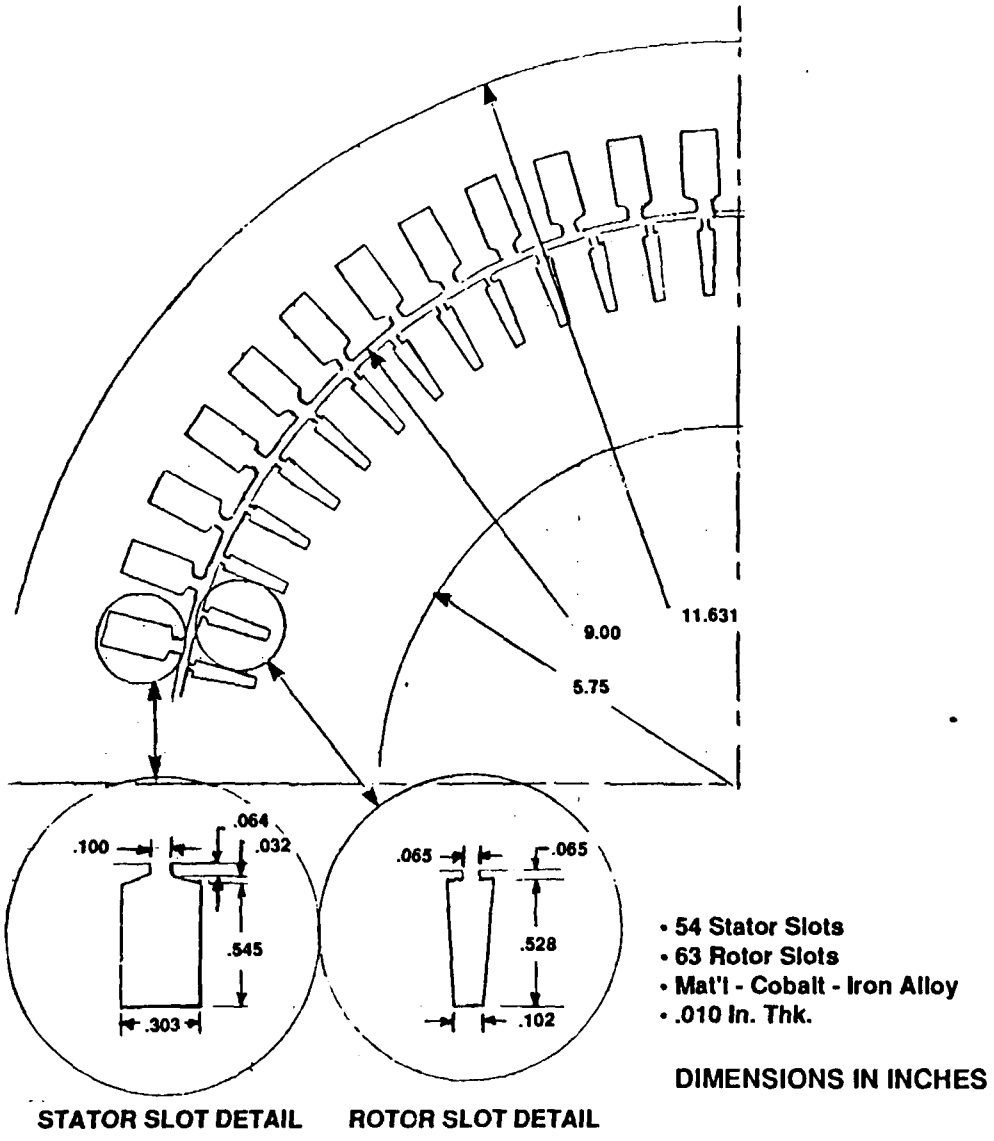

Figure 21. Stator and Rotor Laminations

The type of stator winding selected is a single circuit wave winding which provides the minimum number of internal connections. The end result of this selection is a winding which minimizes the axial length of the wound stator core. The winding diagram is shown in Figure 22. It is described as a three-phase, six-pole, three-lead, single turn full pitch winding. The stator conductors are rectangular in cross section. The coils are partially preformed then inserted in the stator core slots. Following coil insertion, coil end turn forming is completed. Each coil side has two conductors in parallel for a total of four conductors per slot.

The slot insulation system shown in Figure 23 is rated for a 180°C, 600 volt, 450 hertz design. All insulation materials are compatible with the internal oil system coolant (MIL-L-7808). The slot ground wall insulation is a Nomex-Kapton-Nomex composite which has a high tear and cut-through resistance. The ground wall provides a 6600 volt dielectric strength to ground and has long life at elevated temperatures. The film insulation on the winding conductors is a heavy polyamide-imide which is compatible with MIL-L-7808. It has a nominal temperature rating of 200°C. In addition to long thermal life, the cut-through and heat shock tolerance are superior to other types of magnet wire insulation. The wound stator is vacuum pressure impregnated with an epoxy resin which provides resistance to contaminates, seals the winding against moisture absorption and facilitates heat transfer by eliminating air voids in the ground wall system. In addition to the conductor film insulation the stator winding end turn area is insulated with an epoxy resin coating to enhance the heat transfer in this region from the conductor to the oil (MIL-L-7808).

2.3.2.5 Starting and Acceleration Characteristics, Initial Design

The ability of the motor to accelerate the waterjet commensurate with the alternator characteristics was initially analyzed using steady state performance data. The motor voltage and power factor were held constant during the acceleration time period. Figure 24 shows the predicted electrical system voltages and currents under both hot (15°C) and cold (150°C) starting conditions. During starting the alternator will be at 4306 ±RPM and the

STATOR WINDING FEATURES

- Winding Type: Three-Phase Six-Pole Wave Wound WYE Connected Series Winding
- Rectangular Conductors, Form Tunnel Wound
- Full Pitch, 54 Slots, 2-Layer
- Advantages:
  - Minimizes Axial Length
  - All Internal Connections in Common Location
- Common Winding Arrangement for Motor and Alternator

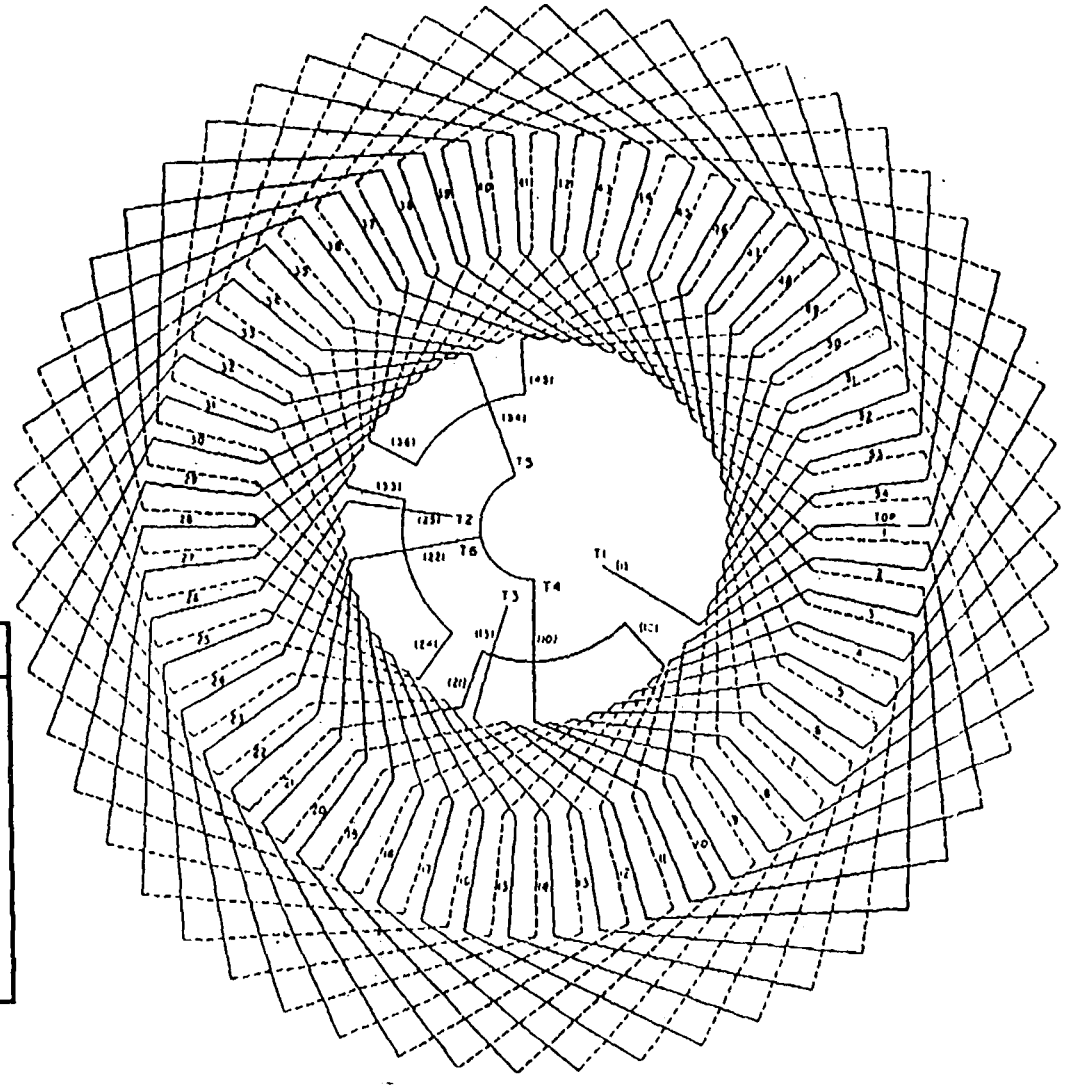

WINDING DIAGRAM

05/204/88/019

Figure 22. Motor Stator Winding Design

SLOT INSULATION SYSTEM

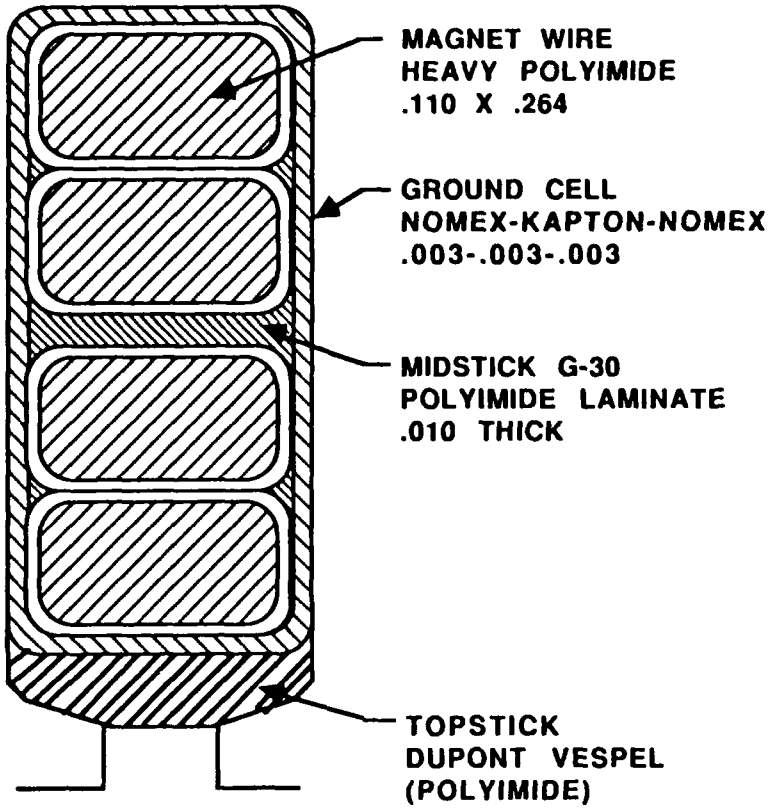

DESIGN REQUIREMENTS

- Insulation - 180°C
- Voltage - 520 Volt RMS Continuous
  2040 Volt Dielectric Withstand
- Frequency - 450 Hz
- Life - 500 Hrs. Operating
  10 Yrs. Storage (-40C to + 125C)
  Oil Resistant (Mil-L-7808)

KEY FEATURES

- Voltage Breakdown >4000 V/Mil
- Vacuum Pressure Impregnated with Epoxy Resin
- Excellent Heat Transfer Characteristics

05/204/88/020-F

Figure 23. Stator Insulation System

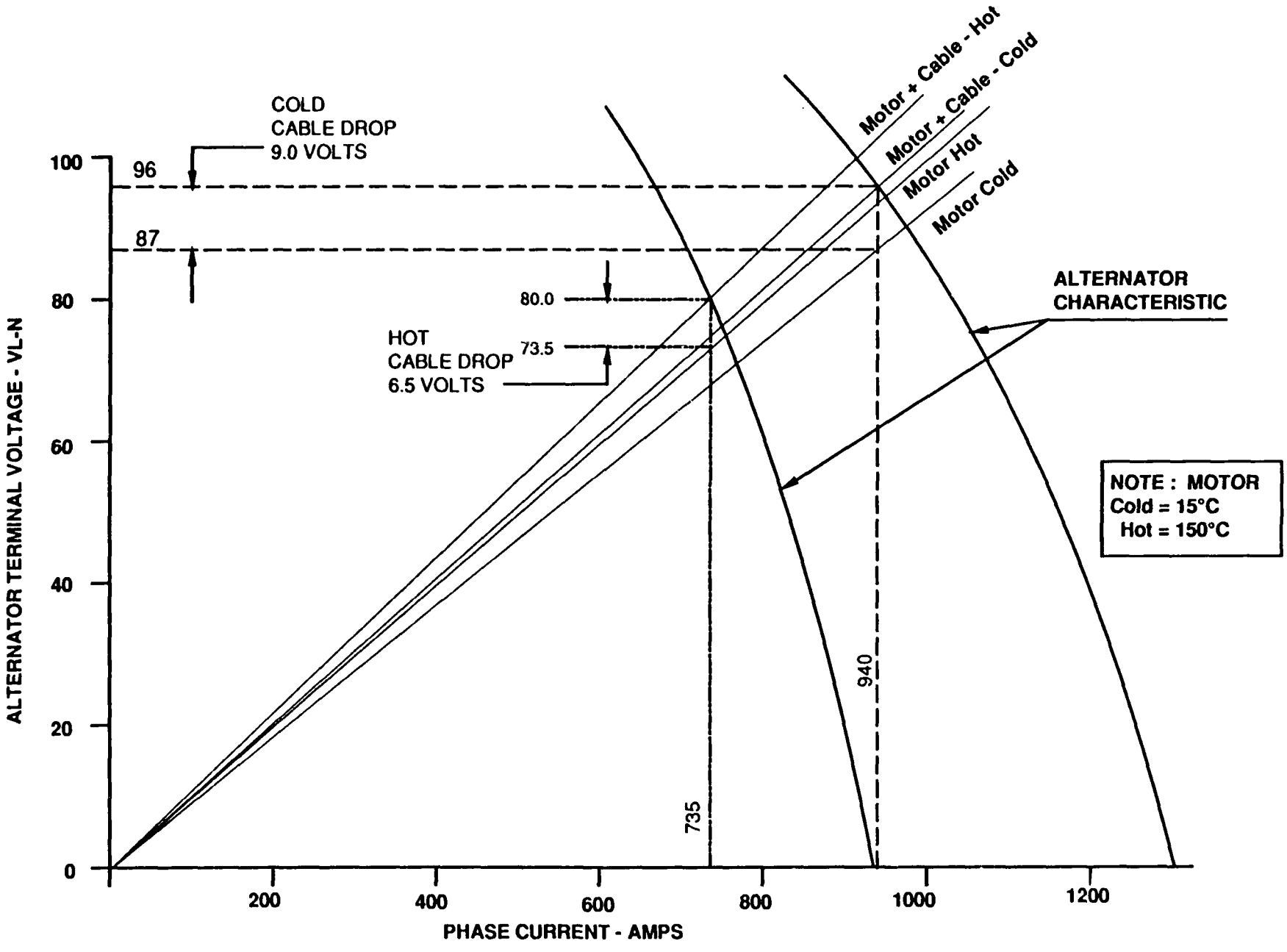

Figure 24. Operating Point Starting Conditions (0 Motor Speed, 215.3 Hz)

system frequency at 215.3 hertz. Alternator no-load voltage at this frequency should be 143.6 volts (L-N) corresponding to rated volts/hz; but, due to the large currents drawn during starting, the motor terminal voltage drops to 87.0 volts for a cold start and 73.5 volts for a hot start. The intersection of the alternator and motor starting characteristics determines the motor starting conditions. The power cable voltage drop (assuming a 4/0 cable of 25 feet in length) for hot and cold conditions are shown.

Once the motor terminal voltage has been determined under starting conditions, the motor speed-torque curve can be calculated (Figure 25). This curve is calculated assuming the motor is at 15 degrees C temperature. The developed motor torque includes the fundamental as well as additional harmonic torques that exist primarily at lower motor speeds. The expected load-torque (reflected to the motor shaft) curve and its associated break-away torque is below the motor torque. The difference between these two curves is the torque available for accelerating the load. Given the accelerating torque and the system inertia, the drive system acceleration time is calculated (Figure 26). The dynamic performance during starting is simulated using the system model. The motor voltage and power factor vary during acceleration and are taken into account in the system model. (Refer to section 2.5, Propulsion System Controller, for a more detailed discussion.)

The worst case starting condition occurs when the drive system is at temperatures corresponding to nominal load conditions. This condition may occur should a restart of the vehicle be required immediately after a full load run. The capability of the drive system to start at elevated temperatures was investigated. The motor terminal voltage was determined from the alternator characteristic to be 73.5 volts (Figure 24). The motor's terminal voltage at elevated temperatures is lower than ambient conditions which provides decreased motor starting torques with an accompanying decrease in starting current. The motor torque (including fundamental and harmonics) and load torque during a hot start are shown in Figure 27. From this, the time for a hot start (restart) was calculated to be approximately four seconds (Figure 28) using the steady state approach. (Refer to the section 2.5, Propulsion System Controller, for the simulated starting conditions using the system model.)

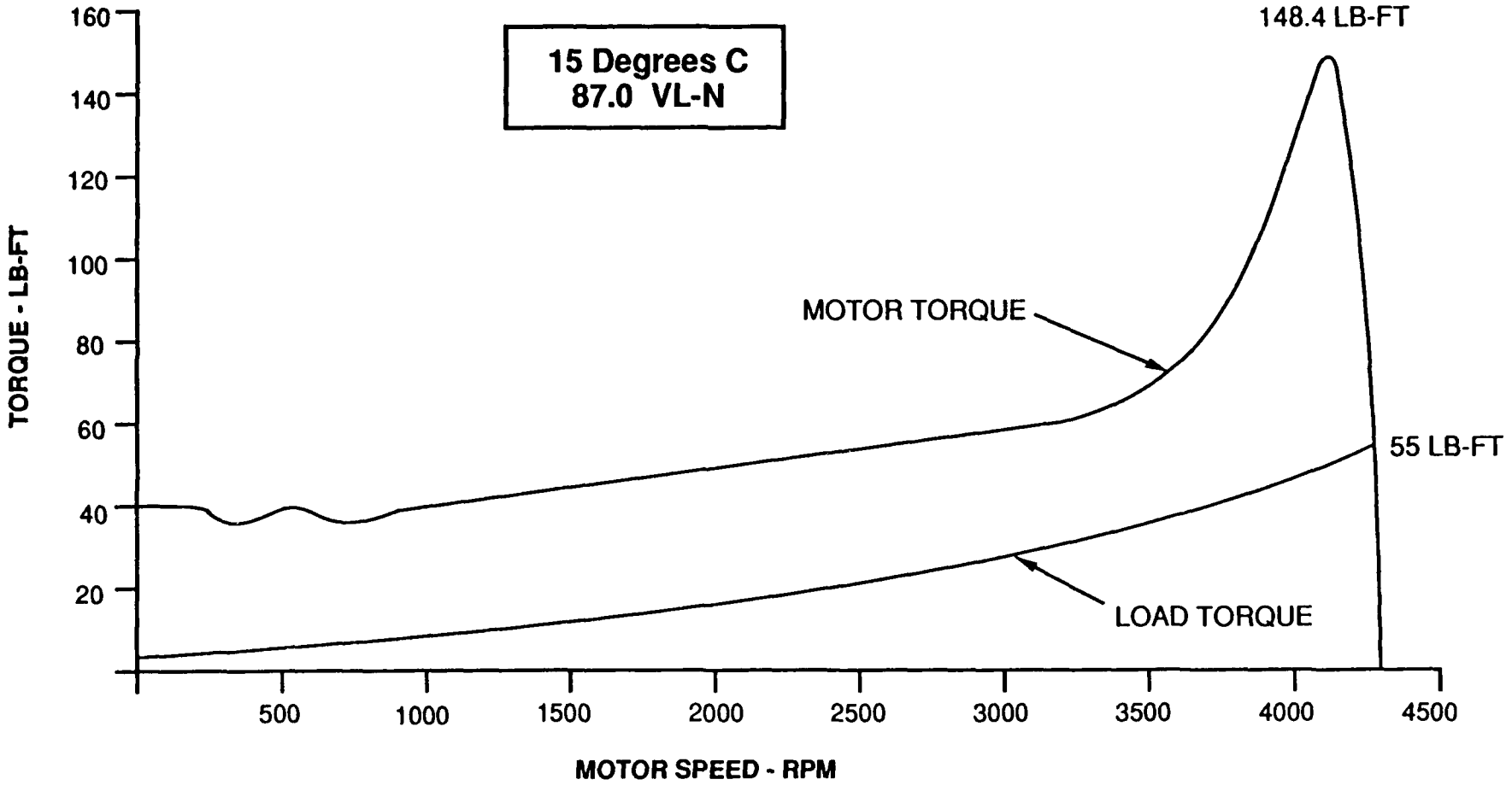

Figure 25. Speed Torque Curves (Cold Starting Condition)

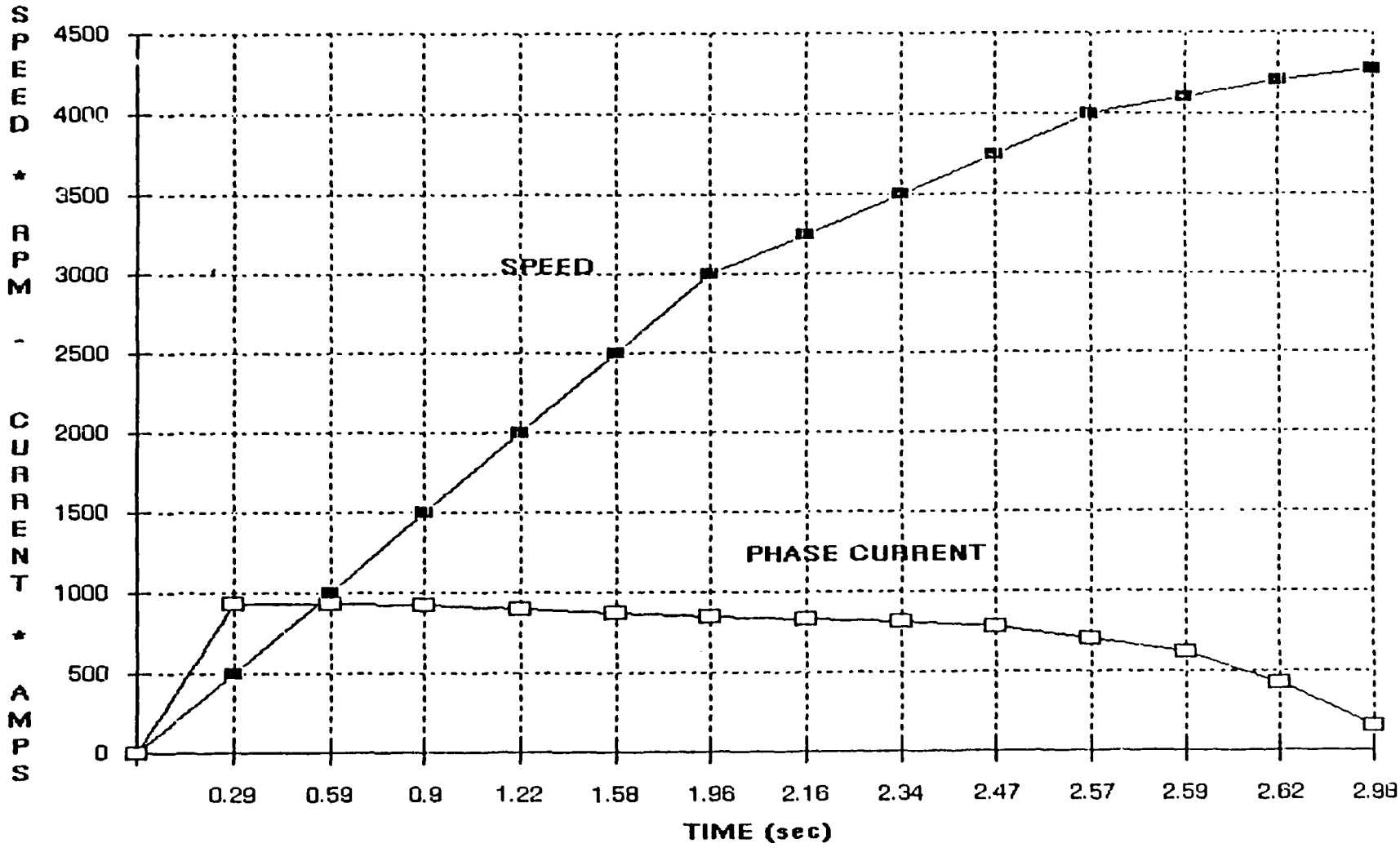

Figure 26. Motor Acceleration (15C)

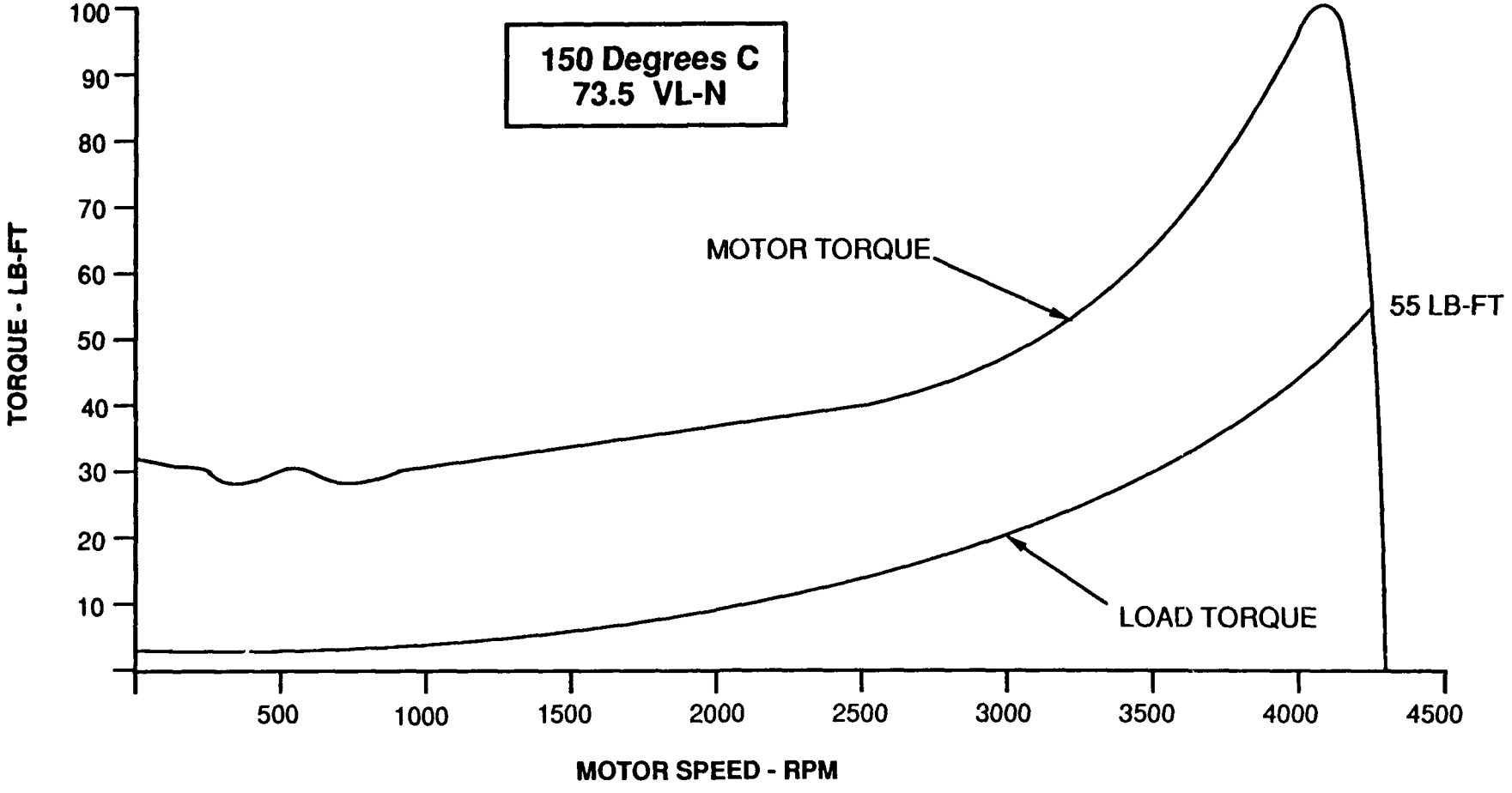

Figure 27. Speed Torque Curves (Hot Starting Condition)

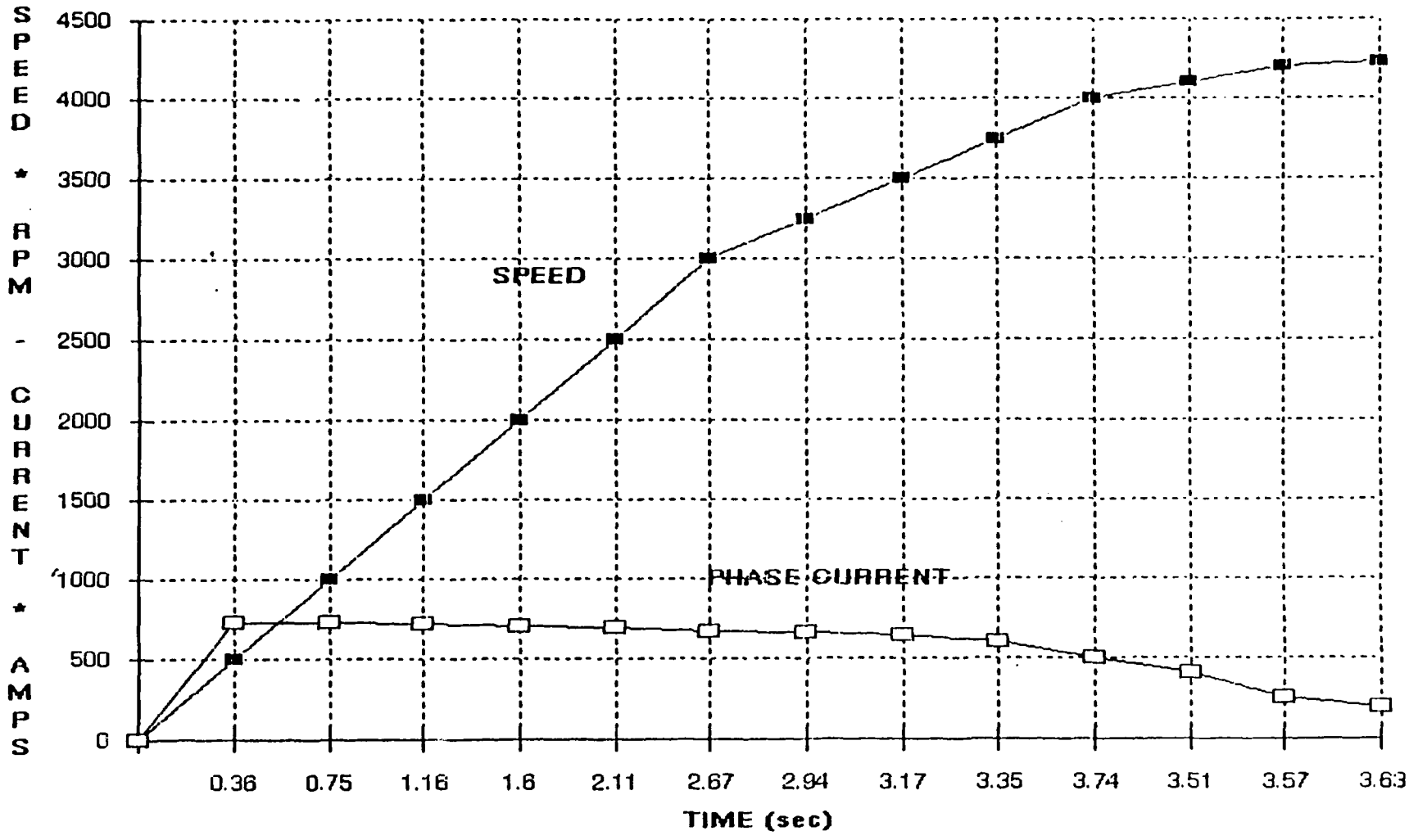

Figure 28. Motor Acceleration (150C)

2.3.2.6 Mechanical Stresses

The mechanical design requirements are summarized in Figure 29. The torque requirements result in shear stress in the stub shaft. The speed requirements result in centrifugal forces which create stresses in many of the shaft components. The shock loads create bending stresses in the stub shafts and bending stresses in the forward bulkhead. The life requirement has an impact on the working stresses in the shaft components.

The rotor assembly (Figure 12) was modeled with finite element analysis. The ANSYS model is shown in Figure 30. Numbers on the diagram represent node and element numbers. The centerline of the shaft runs through nodes 54 and 56.

Shaft stresses due to centrifugal force at 9000 rpm are shown in Figure 31. The safe working stresses in this figure are adjusted for cyclic and temperature effects. The rotor lamination stress is a hoop stress located at the inside diameter of the rotor lamination. The assembly stress in the lamination is not superimposed since the safety factor is quite large and the superposition process adds substantial complexity to the model. The copper end ring stress is also a hoop stress located at the inside diameter of the end ring. The end ring and bar stress is a hoop stress which occurs at the braze joint between the bars and end rings. Assembly stresses due to the shrink ring are superimposed on the end rings since the shrink rings are installed specifically to keep the end ring stresses at an acceptable level.

The shrink ring stress is a hoop stress which is the combined effect of assembly, thermal and centrifugal forces. The safe tensile stress for the shrink ring is not adjusted for cyclic loading because the cyclic stress is small relative to the average stress and the number of stress cycles is at the threshold at which no correction is needed. The shaft stress is a hoop stress located at the point where the stub shafts are welded to the end plates.

The centrifugal stresses of 10500 rpm are shown in Figure 32. Since this speed only occurs in the overspeed test the material properties are not adjusted for cyclic or temperature effects. All stresses are located as described above.

- 250 Ft. Lb. Torque at 9000 RPM Nominal
- 10,500 RPM Overspeed
- Shock Load - 7G All Directions
- 500 Hr. Life

Figure 29. Mechan al Design Requirements

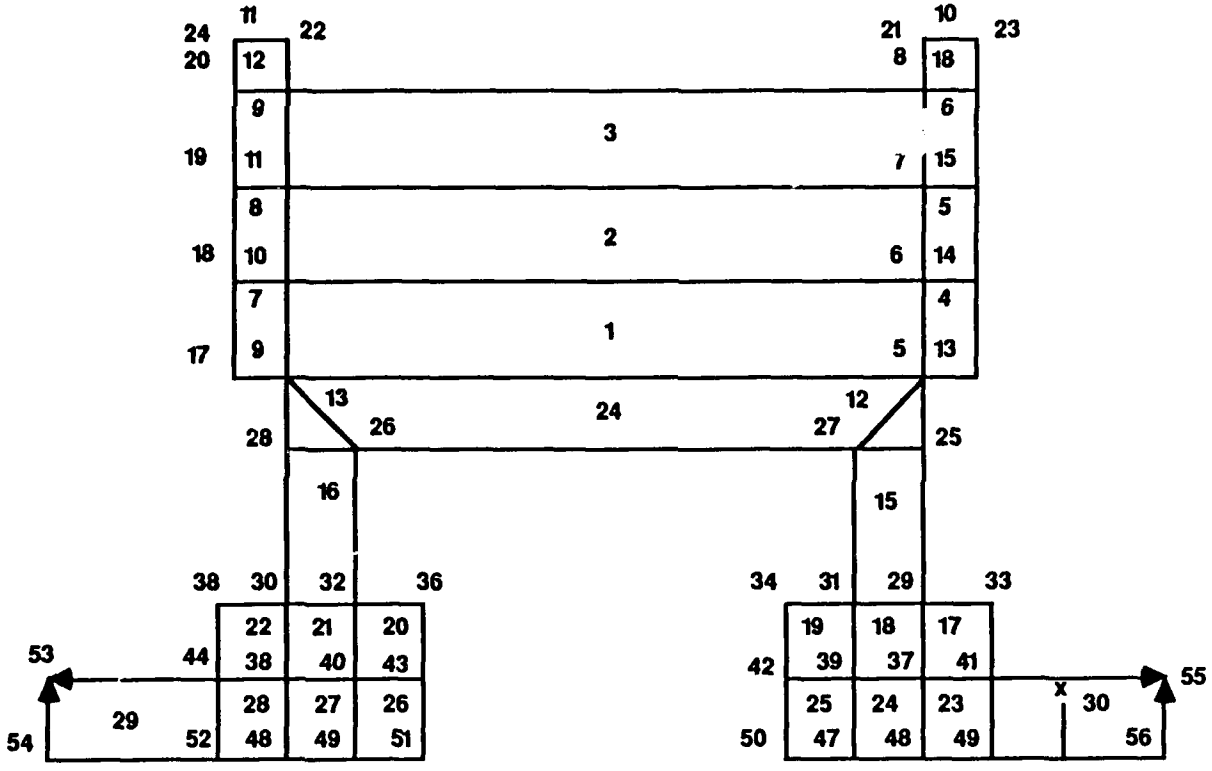

Figure 30. Rotor Ansys Model

Item	Material	Material Properties		Design-Operating	
		Minimum Tensile Yield PSI	* Safe Tensile Stress PSI	Maximum Tensile Stress PSI	Factor of Safety
Rotor Lamination	Iron-Cobalt ASTM801-82 Type 1	30,000	20,000	9,900	2.02
Copper End Ring	Zirconium-Copper CDA15000	32,000	16,000	9,900	1.616
Copper End Ring & Bars	Zirconium-Copper CDA15000 Filler Metal Bag-1 QQ-B-650	32,000	16,000 10,500	6,350	1.653
Shrink Ring	Inconel 625	60,000	51,600+	49,000	1.05
Shaft/End Plate Joint	ANSI 4130 Steel	40,000	35,000	25,200	1.389

* Adjusted for Temperature and Cyclic Effects
+ Adjusted for Temeprature Only (See Text)

Figure 31. Centrifugal Stresses (9000 RPM)

Item	Material	Material Properties	Design-Operating	
		Minimum Tensile Yield PSI	Maximum Tensile Stress PSI	Factor of Safety
Rotor Lamination	Iron-Cobalt ASTM801-82 Type 1	30,000	13,500	2.22
Copper End Ring	Zirconium-Copper CDA15000	32,000	13,500	2.37
Copper End Ring & Bars	Zirconium-Copper CDA15000 Filler Metal Bag-1 QQ-B-650	32,000 40,000	8,600	3.72
Shrink Ring	Inconel 625	60,000	41,600	1.44
Shaft/End Plate Joint	ANSI 4130 Steel	40,000	34,000	1.18

Figure 32. Centrifugal Stresses (10500 RPM)

Bending and torsional stress in the shaft end assembly are shown in Figure 33. The shaft working stresses are adjusted for operating temperature.

The stress and deflection in the forward bulkhead are shown in Figure 34. The working stress is not adjusted since the operating temperature is low and the number of repetitions is not expected to be large.

The assembly stresses in the housing and stator are shown in Figure 35. The worst case stress condition occurs at the low temperature limit since the external housing has a larger coefficient of thermal expansion than the stator. The resultant interference at operating temperature is also shown to demonstrate that the stator does not become loose in the housing under this condition.

Bearing life and shock handling capability are shown in Figure 36. Safety factors are large because bearing size was made large to fit over the shaft which was sized to carry the torque.

The critical speeds are shown in Figure 37. As can be seen, the first critical speed is well above the maximum operating speed of the motor.

Stress calculations are found in Appendix IV.

2.3.2.7 Rotor/Stator Thermal Predictions

A summary of the motor losses at nominal conditions is shown in Figure 38. The rotor losses and a portion of the stator winding end turn losses are rejected to the internal oil cooling system which in turn rejects these losses to seawater via the oil-to-water heat exchanger implemented in the outer motor housing. The remaining motor losses are rejected to seawater by radial conduction through the stator core to the outer motor housing.

Finite difference models were used to predict temperature distribution in the motor wound stator core and rotor cage. The analysis is based on 26.6°C (80°F) seawater flowing past the motor housing at a velocity of 10 ft./sec. The rotor temperature analysis indicates that 904 watts will be transferred across the motor air gap from the rotor O.D. to the I.D. of the stator core under nominal steady state load conditions. The remaining rotor loss is conducted axially along the rotor bars to the rotor cage end rings where it is rejected to the internal oil coolant.

Load	Type of Stress	Point of Maximum Stress	Material	Safe Working Stress PSI	Actual Stress PSI	Factor of Safety
7G Shock	Bending	Stub Shaft Adjacent to Hub	PH13-8 MO Stainless Steel	190,500	2,040	93
1.3 Nominal Torque	Torsional Shear	Stub Shaft Adjacent to Coupling	PH15-8 MO Stainless Steel	75,000	22,600	3.32
Assembly	Tangential	Inside Diameter of Lamination	Permendur V 50% Cobalt Steel	30,000	12,000	2.5

Figure 33. Shaft Stresses

Load	7G Shock = 525/LBF
Type of Stress	Bending
Material	Aluminum 6061-T6
Safe Working Stress	40,000 PSI
Actual Stress	1700 PSI
Factor of Safety	23.5
Deflection	.002 in.

Figure 34. Forward Bulkhead Stress

Maximum Interference

Operating Point = 50°F

Assumptions: Max Interference at Room Temp (.014 in.)

Interference at Operating Point = .016 in.

Item	Material	Safe Stress PSI	Actual Stress PSI	Factor of Safety
Housing	Aluminum 6061-T6	40,000	10,400	3.84
Stator	Permendur - V 50% Cobalt Steel	30,000	10,400	2.88

Minimum Interference

Operating Point: Steady State Full Load
Average Housing Temp 136°F
Average Stator Temp 170°F

Assumptions: Min Interference at Room Temp (.008 in.)

Interference at Operating Point = .004 in.

Figure 35. Housing and Stator Assembly

LIFE

Load Mechanism	Rotor Weight	Spring Washer
Load LBF.	37.5	39.0

Oper Speed RPM	Expected Life Hrs.	Required Life Hrs.	Safety Factor
9000	42,800	500	85.6

SHOCK

Load Direction	Shock Load LBF	Brg Cap LBF	Safety Factor
Axial	525	1,772	3.38
Radial	263	1,136	4.33

Figure 36. Bearing Loads

Shaft Weight: 76 LBM

Bearing Stiffness: 400,000 lb/in

Model Lumped-Mass Modal Analysis Program, CRTSPDM

Results:

1st Critical Speed 16,900 RPM

2nd Critical Speed 40,700 RPM

Figure 37. Critical Speed

416.67 HP
G/Box Eff = 96%

Motor Loss Segregation (Watts)

Stator		Rotor	
Heat Generated			
Sta I^2R	5856	Bar I^2R	2246
Core	1104	E/R I^2R	581
SLL (Stray Load Loss)	777	SLL	777
Windage (Drum)	131	Oil Drag	150
	7868		3754
Heat Transfer			
Rot → Sta (Gap Path)	+904	Rot → Sta	-904
To Housing Conduction Path	8772	To Oil System	2850

Figure 38. Motor Losses/Heat Transfer

The predicted results of the stator analysis are shown in Figure 39 for nominal load conditions. The model used assumed that no heat was transferred from the stator end turns to the internal oil coolant. This assumption produces the worst case stator coil temperature distribution. Winding top coil temperatures are found to be the highest since the losses are larger in this coil and it is further from the cooling jacket than the bottom coil. Since the model assumes that the top and bottom coils are physically disconnected in the end turn area, the temperature difference between coils is higher than anticipated. This is due to the fact that every top coil is physically connected to a bottom coil in the actual winding.

A minor modification to the above model was made to determine the effect of oil cooling of the end turns. The modification consisted of the removal of 1,040 watts from the end turns of the top coils via convection to the cooling oil. This is equivalent to conducting away all the heat generated in this portion of the end turns and is based on a conservative estimate of the amount of heat transferred to the oil via convection.

The results of this modified model are shown in Figure 40. The highest temperature (180°C) is located at the end of the top coil. The insulation system selected for this design will withstand this environment for 500 hours as required.

Steady state rotor cage temperatures at nominal load conditions are shown in Figure 41. The rotor model assumes that no rotor losses flow from the rotor core to the rotor shaft and hub assembly. The only paths permitted for heat flow in the model consist of the motor air gap and the axial route along the rotor cage bars to the cage end rings. This assumption yields a worst case model for the rotor temperature analysis. The primary concern is that no rotor component temperature be in excess of the oil coolant temperature limit which is 180°C (356°F) for nominal conditions and 204°C (400°F) for the overload condition. A radial temperature profile for a rotor end ring is also shown indicating a maximum temperature of 120°C (248°F) at the ring O.D.

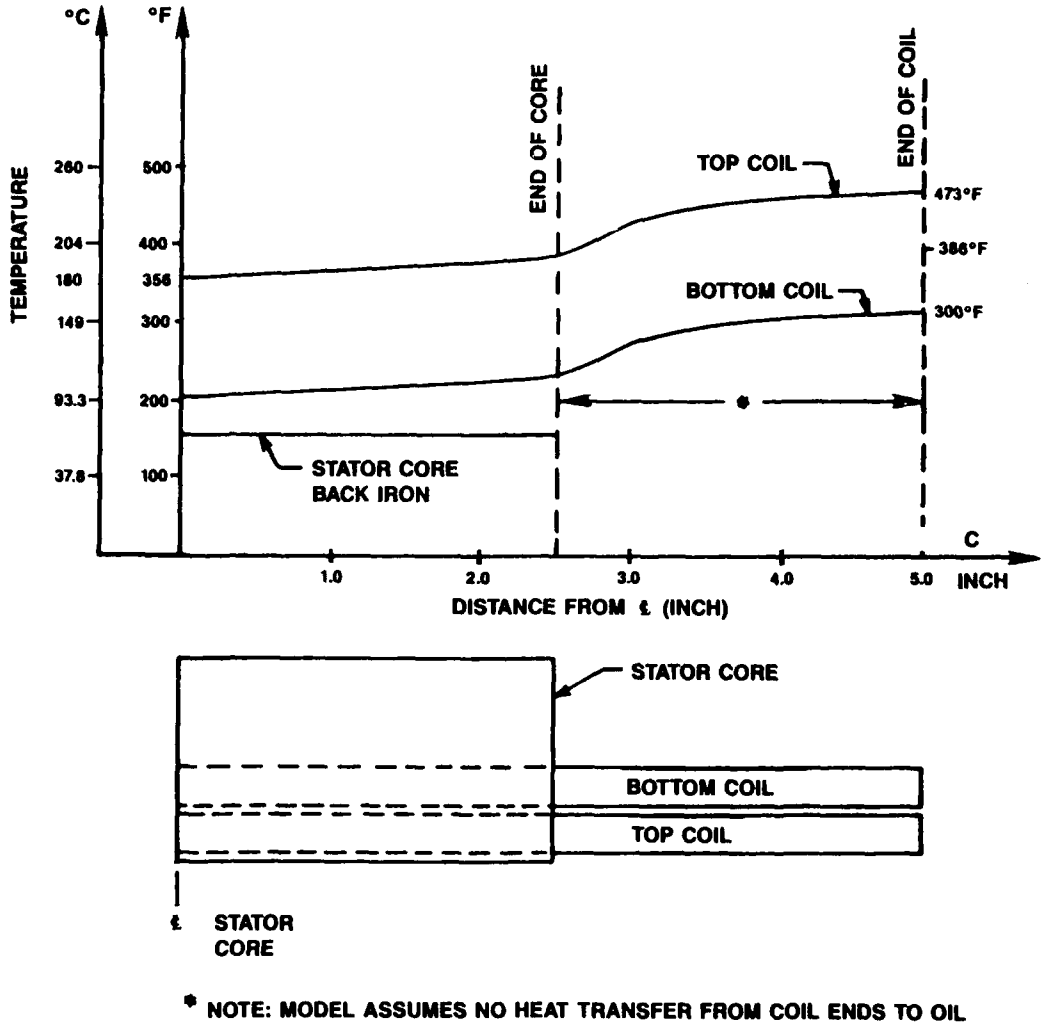

Figure 39. Predicted Steady State Stator Temperatures (Nominal Conditions); Original Model

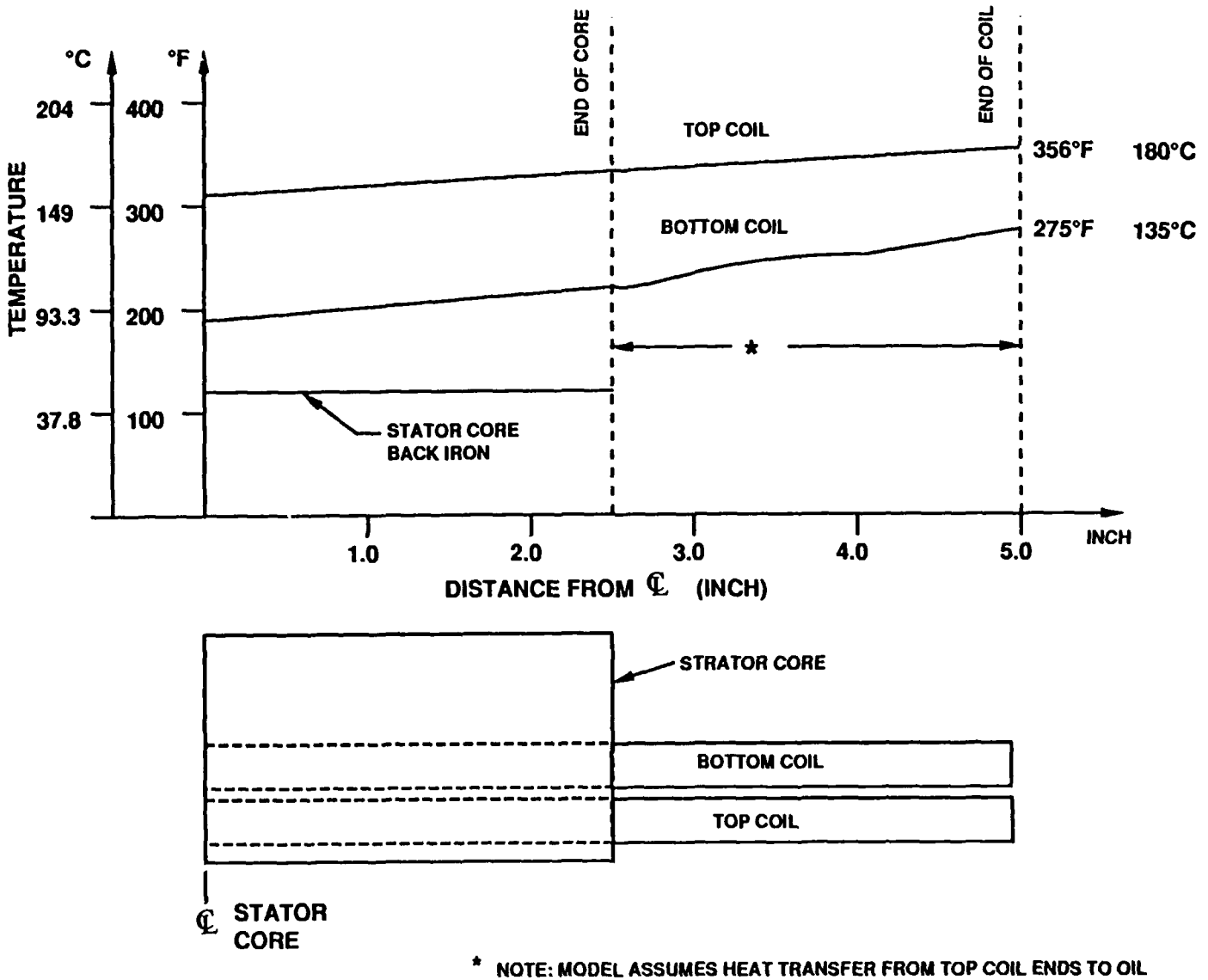

Figure 40. Predicted Steady State Stator Temperatures (Nominal Conditions); Modified Model

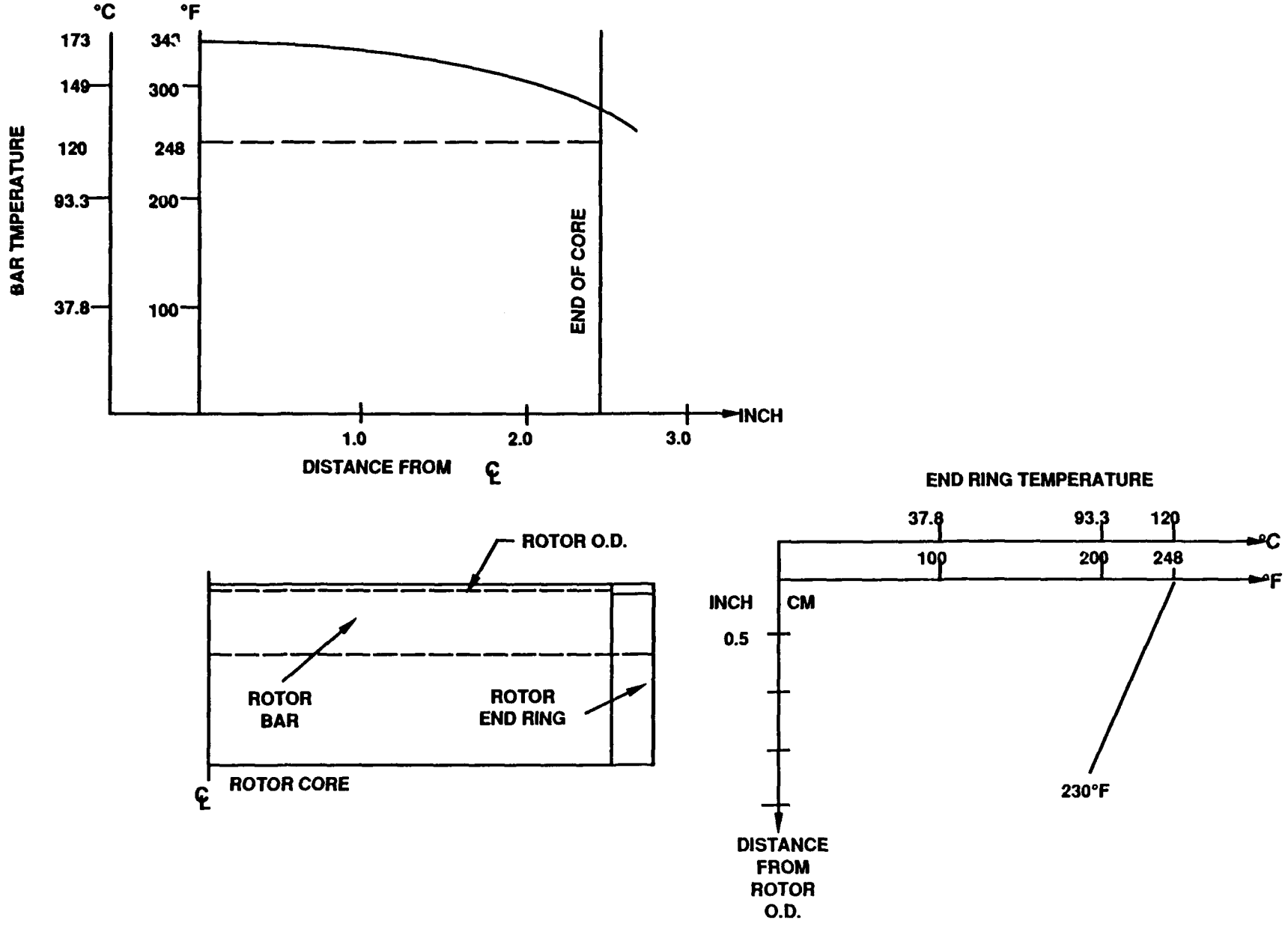

Figure 41. Predicted Steady State Rotor Cage Temperatures (Nominal Conditions)

Rotor bar thermal transient response is depicted in Figure 42. These results indicate the rotor bar thermal response to the 60 second 30% overload condition. The maximum rotor bar temperature after one minute reached 195°C (383°F) and is located at the axial centerline of the rotor. The rotor cage, therefore, has adequate thermal storage to meet the overload requirement. Continued operation at 1.3 overload will result in steady state rotor bar temperatures of 306°C (583°F). This temperature exceeds the maximum allowed oil temperature of 204°C. Therefore, continuous operation at 1.3 overload is not permitted.

2.3.2.8 Motor/SDG Thermal Analysis

A schematic of the oil system is shown in Figure 16. Oil is drawn from the sump in the bottom of the motor through the 20 micron filter into the lubrication pump located in the SDG. The filter is located in the sump and can be removed for cleaning or replacement through an access port in the bottom of the sump. From the pump the oil flows into the heat exchanger surrounding the motor and on into passages which feed lubricating oil to bearings and gears and cooling oil to the rotor. A relief valve at the outlet of the pump prevents excessive pressure from developing.

The assumptions used in the thermal analysis are shown in Figure 43. These assumptions lead to a worst case analysis for the system. The required oil flow rate was established through an iterative process. A safe hot oil temperature was selected based on the SDG manufacturer's recommendation and an estimate was made at the cold oil temperature that could be produced with the heat exchanger. The required oil flow rate was then calculated from the temperature difference and the total heat flow into the oil.

The temperature drop in the heat exchanger was then calculated to verify the cold oil temperature used. The new cold oil temperature was then used to adjust the required oil flow rate and the entire process repeated.

The thermal model is shown in Figure 44. In this model the heat exchanger is treated as two separate units. The first unit surrounds the stator and transfers heat from the stator through its walls to the water outside as well. In addition to this, heat from the oil is transferred to the fins in the outer shell and into the water.

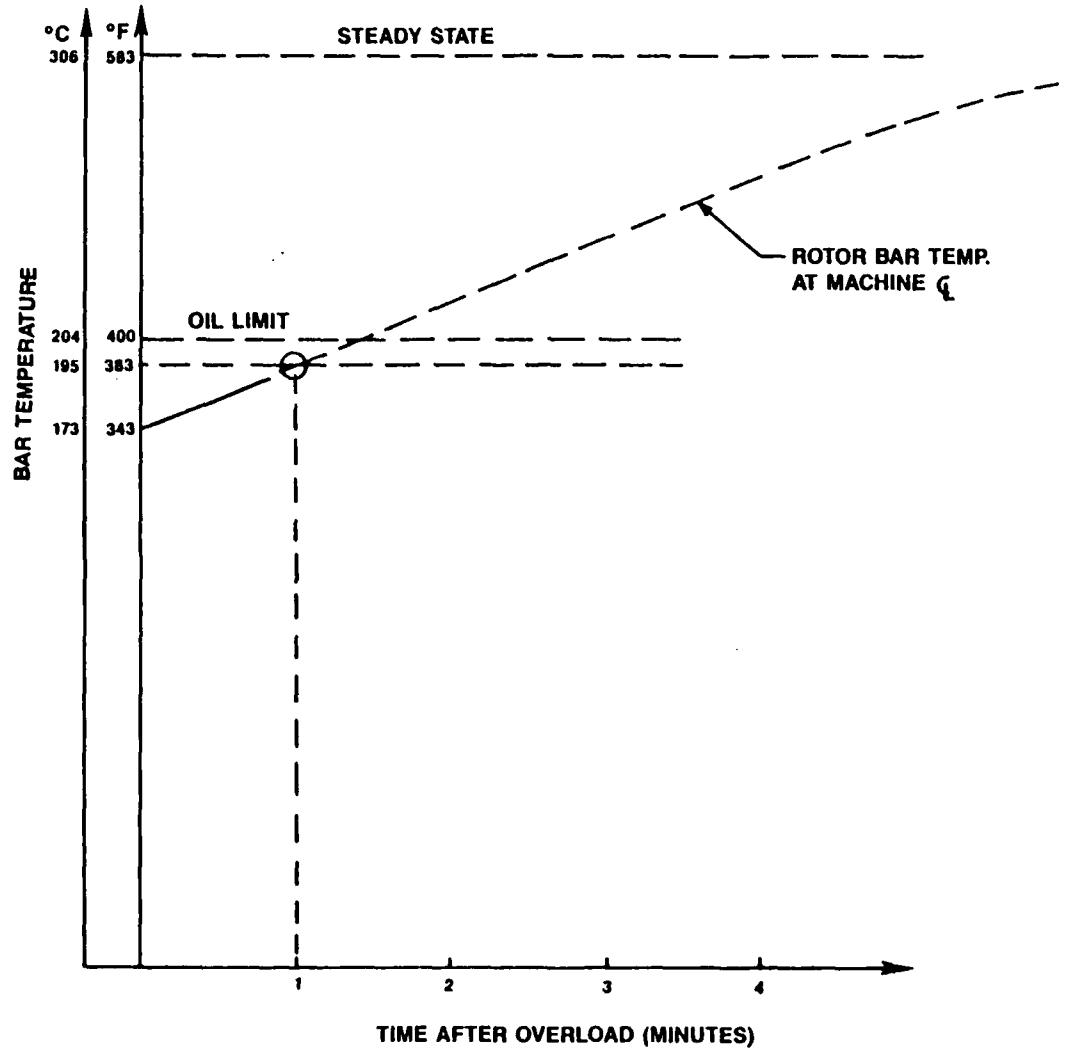

NOTE: MAGNITUDE OF OVERLOAD IS 1.3X NOMINAL

05/204/88/026

Figure 42. Thermal Transient Response of Rotor Cage Bar (1.3 Per Unit Overload)

- Steady State
- 400 HP
- 80 F Water Temperature
- 10 FPS Water Velocity
- Efficiency
  - 96% Gearbox
  - 96.2% Motor

Figure 43. Thermal Design Assumptions (Oil Temperature)

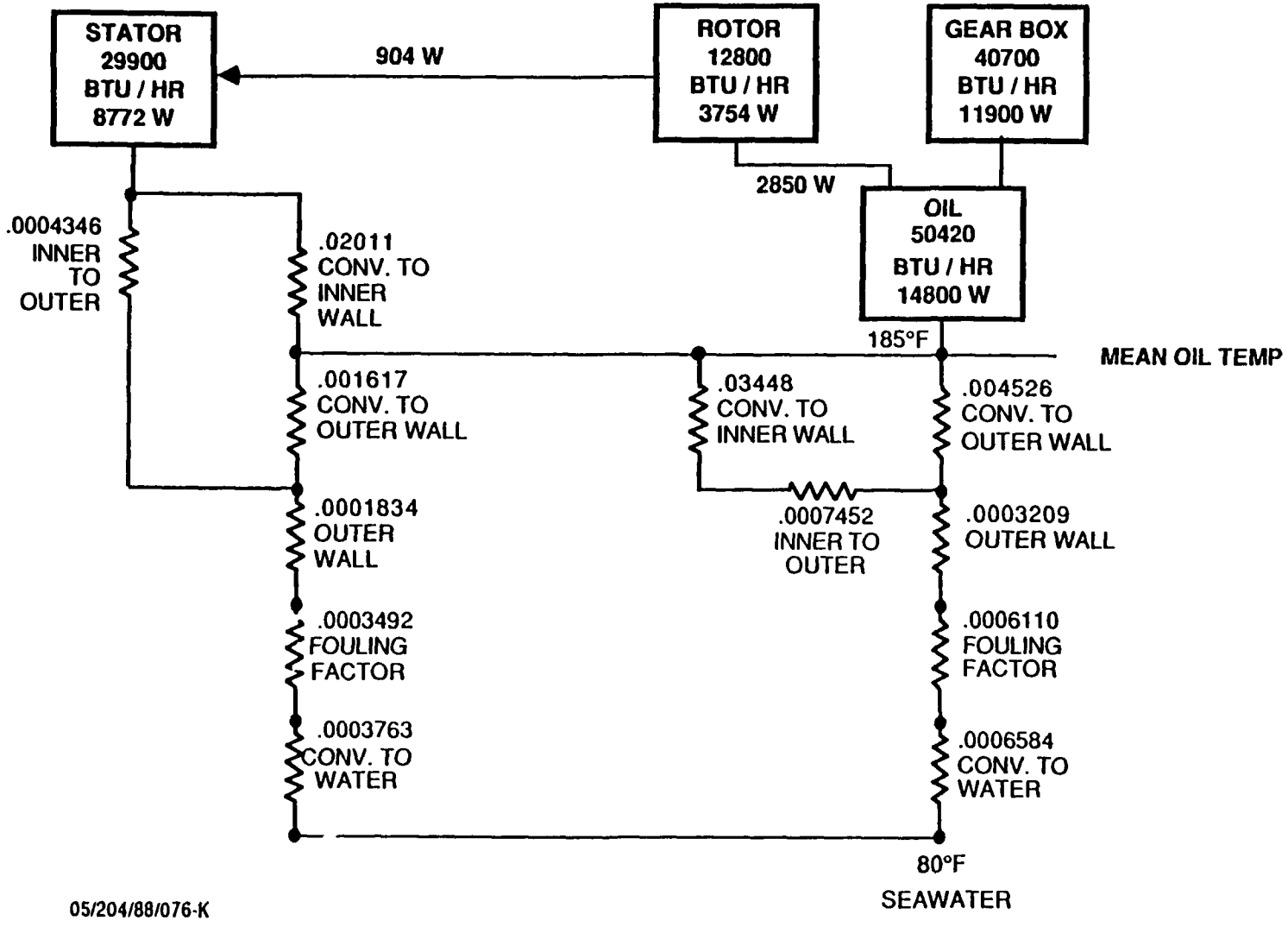

Figure 44 Thermal Model (No End Turn Cooling)

The second unit represents the section of heat exchanger between the stator and SDG and the section between the stator and forward bulkhead combined. This unit transfers heat from the oil to the fins and outer shell to the water but does not carry heat from the stator.

After all thermal resistances were calculated, node equations were written and solved simultaneously with a matrix algorithm. To verify the analytical results an experimental heat exchanger similar in design to that used in the motor was fabricated and tested. The test results are shown in Figure 45.

The thermal model was modified as shown in Figure 46 to include the 1040 watts transferred from the end turns to the oil in the modified stator model. This resulted in a 6 degree F rise in the mean oil temperature prediction. This is offset by the higher than predicted heat flow observed in the experimental heat exchanger and is not expected to occur in the actual design.

The thermal calculations are shown in Appendix V.

2.3.3 Speed Decreasing Gear

2.3.3.1 Design Description

The SDG is a single stage planetary type reducer with three planets and floating sun and ring gears. The general features of the speed decreasing gear are listed in Figure 47. All gears are fabricated from Alloy steel (AISI 9310 in the sun and planet gears and AISI 4150 in the ring gear) and the housing and bulkhead are cast aluminum alloy (A-356) as shown in Figure 48. The planet carrier is made from 17-4PH stainless steel which combines high strength with the corrosion resistance it needs since the output end will be exposed to seawater. The gear teeth are a proprietary spiroid (ITW) design and are ground to a special tooth form which makes it possible to manufacture a sun gear with a small number of teeth without undercutting. This permits a large speed reduction in a single stage.

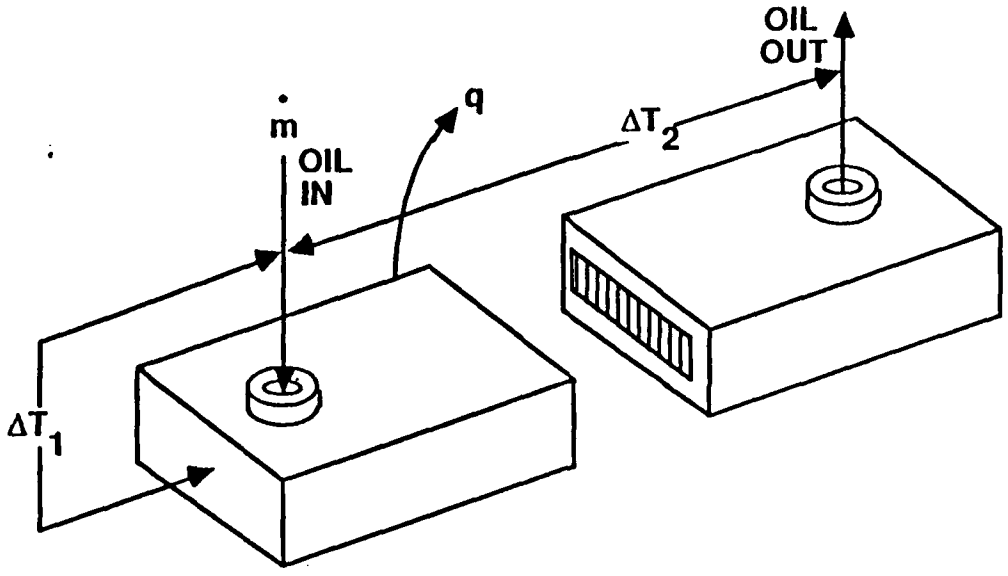

HEAT FLOW PREDICTED BY MODEL

q = 6110 BTU/HR

HEAT FLOW MEASURED

q = 8041 BTU/HR (32% GREATER THAN PREDICTED)

MEASURED DATA:

ΔT_1 TEMPERATURE DIFFERENCE (OIL TO EXCHANGER)

ΔT_2 TEMPERATURE DIFFERENCE (OIL IN-OIL OUT)

$\dot{m}$ MASS FLOW RATE OF OIL

05/204/88/077-k

Figure 45. Model Verification

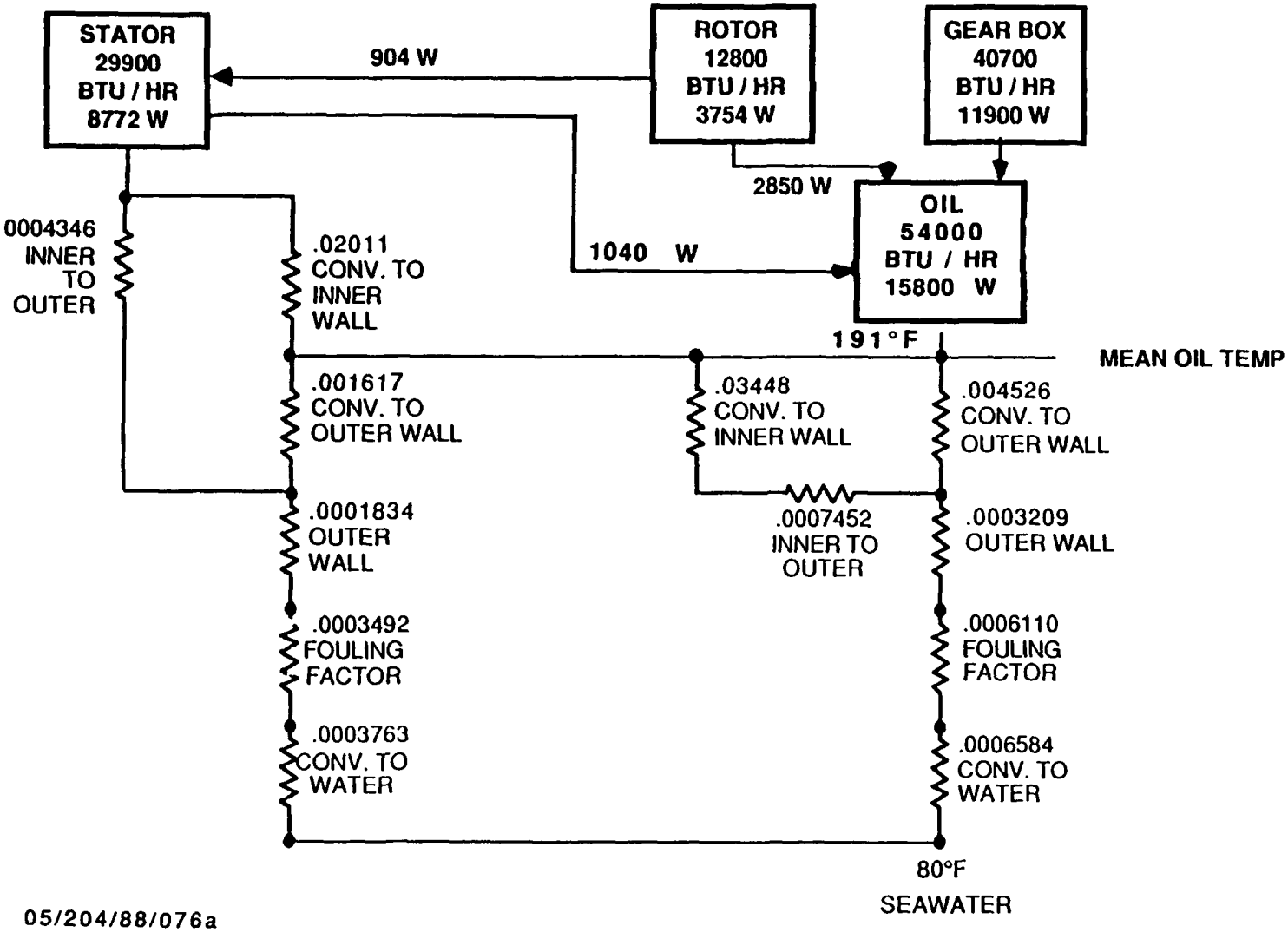

Figure 46. Thermal Model (With End Turn Cooling)

- Gear Ratio 7:1
- Gear System: Planetary with Sun Gear
- Tooth Form: Concurve
- Housing Material: Cast A-356 Aluminum
- Motor Interface: Common Bulkhead
- Oil Pump: Gear Driven

Figure 47. Speed Decreasing Gear

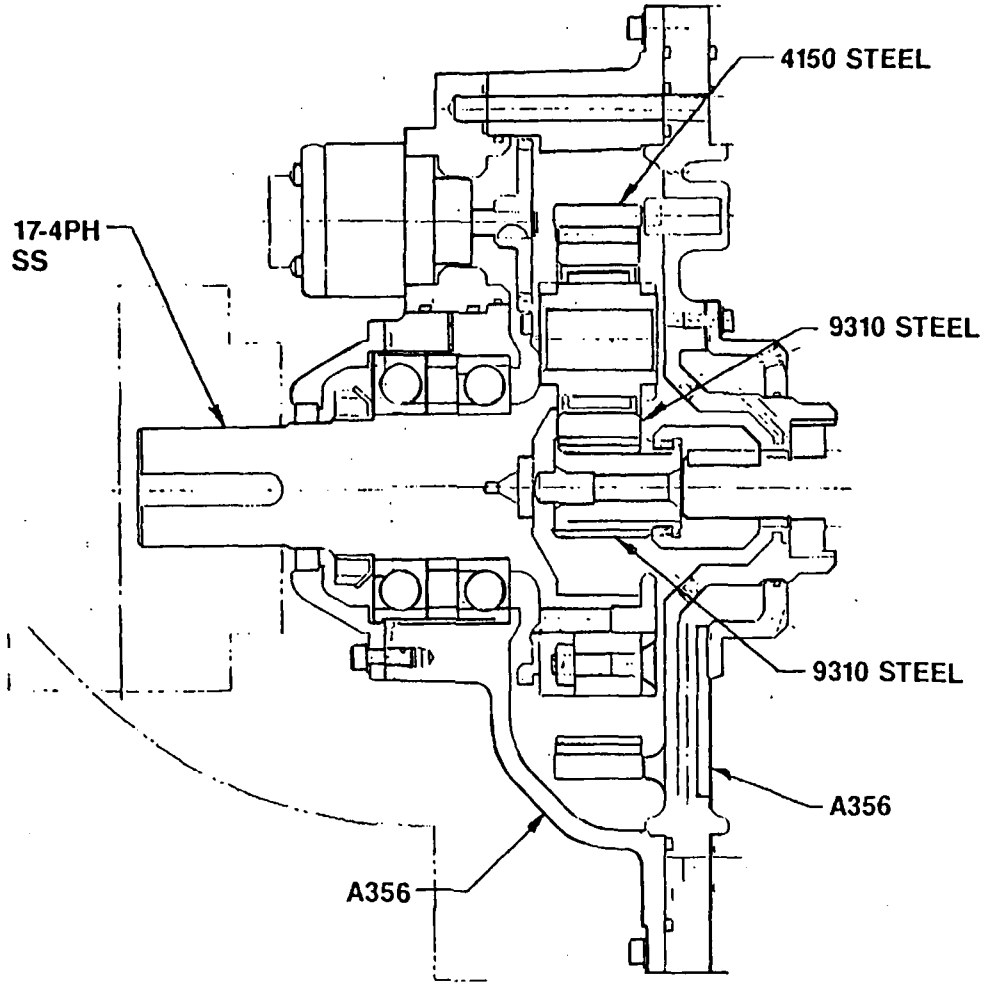

Figure 48 Speed Decreasing Gear Construction

The oil pump is a special gear pump design consisting of steel gears and shafts in a bronze case. A mechanism inside the pump causes the oil to be delivered to the same port regardless of the direction of rotation. A gear on the pump input shaft meshes with a gear on the planet carrier in the SDG. The pump runs at 3125 RPM and delivers 3.5 GPM of oil when the SDG runs at full speed.

Minimum weight and volume were major considerations in the SDG design. The floating ring gear and sun gear more evenly distributes the load among the planet gears resulting in a lighter set of gears for the required power. Weight and volume considerations were also the reasons for the selection of A-356 aluminum for the gearbox and bulkhead castings. The gearbox weight breakdown is given in Figure 49.

2.3.3.2 GEAR TOOTH STRESSES

All stress calculations for Concurve gear teeth are done by Spiroid developed computer programs. The general approach is conventional but several refinements have been made to help create a more comprehensive stress analysis.

Bending stresses are calculated for two points on both pinion (sun) and gear (planet): 1) tip load assuming only one tooth carrying the full load (actual stresses are half this value since the load is actually shared by two teeth in accurate gearing) and 2) "worst point load" (highest point of single tooth contact).

Compressive (Hertz) stresses are calculated for many points along the tooth profile from tooth tip to lowest point of contact.

The stresses in the ring gear teeth are not a factor in the gearbox design since they are much lower in value than the sun gear and planet gear stresses. Therefore only the sun and planet gear stresses are shown.

Item	Weight, lbM
Output Shaft Carrier	8.66
Housing	10.87
Bulkhead	11.51
Planet Gears (3)	5.81
Ring Gear	6.41
Pump	4.50
Misc.	18.74
Total	**66.50**

Figure 49. Speed Decreasing Gear - Weights (lbm)

Loads used for stress calculations were derived from a steady state input horsepower to the gearbox of 416 horsepower. In evaluating maximum torque overload stresses, a 1.3 factor was used. These stresses were then compared with the bending yield strength of 135,000 psi and compressive (Hertz) yield strength of 450,000 psi for 9310 alloy steel used in both gears) to determine factors of safety. Figure 50 summarizes stress analysis results.

Stresses for other components of the SDG are shown in Figure 51. The stresses in the input key and input coupling are directly due to the input shaft torque. The ring gear tang and bulkhead dowel pin prevent rotation of the ring gear. There are two dowel pins and two sets of tangs. The stresses are calculated in the basis of the entire load on one dowel pin. The calculations for the above stresses are found in Appendix IV.

2.3.4 Coupling

2.3.4.1 Design Description

The coupling shown in Figure 10, is a double flex gear type made of 316 stainless steel. Seals at each end of the sleeve retain lubricant in the coupling. This design was selected on the basis of minimum size and weight and the capability to operate under seawater.

2.3.4.2 Mechanical Stresses

The coupling was sized by derating a known design of alloy steel on the basis of the comparison of its yield strength compared to 316 stainless steel. The maximum torque rating (5180 ft-lb) provides a safety factor of 2.37 for 1-3 nominal overload condition.

Miscellaneous Stresses

Stresses for other components of the SDG are shown in Figure 51. The stresses in the input key and input coupling are directly due to the input shaft torque. The ring gear tang and bulkhead dowel pin prevent rotation of the ring gear. There are two dowel pins and two sets of tangs. The stresses are calculated on the basis of the entire load on one dowel pin. The calculations for the above stresses are found in Appendix IV.

Sun/Planet Gear Tooth Stress Analysis Summary

Gear	Torque/ Tooth Load (HP)	Root Bending Stress	Bending Stress Allowable	Safety/ Service Factor	Compressive (Hertz) Stress	Compressive Stress Allowable	Safety Service Factor
Sun	2942 in. lb./ 1401 lb. T.L. (416 HP)	20,404 PSI	**50,500 PSI	2.48	177,320 PSI	**230,000 PSI	1.30
	3825 in.lb./ 1821 lb. T.L. (1.3 x overload)	26,460 PSI	135,000 PSI	5.10	202,160 PSI	450,000 PSI	2.22
Planet	1401 lb. T.L. (416 HP)	20,845 PSI*	**53,000 PSI	2.54	177,320 PSI	**250,000 PSI	1.40
	1821 lb. T.L. (1.3 x overload)	18,948 PSI	135,000 PSI	7.12	202,160 PSI	450,000 PSI	2.22

* Planet gear tooth bending fatigue stresses include a 1.43 factor to account for reverse bending of planet gear teeth.

** Adjusted for cyclic effects.

Figure 50. Gear Tooth Stresses.

Item/Material	Type of Stress	Safe Working Stress PSI	Actual Stress PSI	Factor of Safety
Input Shaft Key 4140 Steel	Shear	66,000	24,920	2.65
	Compressive	132,000	49,000	2.69
Input Coupling 4150 Steel	Shear (in neck)	72,000	4,320	16.7
	Shear (in spline teeth)	72,000	8,020	8.98
	Compressive (in spline teeth)	145,000	10,100	14.4
Ring Gear Tang 4150 Steel	Bending	145,000	62,400	2.32
Bulkhead (seat for dowel pin) A356 Aluminum	Compressive	22,000	11,000	2.00

Figure 51. SDG Stresses – at 1.3 Nominal Torque

2.4 Power Cable

As shown in Figure 1, the power cable transmits the electrical energy from the alternator to the motor/SDG. Three cables are required, one for each of the three phases of the motor. The cable was selected based upon the design requirements shown in Table 6.

TABLE 6. CABLE REQUIREMENTS

ELECTRICAL	MOTOR CURRENT		392 A_{rms} continuous 531 A_{rms} 60 seconds 1,000 A_{rms} 5 seconds
	DIELECTRIC VOLTAGE		1,000 V_{rms}, 450 Hz continuous 2,040 V_{rms}, 60 Hz 60 seconds
PHYSICAL	PRIMARY INSULATION		200°C
	SIZE		4/0 AWG
	BEND RADIUS		1 FT. Max
	WEIGHT		.944 LB/LINEAR FT. NOMINAL
ENVIRONMENTAL	COMPATIBILITY		OIL, SEAWATER AND ABRASION RESISTANT
	OPERATING	TEMPERATURE	0-32°C
		LIFE	500 HR MIN
	STORAGE	TEMPERATURE	-40 to 125°C
		LIFE	10 YR, DAMP SALT AIR

The selected 4/0 AWG cable results in a nominal current density of 2424 amps/in^2. A pictorial of the cable is shown in Figure 52. The conductor has 259 strands of 21 AWG tinned solid wire. This stranding insures that the cable can meet the bend radius requirement. The primary insulation is silicon rubber impregnated glass fiber overwrapped with mylar tape. The outer jacket is polyurethane with an internal kevlar braid. The cable has a nominal outside diameter of 1.015 in.

Power Connector

The main lead power connector is shown in Figure 53. There are three such connectors for each motor. The main lead power connector consists of the power feed through, the bolted joint and the power connector housing.

The three power feed throughs are fabricated from oxygen free copper (OFC) rod for maximum conductivity and are individually brazed to their respective phase winding connection. The current density of the power feed through at the connection is approximately the same as that of the phase winding. The power feed through is electrically insulated from the motor housing via vespel bushings and is sealed with Viton "O" rings. The vespel material and the viton o-rings were selected because of their compatibility with the coolant oil (MIL-L-7808). The viton o-rings will maintain their elasticity when subjected to the coolant oil. The power feed through and the cable assembly is silver plated at the bolted joint to improve electrical conduction with the mating parts and to eliminate oxidation of the copper feed through. The power connector housing is fabricated from aluminum bar and has a polyurethane boot at its inside diameter to provide the necessary environmental seal and ground insulation.

2.5 Propulsion System Controller (PSC)

The controller must provide excitation control for the AC alternator in response to the prime mover speed so that the volts/hertz ratio of the alternator output is kept essentially constant. This provides required AC power to the motor for full output torque capability and variable speed proportional to the prime mover speed. System component characteristics are presented in other portions of this report.

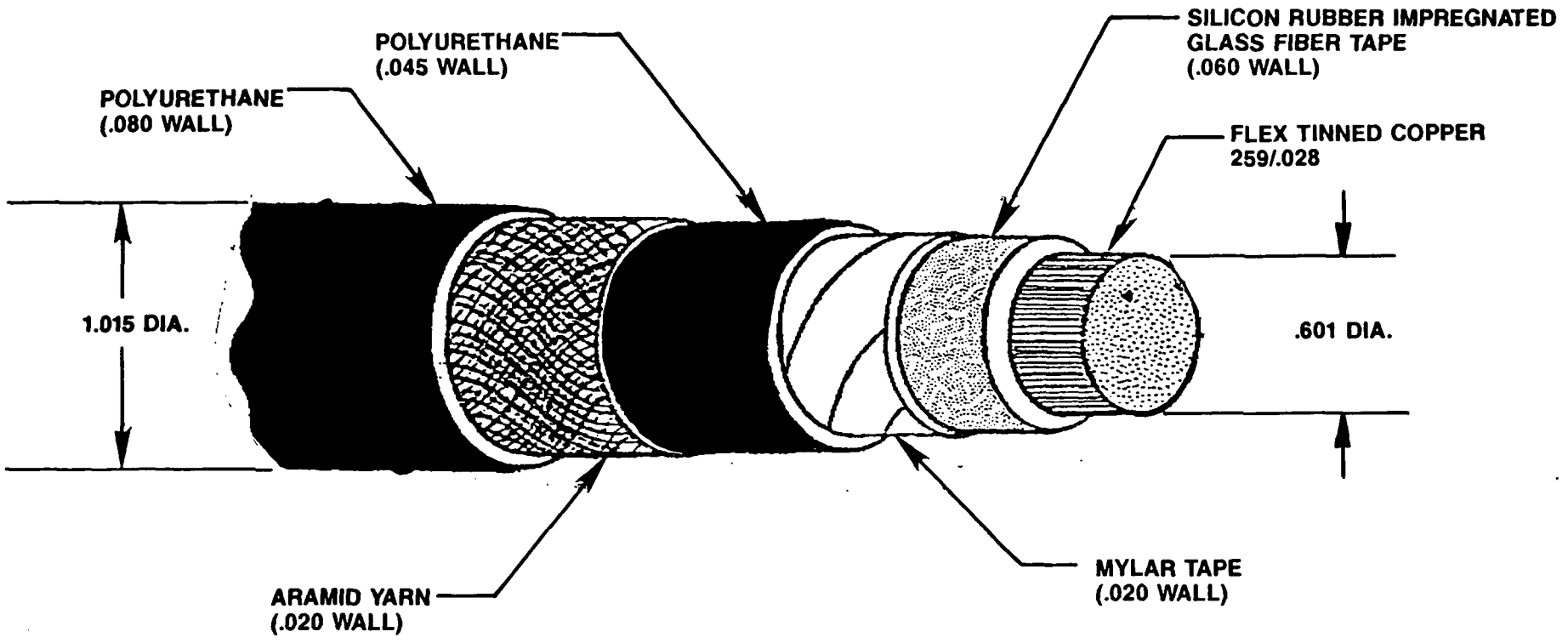

DIMENSIONS IN INCHES

Figure 52. Motor/Alternator Cable

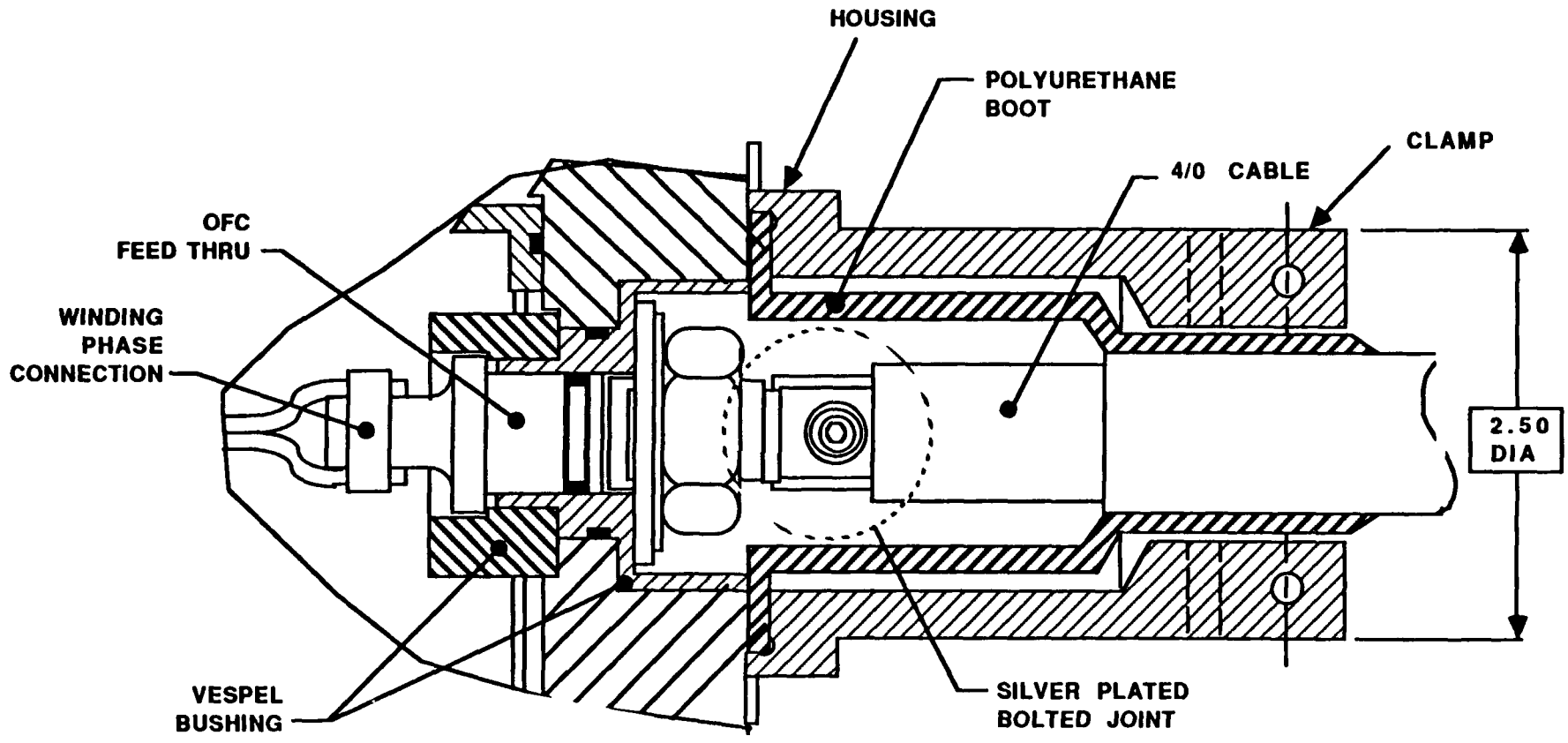

Figure 53. Main Lead Power Connector

In addition to the above requirements the controller must monitor and provide inputs to the display panel for the following parameters: component temperatures; motor RPM; start/stop or run action of this system in response to operator command; and fault indication and automatic shut-down to protect system hardware.

2.5.1 Performance Requirements

Inputs:

The controller shall have the necessary inputs to monitor the alternator and the motor/SDG critical temperatures which limit system performance. Motor RPM shall be monitored.

Provisions shall be made to start, stop and reliably safeguard the system during its operation. Multiple safeguards must be used to ensure positive system control under adverse malfunction.

The vehicle operator's actions (start, stop, speed adjust, etc.) and the automatic sequencing and control of each of the alternators and motors must be accommodated by the controller.

The alternator permanent magnet generator (PMG) shall be used as the volts/hertz reference signal for closed loop feedback control of the propulsion system.

Outputs:

The primary output of the controller shall be excitation current to the rotary exciter field located in the alternator. The current shall be an outcome of the closed loop control of the alternator output terminal voltage and the reference voltage (PMG output) representing the prime mover speed. This field excitation shall be satisfactory for system control from start-up through full load, load transient (as described below) and orderly shut-down.

The secondary outputs of the controller shall provide necessary drives to the control panel instrumentation for visual indication of temperatures, propulsor speed and operating modes as well as vehicle operator's activities.

System Stability:

The controller shall provide the above described system with alternator terminal voltage control to follow the reference signal to within +/- 3% of its linear operating range excluding transients. When load transients occur, a sightly underdamped (vs. overdamped) system response is preferable to improve response time. The prime mover accelerates the alternator from 4300 RPM to 9000 RPM in one second. The closed loop band width of this control system shall accommodate the response of the prime mover.

System Start-up:

The controller shall support the alternator operational speed range of 4300-9000 RPM as provided by the prime mover. At start up, the alternator speed shall be 4300 +/- 100 RPM. The propulsion system must start under the environmental conditions stated.

At room ambient conditions (20-25°C), the controller must provide the necessary alternator excitation to support a motor starting current of not less than 900 amperes RMS. The motor acceleration from 4300 to 9000 RPM shall be completed within five seconds to avoid thermal damage to the system components. Failure to start must be safely aborted. The start-up sequence can be repeated within the propulsion system safety protection limits.

Load Transients:

During the propulsion system's prime mover acceleration from start to full speed (corresponding alternator speeds of 4300 - 9000 RPM), the waterjet may experience transients ranging from no load to full load in 0.1 second. The controller must provide the necessary alternator excitation and subsequent output current to support the induction motor requirements resulting in continuous system operation. In addition, the instantaneous unloading of the waterjet shall not invoke a system shut-down or produce a damaging transient. A one time, one minute, 1.3 system overload must be supported by the controller hardware.

System Shut-down:

The controller shall provide an orderly shut-down of the propulsion system. It shall also provide for instantaneous operator initiated system shut-down. The controller shall have system safety/protection functions built in its hardware and shall include mechanical interrupt capability of the alternator exciter field current. This shall be accomplished with a relay having normally open contacts.

Acoustic Noise:

The controller hardware shall not emanate acoustic noise to the environment below 20 khz at intensities perceptible to the human ear 3 feet from the equipment.

Humidity and splash proof enclosure:

The controller hardware must be operational in the salt air environment and must have a splash proof enclosure as a minimum. Shelf life shall be considered in sheltered environment only.

A detailed description of the PSC requirements is contained in Appendix I, Interface Specification.

2.5.2 Approach

The specifications which were the key drivers of the electrical design will be reiterated along with the design impact.

The design drivers were the size/weight requirements (1 cubic foot and 20 pounds) and the requirement for safe shutdown in cases of various fault modes (overcurrent, overtemp, excessive start time, excessive motor slip). The size/weight limitations disallowed the use of conventional switchgear (circuit breakers, fuses, contactors). Monitoring of fault conditions is performed by a microprocessor interfaced to RTD's, current transformers, and tachometers. Shutdown of the regulator is done electronically with two backup modes of shutdown, the last being to physically open the 150V supply from the field regulator amplifier using a small vacuum relay.

The requirement of monitoring multiple points in the Propulsion System Controller (PSC) also drove the design to a microprocessor with a multiplexer and an analog to digital converter.

The characteristics of the alternator and field exciter and the induction motor established the starting and running power levels of the PSC. About 75 watts output is needed to run the motor at 9000 rpm with nominal load. About 800 watts is needed for starting. The controlled variable is the alternator voltage, which must follow the prime mover speed to keep constant V/Hz. The actuated variable is the exciter field current. For the motor to start in 3 seconds at a prime mover speed of 4300 rpm, the alternator/motor line current must reach 900 amps for an ambient start (25 degrees C). Exciter field current of 9 amps gives 1000A peak during ambient start and 800A peak during a hot start (150 degrees C motor). System modeling showed that for nominal alternator parameters, 7A exciter current is sufficient. A 9A current limit was used to assure a robust system with respect to system parameter variations.

The field regulator bus voltage was selected at 150V to enable the field current to be forced faster than the time constant of the exciter field (L/R=0.1 Sec). With 150V bus and 9 Ohm max field resistance, current limit can be reached in .08 second. This was selected to satisfy the worst case load transient. This transient was hypothesized to be the case of the waterjet coming out of the water (fully unloading) and then being put back into the water (fully loading). Whether this is realistic or not is not known at this time, but it is used as a design goal. If the waterjet is fully loaded instantaneously after being out of the water, the system only recovers from the transient if the waterjet was unloaded no more than 75% (25% remaining) and then full load reapplied. With a more realistic transient of going from no load to full load with a .1 second ramp time, the system can respond with a 100V bus and 6A. Since the actual worst case transient is not known, the 150V, 9A levels in the PSC will be used to assure robustness. See section on system modeling for more detail.

The available input source is 28VDC at a max power of 2KW. Since 150VDC bus is desired, some type of voltage step-up is needed. If the 28V was fairly constant and the load was fairly constant, the 28V could be chopped at a high frequency, put through a step-up transformer, rectified and filtered to obtain 150VDC. However, 28V can vary +/-4V and the 150V load can vary from 0.5A to 6A; therefore, regulation is needed. Output voltage will be sensed and compared to a reference; the error signal will be used to pulsewidth modulate the chopped AC waveform to compensate for line and load variations. The bandwidth of this boost converter should be much greater than the field regulator current loop bandwidth (50 Hz). 1 KHz open loop crossover is the design goal. The switching frequency should be at least 10X the bandwidth. Higher frequency, however, reduces the size of the magnetics and filter capacitors. 60 KHz was selected as a compromise between size and efficiency. The 2KW limitation on 28V power necessitates that the field controllers start sequentially since each requires greater than 1000W during the 3 second starting interval.

The alternator voltage must be controlled to follow the prime mover speed in order to maintain constant V/Hz in the induction motor. Since the prime mover can go from idle to full speed in about 1 second, the alternator voltage controller (field regulator) must have a bandwidth of at least 5Hz. To obtain this bandwidth for small signal perturbations, the main field pole (0.46Hz) must be cancelled with a lead network. An integrator was also used to zero the steady state error voltage. By controlling the integration constant (1/RC), the open loop crossover can be selected. The crossover is nominally 6.7 Hz. An inner current loop is utilized also to control exciter field current and limit the maximum exciter current to 9A. This inner loop crosses over at 67 Hz nominal (10X voltage loop).

In order to adequately control the field current, the regulator must be able to force current down as well as up (instead of merely freewheeling to zero with L/R time constant). A full wave, half-controlled power bridge is used (two mosfets and two diodes). The mosfets are pulsewidth modulated at a fixed frequency of 20KHz, just above the audible range.

Due to the close proximity of power circuits and low level analog and digital circuits, noise management had to be considered carefully. The following safeguards were implemented to prevent problems:

1. High current carrying conductors and their returns were run as twisted pairs to minimize radiator loop area.

2. All logic circuits are cmos technology, which has good noise immunity.

3. The logic circuitry was layed out with multilayer boards, including a ground plane and a power plane for low receptor loop area.

4. Three isolated grounds are used in the PSC to prevent ground loops and noise coupling.

5. Physical separation of power leads and harnesses from signal leads and harnesses was implemented to prevent crosstalk.

6. An LC filter was put in between the 28VDC source and the boost converter power bridge to reduce the switching frequency and its harmonics on the 28V source. This 28V source is the input for all of the DC to DC converters used on the various cards.

2.5.3 Boost Converter Description

The boost converter produces a constant 150VDC output voltage to be used by the field regulator. Regulation is provided against line changes of the 28VDC source (+/-4V) and load changes demanded by the field regulator (0.5A to 6A). Each block of the block diagram in Figure 54 will be described briefly.

The EMI filtering consists of an input LC filter. The inductor is 5UH at 50ADC with a resonant frequency in the megahertz region. The capacitor consists of six 1400UF aluminum electrolytics in parallel to satisfy RMS current requirements and two 30UF polypropylene capacitors (located right at the power mosfets) to offset line inductance at the high frequency components of the switching waveform. These high frequency capacitors keep the voltage overshoot at an acceptable value. A damping resistor (0.02 Ohms) is put in series with the choke to prevent oscillations due to negative input impedance of the converter. The EMI filter smooths the current in the 28 VDC source to reduce conducted and radiated emissions to other circuits within the PSC as well as other external equipment connected to the system 28V source.

The power mosfet full H-bridge consists of two power cubes, each one being a half-bridge with 72A RMS current capability. The mosfets are pulsewidth modulated at 60 KHz to provide a variable duty cycle AC square wave to the primary of the step-up transformer. The primary current is limited to 70A by the pulsewidth modulator. The transformer is a high frequency design, ferrite pot core with extremely low leakage inductance. This is necessary to push the required peak currents through the converter at the operating frequency and duty cycle. The secondary currents (as required by the field regulator) vary from 0.6A (steady state) to about 6A (motor starting). This translates to 5.4A to 54A peaks in the transformer primary.

The transformer output is rectified and filtered to obtain a smooth 150VDC output voltage. This voltage is sensed and sent to the voltage controller where it is used to generate an error signal. The error signal is used as input to the pulsewidth modulator to adjust the duty cycle.

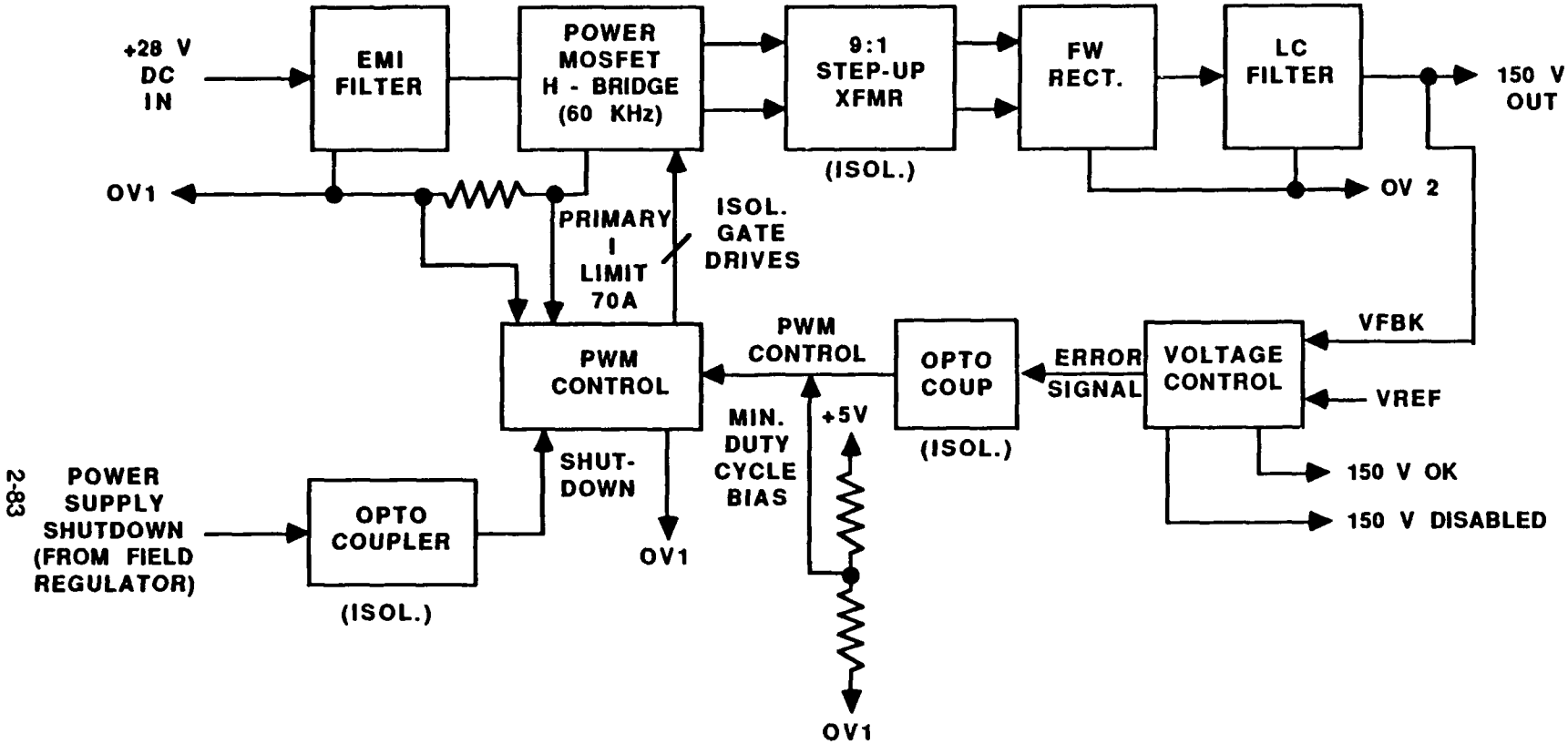

Figure 54. Boost Converter Block Diagram

It should be noted that three isolated grounds exist in the system; 0V1 is the system ground tied to the 28V source and the boost converter power bridge; 0V2 is the field regulator high voltage ground tied to the 150V bus and the exciter field; and 0V3 is the low level control and logic ground. Opto-couplers are used throughout the system to keep these grounds isolated from one another.

Three other signals, related to fault shutdown, can be seen in the block diagram. 'Power supply shutdown', from the field regulator, tells the boost converter to shutdown due to a failure in the main shutdown mode. The main shutdown mode is a regulator disable signal which turns off the current to the exciter field. When this fails, the 150V bus is instructed to shutdown by means of the 'power supply shutdown' signal previously mentioned. '150V disabled' signal tells the field regulator if this has been successful. If in a set time interval, neither the field current or the 150V have shutdown, the field regulator issues an 'abort' signal to the relay board. This opens up the 150V to the field regulator bridge by means of a vacuum relay.

The '150V OK' signal is a signal looked at by the logic card to prevent start-up of the regulator in event of low or high bus.

2.5.4 Field Regulator

The field regulator, see Figure 55 controls the alternator voltage by means of the exciter field current. The reference which the alternator voltage must follow is the permanent magnet generator (PMG) rectified average voltage, which is proportional to alternator and prime mover speed. The higher the required alternator voltage, the more exciter field current that must be supplied. The relationship is non-linear due to saturation of the various machines. 9A is the exciter field current limit set by the field regulator current controller.

The exciter field is pulsewidth modulated at 20 KHz by a full-wave, half-controlled mosfet bridge to obtain the requested current. The field current is sensed by a Hall effect sensor and sent to the current controller. The reference for the current controller is the error signal generated by the alternator voltage controller. The alternator voltage controller, which uses proportional plus integral control, compares the isolated voltage feedback signal from the power sensing box to the voltage reference, generated by the PMG. System shutdown, under normal and fault conditions, is controlled in the field regulator. The signal 'regulator enable', which comes from the logic card, is used to turn the field regulator on and off via the shutdown pin on the pulsewidth modulator. If the current does not decay to near zero in a set time interval, the field regulator sends a 'power supply disable' signal to the boost converter. It then waits to get a handshake ('150V off') verifying that the 150V bus has decayed to some lower voltage. If this handshake does not occur, the field regulator issues an 'abort' signal to the relay board. The relay board energizes a vacuum relay to remove the 150V from the field regulator bridge causing the alternator voltage to go to zero.

As in the boost converter, opto-couplers are used to maintain isolation between the various grounds in the system.

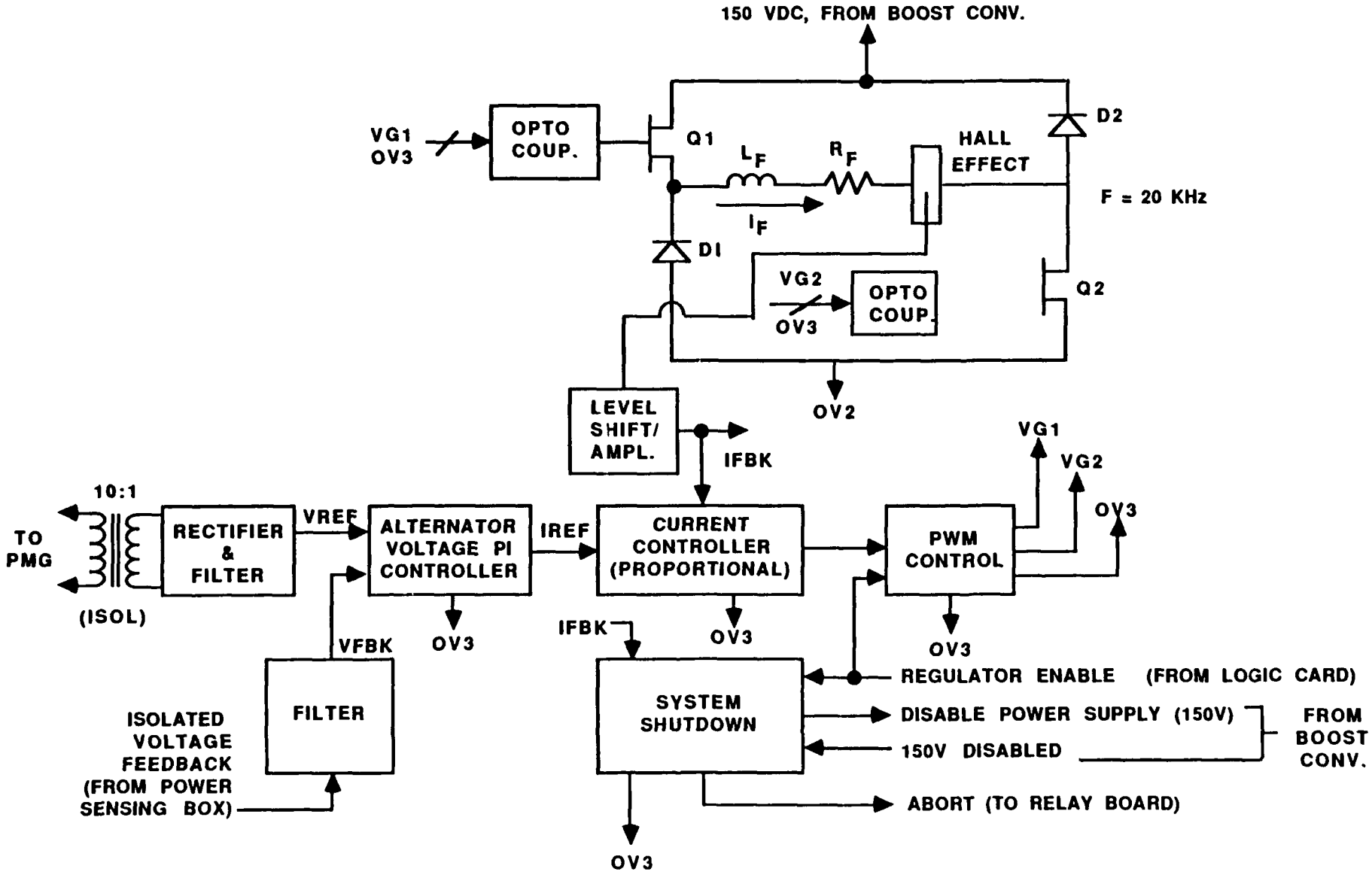

05/204/88/030-F

Figure 55. Field Regulator Block Diagram

2.5.5 Signal Conditioning Card

The purpose of the signal conditioning card is to provide circuitry which will condition the signal levels of the various sensors for conversion to digital data. This card consists of:

11	Identical RTD Circuits
1	Instrumentation Amplifier Circuit
2	RMS-to-DC Circuits, Each with a Post-Amplifier
1	16-Channel Signal Multiplexer (MUX)
1	1 Bridge Excitation Regulator

A block diagram of the Signal Conditioning Card is shown in Figure 56.

The RTD circuits condition the signals from the temperature sensors. There are four alternator stator RTD's, six motor stator RTD's and one motor oil temperature RTD. Each circuit consists of a current source to excite the RTD, a filter to provide noise immunity, a differential amplifier, and a level-shift/gain stage which subtracts an offset and provides amplification. Each RTD circuit output goes to the MUX. Additionally, the output of the motor oil temperature RTD circuit leaves the card as a separate line to the logic card.

The instrumentation amplifier circuit conditions the motor oil pressure signal from a pre-amplifier embedded in the motor. It provides amplification and filtering. The output of this circuit goes to the MUX and also leaves the card as a separate line to the logic card.

The RMS-to-DC circuits convert the AC signals from the current sensors to a DC signal which can easily be digitized. These circuits, by the nature of the AC to DC conversion process, also provide signal filtering. Each circuit also has a post amplifier which provides additional signal amplification.

The 16 channel mux provides a means for one A-to-D converter to digitize up to 16 different signals. The signal to be digitized is selected by a 4-bit digital code outputted to the MUX by the logic card.

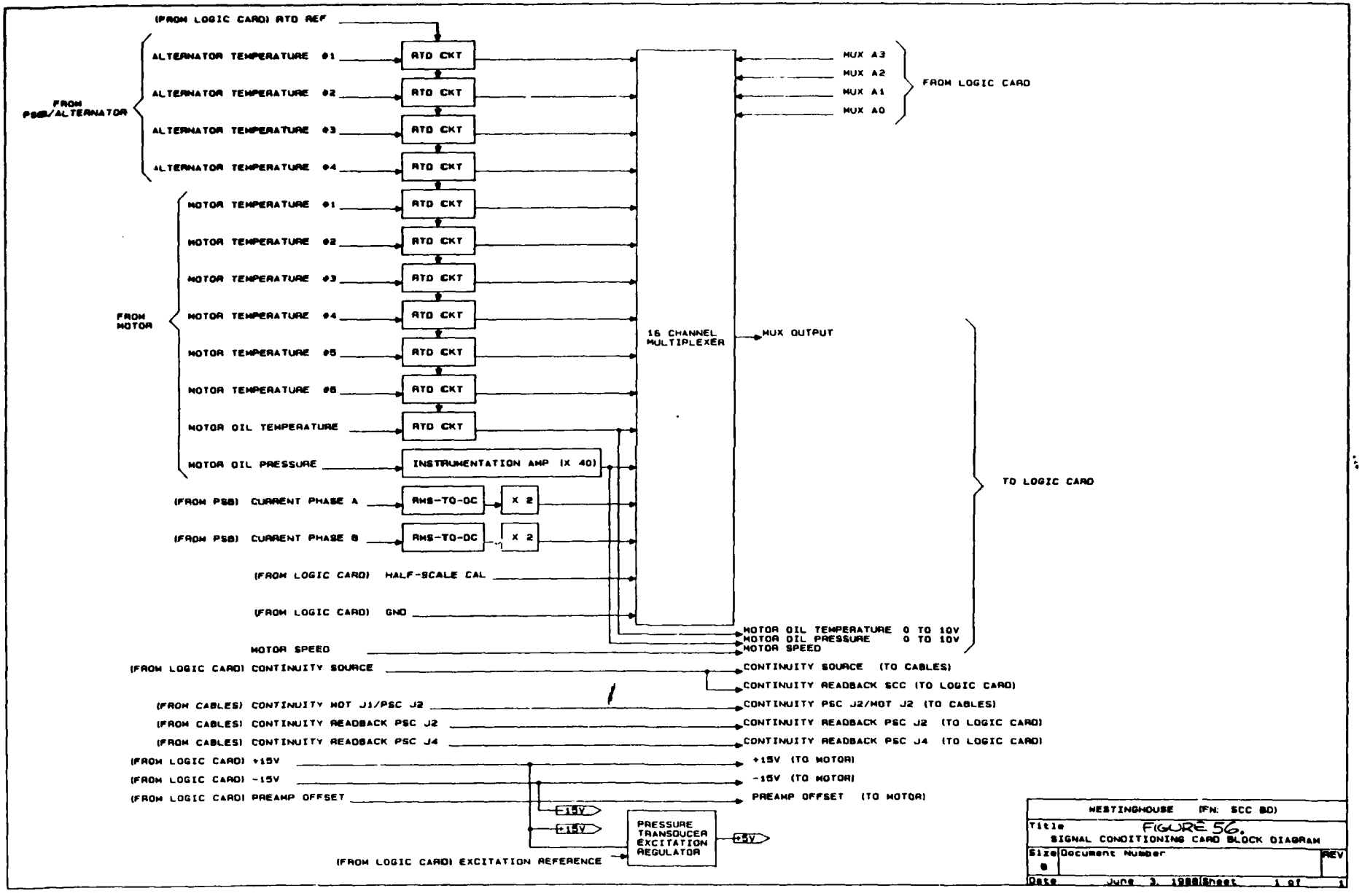

05/204/88/84

Figure 56. Signal Conditioning Card Block Diagram

The bridge excitation regulator converts +15V to +5V to provide excitation for the motor oil pressure transducer. This regulator is protected against a short circuit on its output.

2.5.6 Logic Card

The Logic Card provides circuitry to implement the following functions:

- o Control of PSC operating modes
- o Interface to vehicle controller
- o Monitoring of alternator/motor system status
- o Control of REGULATOR ENABLE signal
- o Communication of system status to vehicle controller

A block diagram of the Logic Card is shown in FIGURE 57. A description of each block is as follows:

VEHICLE CONTROLLER INTERFACE: This interface allows the vehicle controller to control PSC operation and to receive system status. The inputs/outputs of this block are optically-isolated from the vehicle controller.

SEQUENCER: This block provides circuitry to sequence the PSC operating modes. It also generates the REGULATOR ENABLE signal based on operating modes and fault status.

WATCHDOG CIRCUIT: The purpose of this circuit is to provide fault tolerance in the event of a microcontroller hardware/software failure. If the microcontroller fails to reset this circuit within a specified time period, it will cause the sequencer to disable the regulator.

CLOCK/RESET CIRCUIT: This circuit provides 3 crystal oscillator-based clock frequencies: 6 MHz, 3 MHz, and 1 MHz; additionally, it provides a clock synchronized power-on reset circuit. The clock synchronization keeps circuitry reset until the clock has started.

MICROCONTROLLER/ADDRESS LATCH/DECODER: This block is the central element of the Logic Card. The microcontroller is responsible for executing system software and determining fault status. Additionally, it contains:

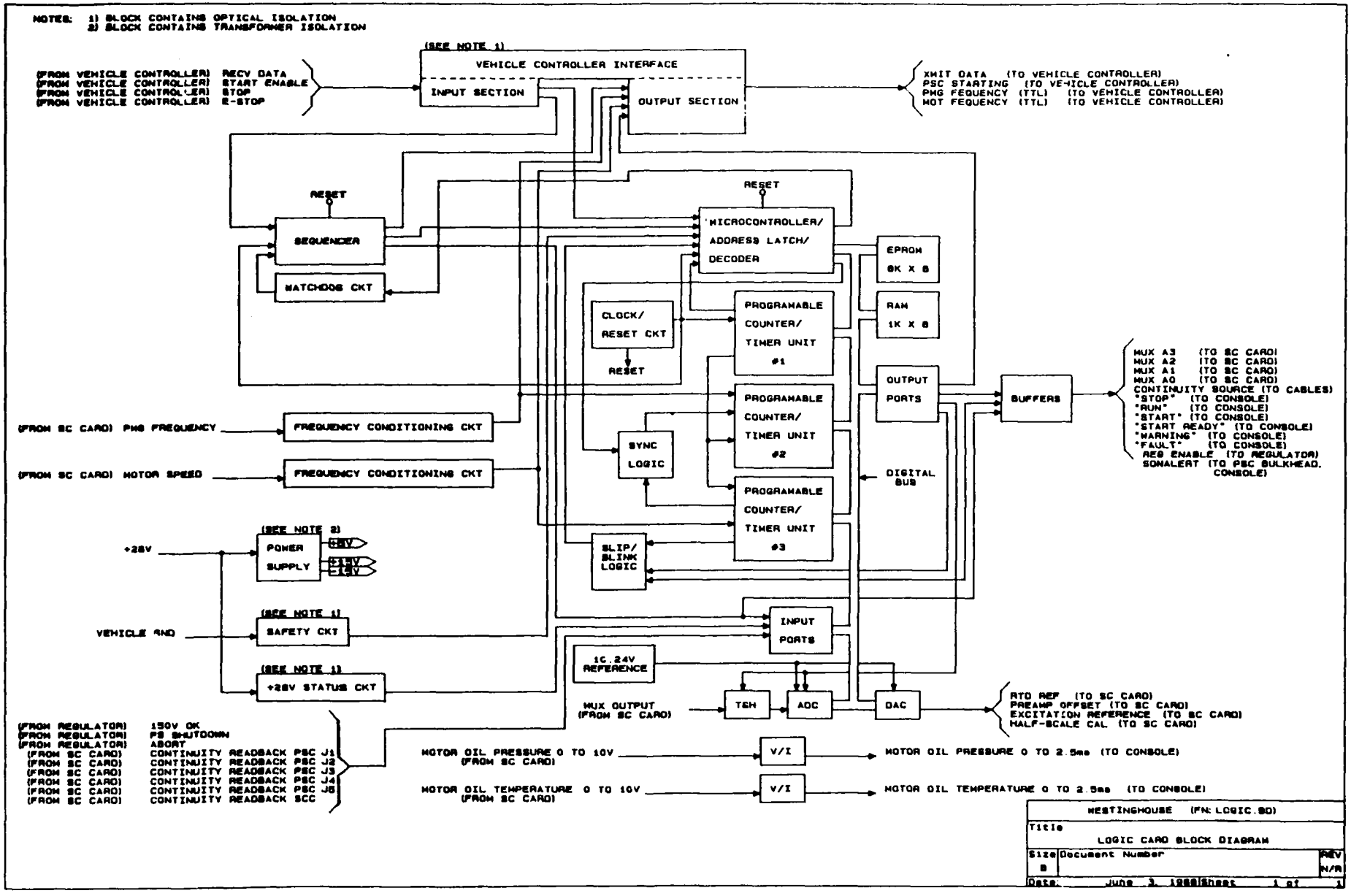

Figure 57. Logic Card Block Diagram

- o An onboard serial port with interrupt for status communication to the vehicle controller
- o A nine bit input/output port
- o Two 16 bit counter/timers, each with one interrupt
- o Two additional interrupts
- o Bus control logic
- o 128 bytes of RAM

The address latch and decoder provide the additional logic required to control activity on the digital data bus.

EPROM: This block consists of the single I.C. used to store the software program.

RAM: This block consists of the single I.C. used to store temporary data values generated during the execution of the program.

FREQUENCY CONDITIONING CIRCUIT: This block provides signal conditioning to translate the input voltage to TTL levels. It also provides filtering and hysteresis to increase noise immunity.

PROGRAMMABLE COUNTER/TIMER UNIT (PCTU) #1: Provides 300 KHz and 1 KHz clocks.

PROGRAMMABLE COUNTER/TIMER UNIT #2: Provides 1 counter to scale the PMG frequency and 1 timer to measure its period.

PROGRAMMABLE COUNTER/TIMER UNIT #3: Provides 1 counter to scale the motor frequency and 1 timer to measure its period. An additional counter is used to generate the blink frequency of the "WARNING" lamp.

SYNC LOGIC: Provides circuitry to synchronize PCTU #2 with PCTU #3 so that slip can be measured.

SLIP/BLINK LOGIC: Provides circuitry to implement slip interrupt and "WARNING" lamp blinking functions.

INPUT PORTS: Provides a means of inputting parallel digital data into microcontroller.

OUTPUT PORTS: Provides a means for the microcontroller to output parallel digital data.

BUFFERS: These circuits increase drive capability for output signals that leave the card.

T&H (TRACK AND HOLD): This circuit, when commanded, holds an analog signal value constant so that it can be digitized.

ADC (ANALOG TO DIGITAL CONVERTER): Provides a means to convert analog signal information into digital data for use by the microcontroller. The ADC has a resolution of 8 bits.

DAC (DIGITAL TO ANALOG CONVERTER): Provides a means for digital data from the microcontroller to be converted into analog signals. The DAC has a resolution of 8 bits.

10.24V REFERENCE: Provides a scaling voltage for the ADC and DAC such that each bit of digital data is equivalent to 40 mV of analog signal.

V/I: This circuit converts a signal voltage into a proportional current for use in driving an analog panel meter.

POWER SUPPLY: This is an on-card DC-to-DC converter which converts +28V to +5V, +15V, and -15V.

SAFETY CIRCUIT: This circuit alerts the microcontroller when an excessive voltage exists between VEHICLE GND and PSC GND. The microcontroller will respond by beeping an audible alarm both in the PSC and at the test console. Additionally, a warning message will be sent to the vehicle controller. The purpose of this circuit is to protect personnel during PSC service operations and to alert operators of the existence of a hardware fault.

+28V STATUS CIRCUIT: This circuit alerts the microcontroller when the primary DC voltage is outside a specified boundary. The microcontroller will respond by sending a warning message to the vehicle controller.

2.5.7 Microcontroller Software Description

The PSC software has two primary functions:

1. Control of the REGULATOR ENABLE signal based on the status of system sensor signals with respect to limits.

2. Communication of fault status to the vehicle controller.

The PSC has three modes of operation: PRESTART, START, and RUN. Mode control is performed by the sequencer, which is a separate hardware block from the microcontroller. The software is mode dependent, however, and the microcontroller must monitor the mode command inputs from the vehicle controller.

The rationale in having a sequencer in addition to the microcontroller (which could have easily performed the mode control directly) is that a level of hardware redundancy is provided. This redundancy provides fault tolerance to a single point failure if it occurred. If there is a software fault, mode control will not be chaotic, since it is performed in a separate hardware block. Alternately, the sequencer does not have absolute control over start-up; it is dependent on microcontroller-generated start ready and fault signals. The microcontroller provides the means to monitor the sequencer's start timer and regulator enable output. If a hardware fault occurs in the start timer, the microcontroller can provide a fault signal to the sequencer which will disable the regulator.

The software for the PSC can be partitioned into two major sections:

1. The main program, which performs the two primary functions described above.

2. The data acquisition section, which determines the status of the system sensor signals with respect to limits.

Note that both sections of the software are mode dependent.

A flowchart for the software is shown in FIGURE 58 (a), (b), (c) and (d). At the beginning of the main program, the microcontroller sets up its internal registers and peripheral devices. It then enters the PRESTART mode. Its first action in this mode is to start a 10 ms sampling timer. It then enters a data acquisition subroutine, where it samples a set of PRESTART parameters and compares them to limits appropriate for that mode. If a parameter is sampled and a WARNING limit is exceeded, a WARNING flag for that parameter is set. If, additionally, a FAULT limit is exceeded, that parameter will be sampled two more times immediately after the first. If the FAULT limit is exceeded on all three samples, then a FAULT flag is also set. The microcontroller then finishes acquiring data for the rest of the PRESTART parameters and exits the subroutine. When it re-enters the main program, it checks to see if any WARNING/FAULT flags were set. IF any FAULT flags are set, the microcontroller will jump to a shutdown routine. The shutdown routine will disable the regulator and send FAULT status to the vehicle controller/CRT. There is no great significance to this in the PRESTART mode, since the regulator remains disabled until the START mode. However, it does mean that the command to start the motor will be ignored until all faults have been cleared. If any WARNING flags are set, the WARNING lamp will be flashed.

The microcontroller will continue to execute the main program. It will exit the PRESTART mode when there are no faults and the mode-select criteria for the START mode have been met. Otherwise, it will continue to loop in the PRESTART mode, acquiring sensor data on a 10 ms interval.

The START and RUN modes operate analogously to PRESTART with these distinctions:

- The parameters samples and their limits are functions of the mode.
- Entering the shutdown routine because of a fault will cause a jump back to PRESTART.
- The non-synchronizable parameter, slip, is measured. Its sampling interval is variable in length and the beginning of this interval is random. Because of this, the microcontroller samples it on an interrupt basis.

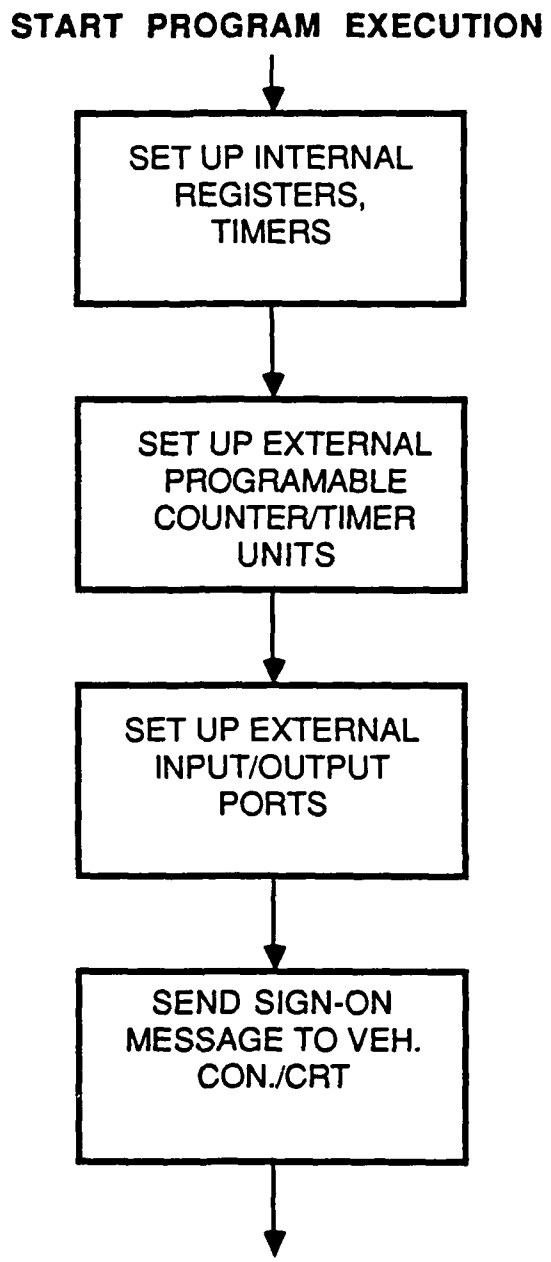

Figure 58. (a) Microcontroller Software Flow Chart

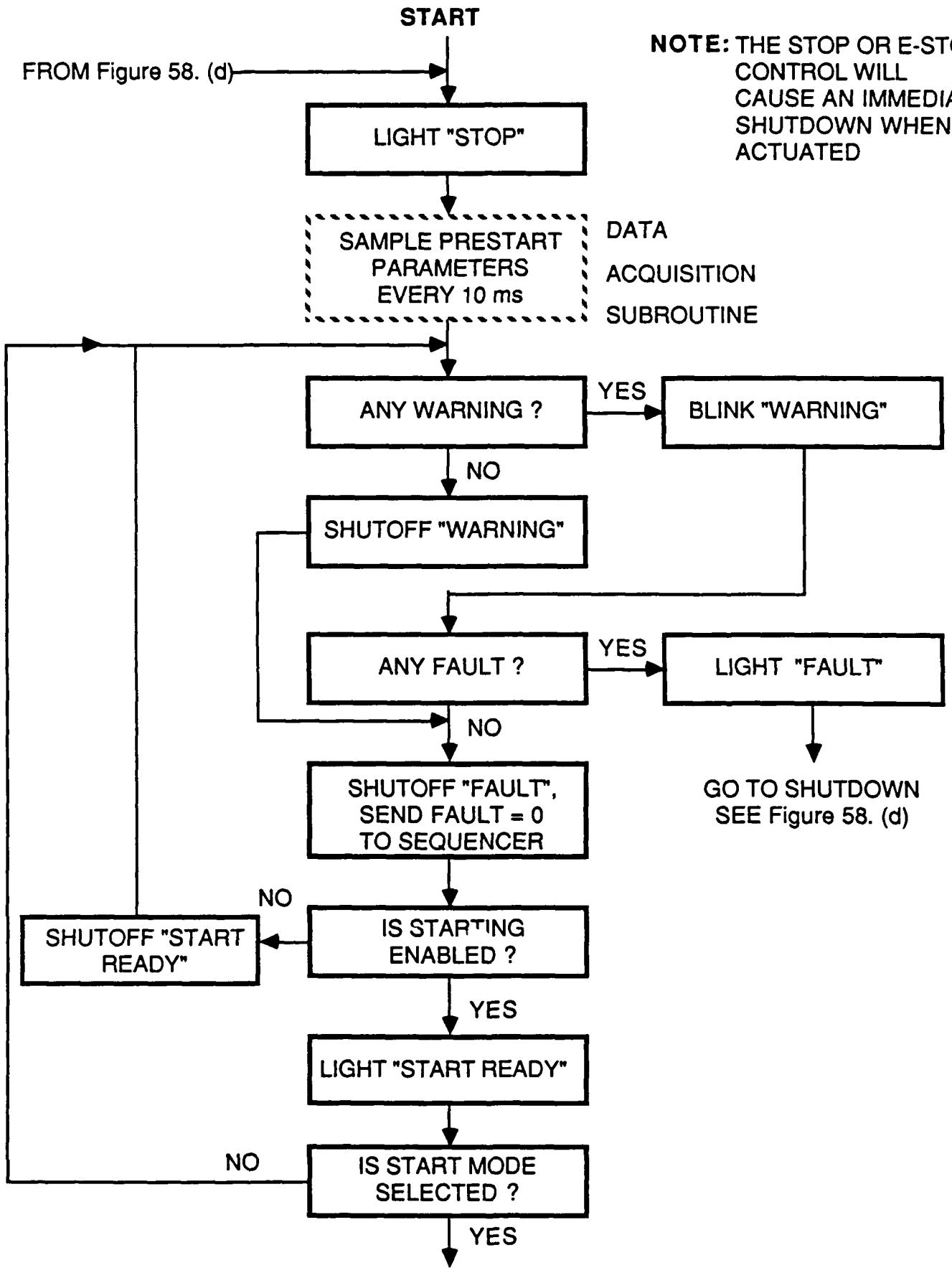

05/204/88/066-A

Figure 58. (b) Microcontroller Software Flow Chart (Prestart Mode)

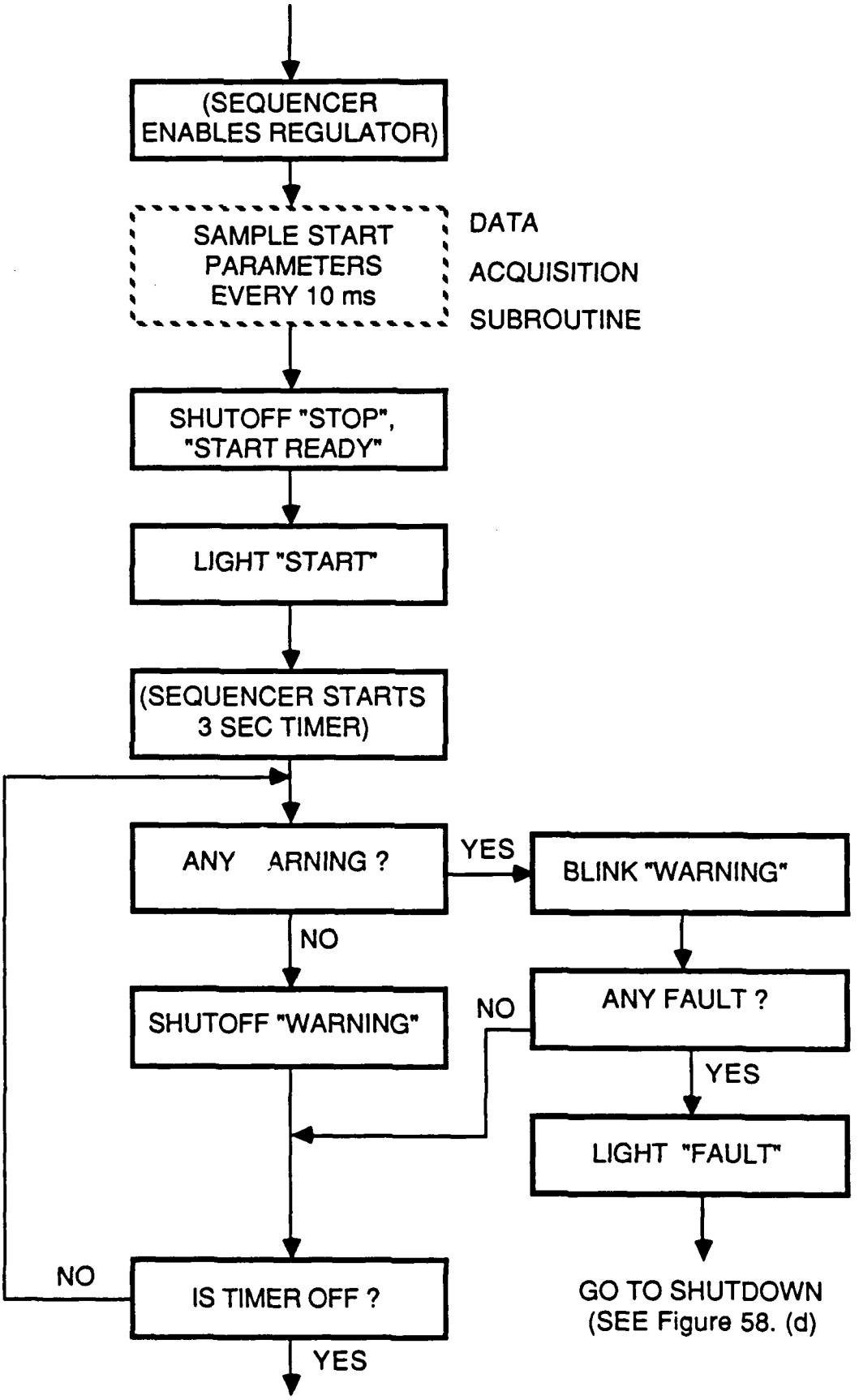

05/204/88/065-A

Figure 58.(c) Microcontroller Software Flow Chart (Start Mode)

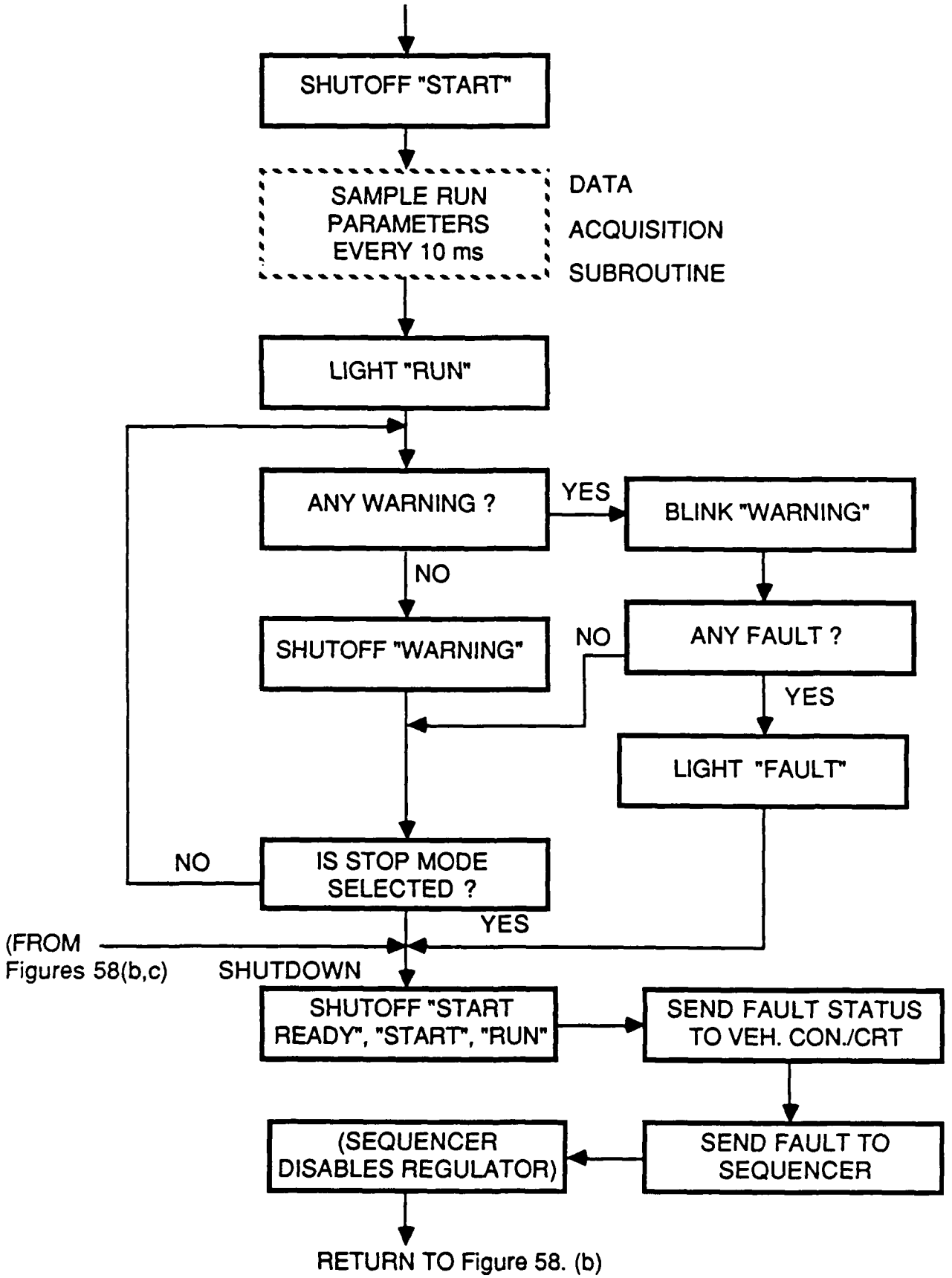

Figure 58. (d) Microcontroller Software Flow Chart (Run Mode/Shutdown Sequence)

2.5.8 Boost Converter Stability Analysis

The boost converter must be able to respond to any load demands put on it by the field regulator current loop. This loop has a bandwidth of 66 Hz. To insure response a boost converter closed loop bandwidth of 5 to 10 times 66 Hz is required, thereby minimizing interaction with the field regulator. One KHz was the design goal.

The control diagram of the converter is shown in Figure 59. The complex poles of the converter's LC filter occur at 196 Hz for nominal components (CF=1300UF,LF=500UH). This frequency moves to 160 Hz for the max tolerance on the capacitor (+50%). The control philosophy is to approximately cancel the LC filter poles with two lead networks and to use an integrator to zero steady state error. Figure 60 shows the open loop bode plot of the converter with the extremes of CF. The compensator lead networks place zeroes at 160 Hz and 190 Hz. The LC filter poles are located between 160 Hz and 196 Hz. The two extreme crossovers are shown at 828 Hz and 1.2 KHz with corresponding phase margins of 88 and 92 degrees. Sufficient bandwidth and stability have been realized.

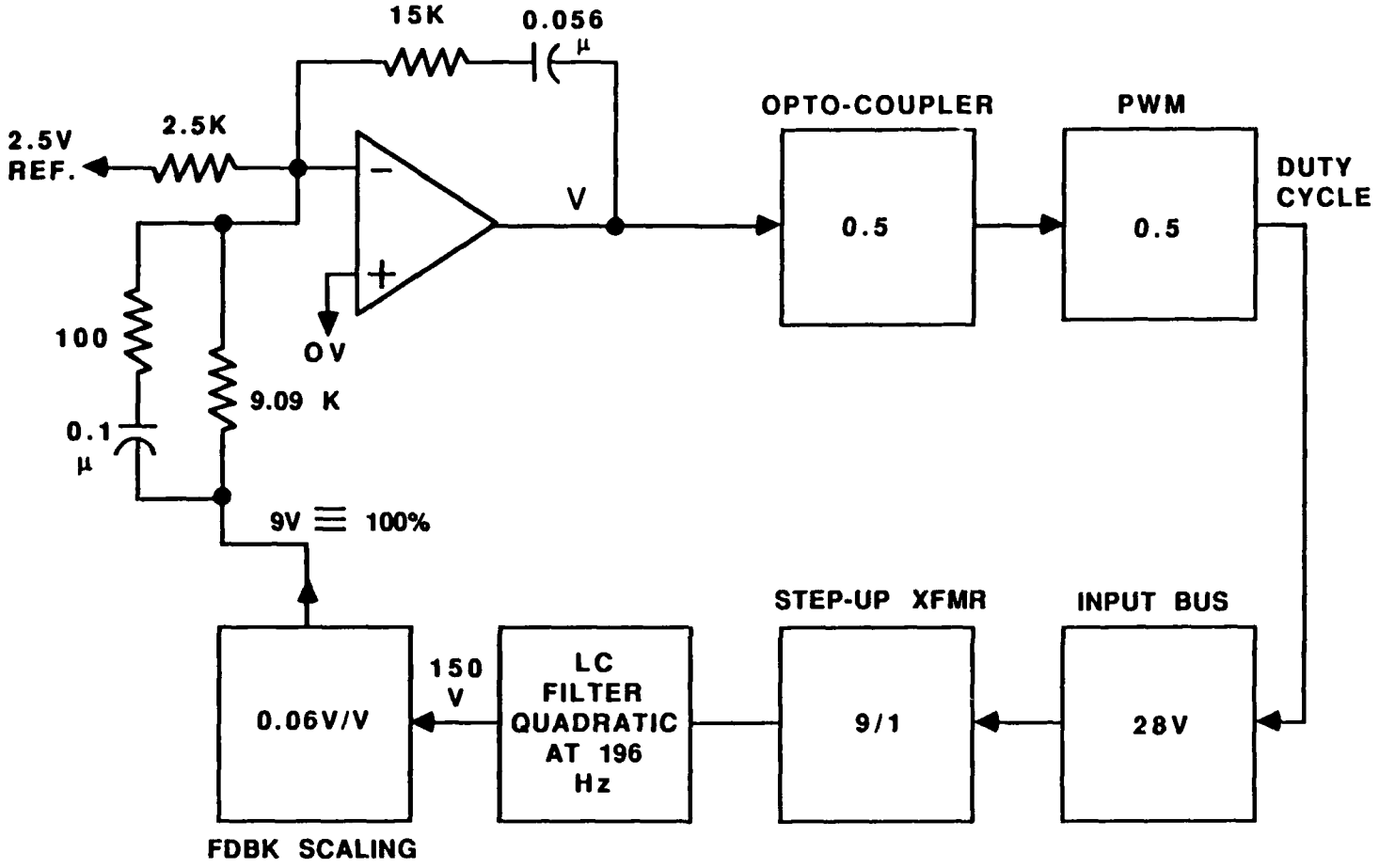

$$\text{T.F.}_{\text{Open Loop}} = \frac{\overbrace{[\,(9.09k \times 0.056\mu)^{-1} \times 0.5 \times 0.5 \times 28 \times 9 \times 0.06\,]}^{6187} \times \left(1+\frac{S}{2\pi \times 255}\right)\left(1+\frac{S}{2\pi \times 190}\right)}{S \times (\text{Quadratic at 196 Hz})}$$

$$F_{co} \simeq 1 \text{ KHz}$$

Figure 59. Boost Converter Voltage Loop Control Diagram

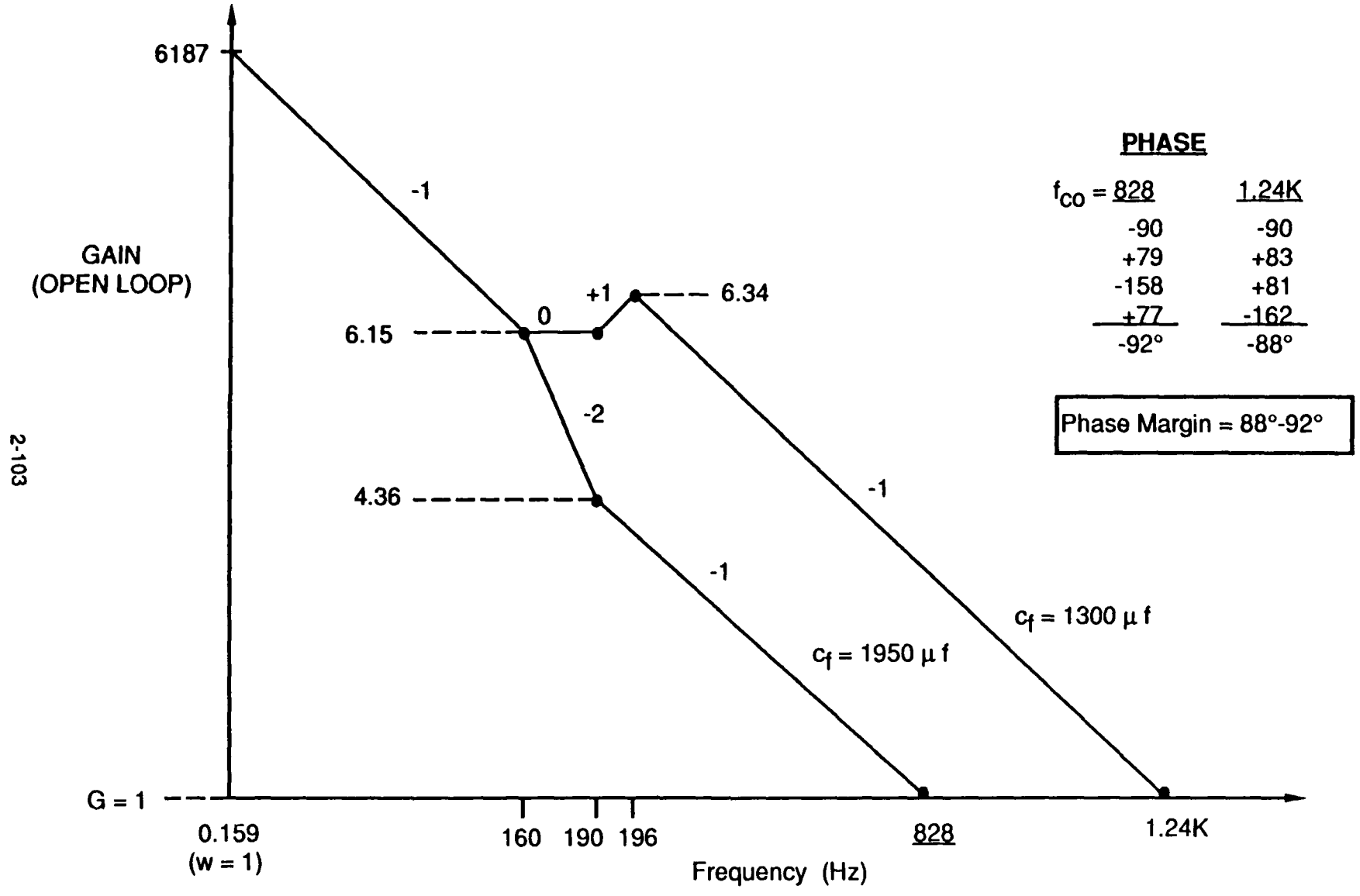

Figure 60. Boost Converter Bode Plot

2.5.9 Field Regulator Small Signal Stability Analysis

The alternator voltage controller (field regulator) must respond to prime mover changes on the order of 1 Hz frequency. Five to ten times this frequency is therefore required as a closed loop bandwidth of the controller. Figure 61 shows the control diagram. The current loop pole and the voltage filter pole are both located more than 10 times the open loop crossover frequency and thus can be ignored for the analysis. The only time constant which affects the response is the main field time constant (2.88 RAD/SEC or .46 Hz). The control philosophy is to cancel this pole with a lead network at 2.8 RAD/SEC, and to use an integrator to zero steady state error. The required crossover can be obtained by adjusting the integration constant (1/RC) of the controller. Figure 62 shows the bode plot of the resultant system with an open loop crossover of 6.7 Hz. The final compensated system looks like a simple integrator with phase margin of 90 degrees.

The inner loop (current controller) control diagram is shown in Figure 63. The single time constant of the system is the exciter field L/R time constant. Proportional control is used since some current error is acceptable. The gain of the current error amplifier is adjusted to obtain the required bandwidth of 66 Hz. This can be seen in Figure 62.

2.5.10 Mechanical Packaging

The propulsion system controller, see Figure 64, is assembled in an aluminum box with a removable heat sink on one side. The overall dimensions of the box are 10.06 wide by 13.00 high by 12.00 deep. Further dimensional information can be found on the ICD drawing E77857.

The high power elements of the circuit are mounted directly on the heat sink. Boost converter and field regulator PWB's are also mounted on the heat sink to minimize lead lengths in these circuits. Heavy components are mounted to the heat sink or walls of the box keeping the PWB's light and capable of enduring the shock loads. This arrangement is also convenient for testing the boost converter and field regulator circuits since the entire unit can be removed from the box giving easy access to all components.

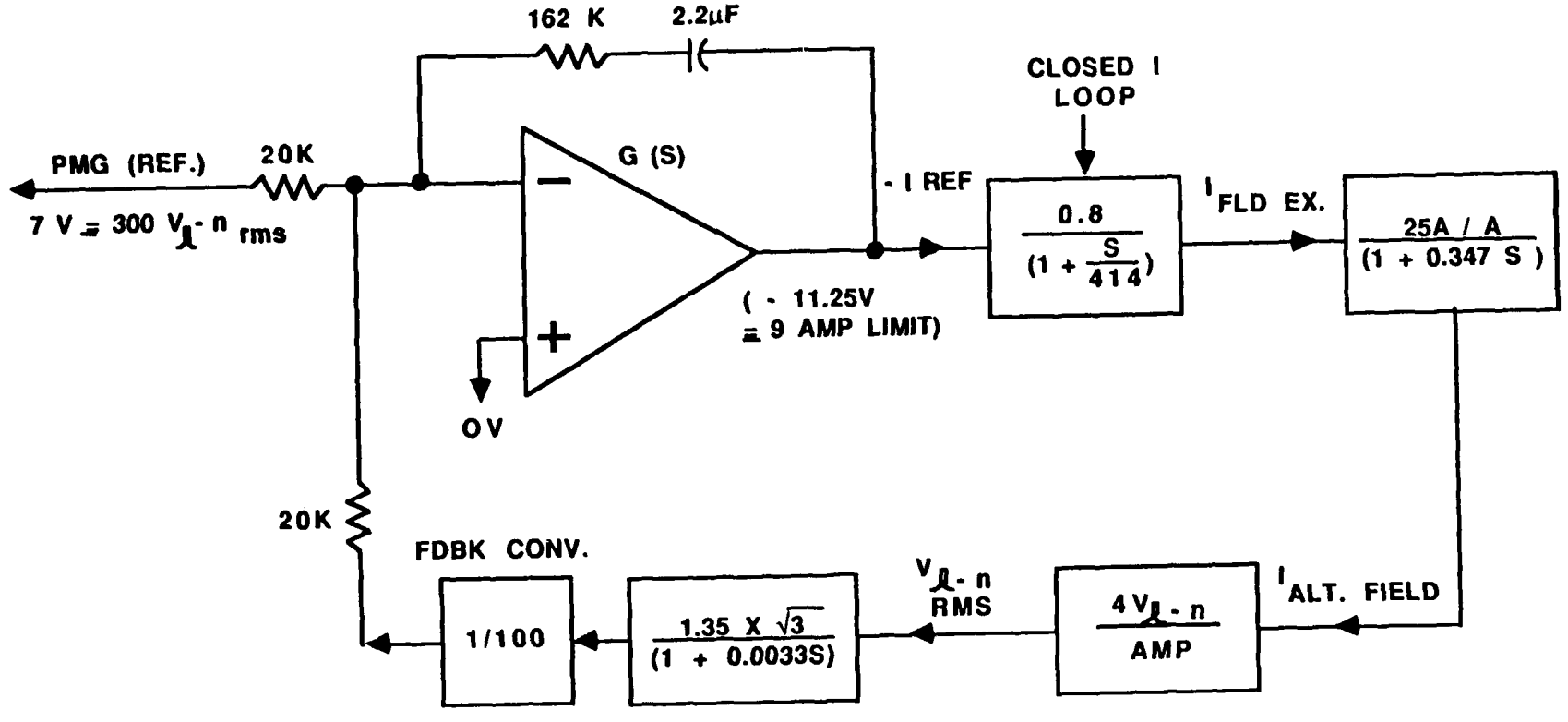

$$TF = G(S) \times \frac{1.87}{\left(1+\frac{S}{414}\right)\left(1+\frac{S}{2.88}\right)\left(1+\frac{S}{303}\right)} \cong \frac{\left(1+\frac{S}{2.8}\right) \times 23}{S} \times \frac{1.87}{\left(1+\frac{S}{2.88}\right)}$$

$$= \boxed{\frac{42.5}{S}} \qquad F_{co} \simeq 6.7 \text{ Hz}$$

Figure 61. Alternator Voltage Loop Control Diagram

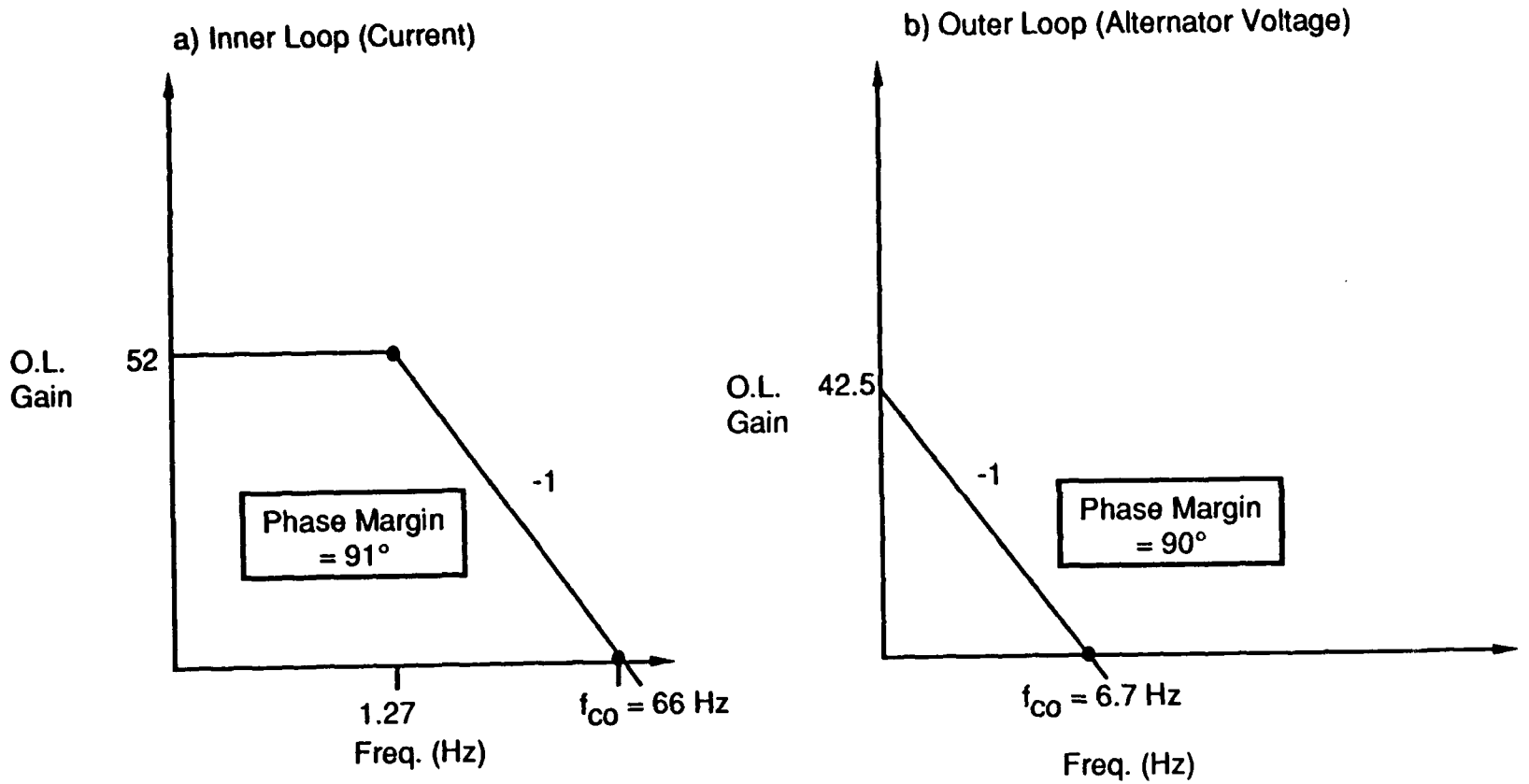

Figure 62. Field Regulator Bode Plots

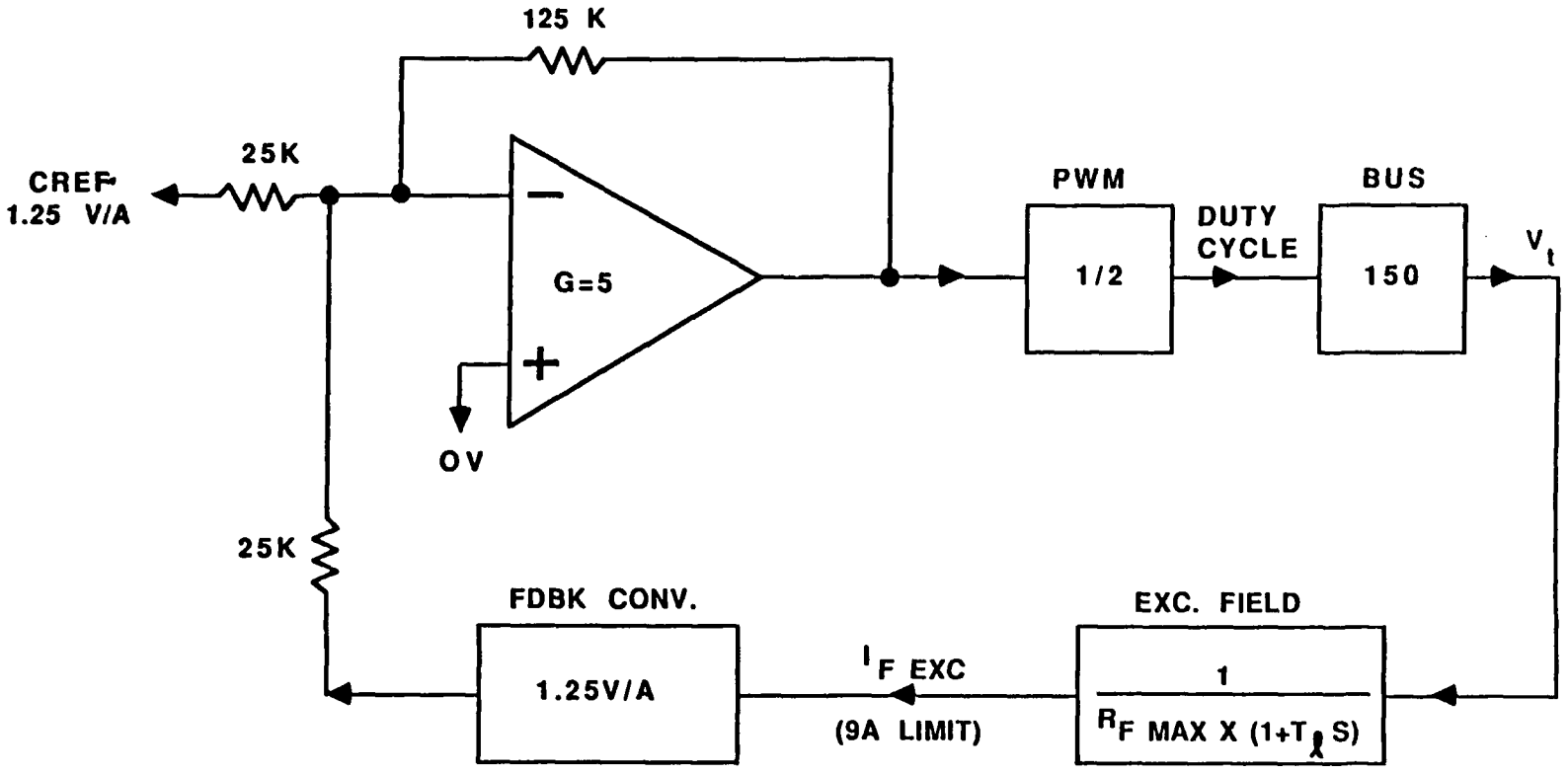

$$TF_{O.L.} = 5 \times 1/2 \times 150 \times 1/9\Omega \times 1.25 \times \frac{1}{R + S/8}$$

$$= \boxed{\frac{52}{(1 + S/8}} \qquad (8 \frac{RAD}{SEC} = 1.27\ Hz$$

$$F_{co} \simeq 66\ Hz$$

Figure 63. Current Loop (Inner Loop) Control Diagram

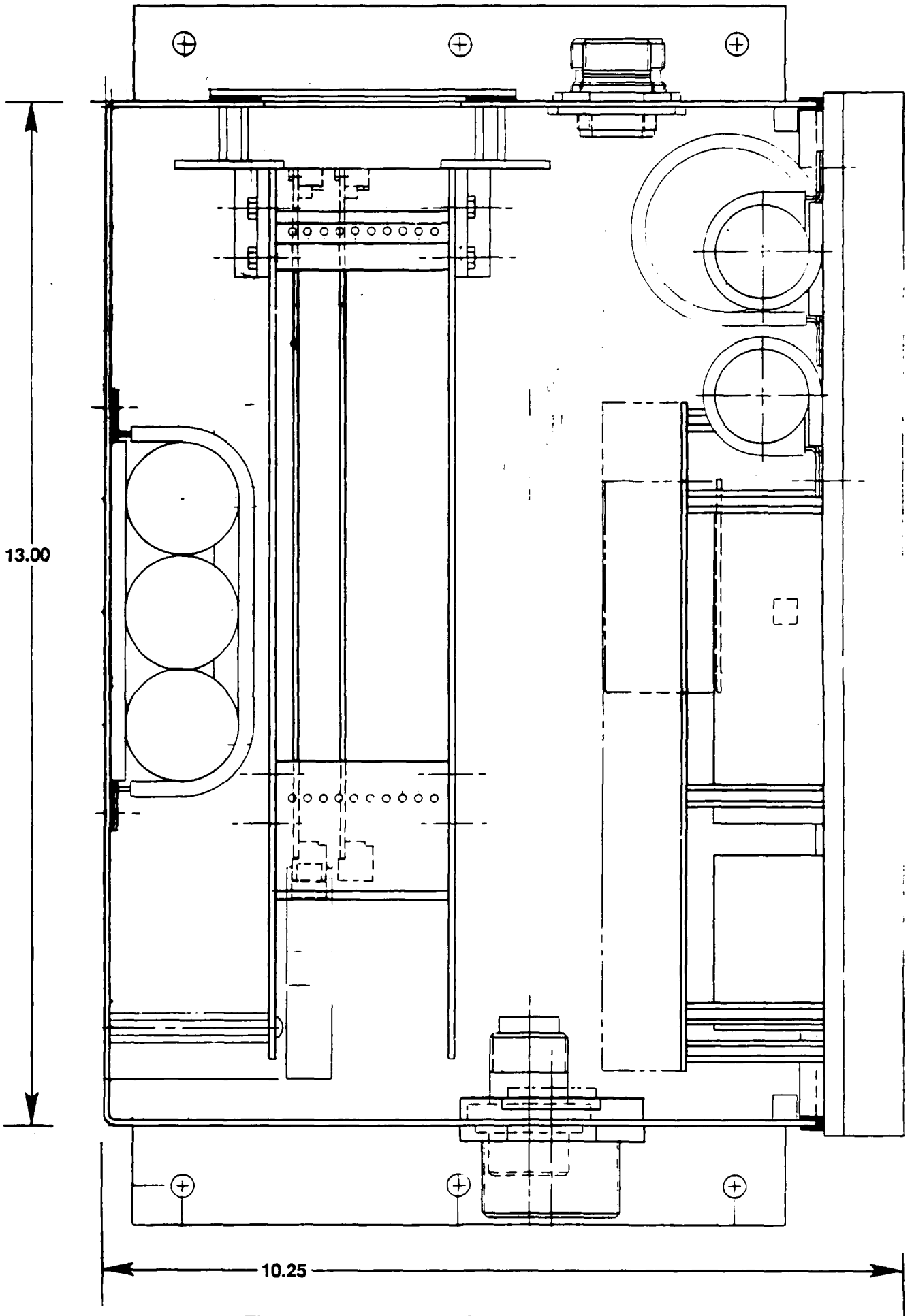

Figure 64. Propulsion System Controller

The signal conditioning card and logic card are mounted in a standardized aluminum/plastic card rack which is mounted inside the box. This gives the PWB's adequate support for the shock loads. A removable cover over the card rack makes it possible to instack extender cards for testing purposes. The rack has one spare card slot.

The box has been fabricated from aluminum to minimize weight. Commercially available boxes were investigated but could not meet the requirements for volume. The cover and heat sink are sealed to keep out dust and fluids.

2.5.11 Thermal Analysis

A thermal analysis was performed on the power circuitry located on the extruded heatsink. This consists of the boost converter power bridge and the field regulator power bridge. One computer program calculates the power losses of the power components for the inputted operating conditions and a second program calculates the junction temperatures of the power semiconductors. Two conditions were examined; steady state operation at top speed was looked at (2-3 amps exciter field current), and a restart condition where the system was restarted (9 amps exciter current for 3 seconds) after steady state temperatures had been reached. All semiconductor junctions were well below 125 degrees C (150 degree C rated) for the worst case condition of restart. The details of the analysis and the actual temperatures are included in Appendix 7.

In the thermal analysis of the system, all the heat generated remotely from the heat sink was treated as flowing through the top and bottom and two sides of the PSC box. With a total heat load of 28 watts the wall temperature was calculated to be 66°C (in a 50°C environment). This is well below the 85°C rating of the electronic components. Based on this result more complex analysis of the heat transfer process inside the box was considered unnecessary.

2.5.12 Power Sensing Box (PSB)

The Power Sensing Box, see Figure 65, contains the hardware for sensing the alternator phase current for both load and fault monitoring and the hardware for sensing the terminal voltage (feedback voltage) for the volts/hertz regulator. The PSB is located on top of the alternator and is mounted to the power terminal board. The electrical schematic of the current sensing hardware is shown in Figure 66. The stepdown current transformers are custom designed and fabricated to fit within the PSB. The transformers are wound with a 2000:1 turns ratio. The output of each is connected to a burden resistor whose signal goes to the Propulsion System Controller (PSC). Since a three wire system is used between the alternator and the induction motor, only two current transformers are required to monitor the three phase power (the vector summation of the phase currents is zero).

The electrical schematic of the voltage feedback signal that is sent to the volts/hertz regulator is shown in Figure 67. The three phase voltage transformer, a full wave bridge rectifier and the burden resistor are also mounted in the PSB. The transformer has a 50:1 stepdown ratio. The rectifier and burden resistor convert the transformer output to a DC signal which goes to the volts/hertz regulator.

The power cables connecting the alternator to the motor are fed through grommets located on the PSB. The input and output wires for the current and the voltage sensing circuits are soldered to connector receptacles mounted on the PSB wall. The RTD (Resistance Temperature Detector) probes that sense alternator temperatures are held in place by compression fittings on the PSB. The RTD output wires are soldered to a second connector receptacle also on the PSB.

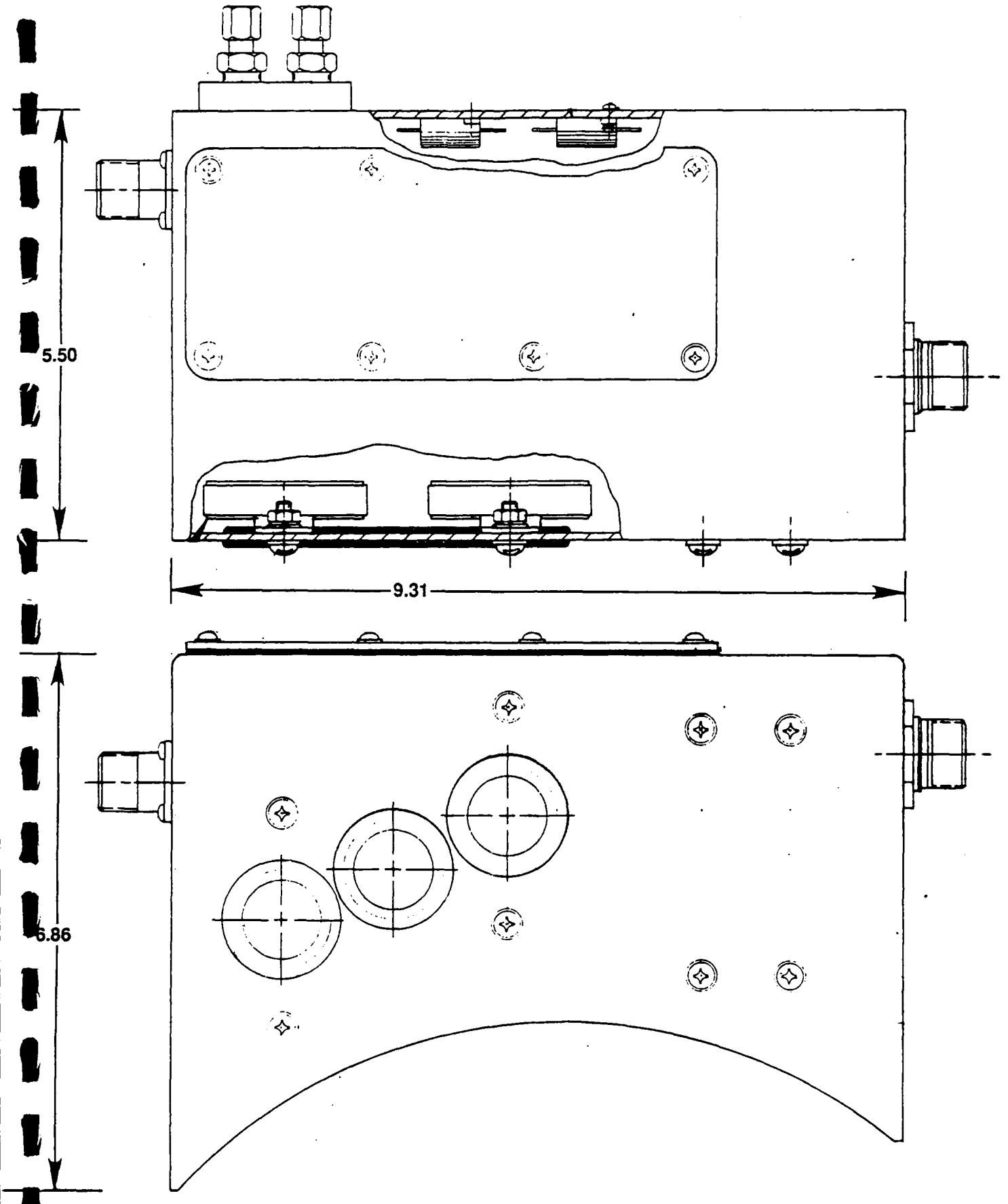

05/204/88/079

Figure 65. Power Sensing Box

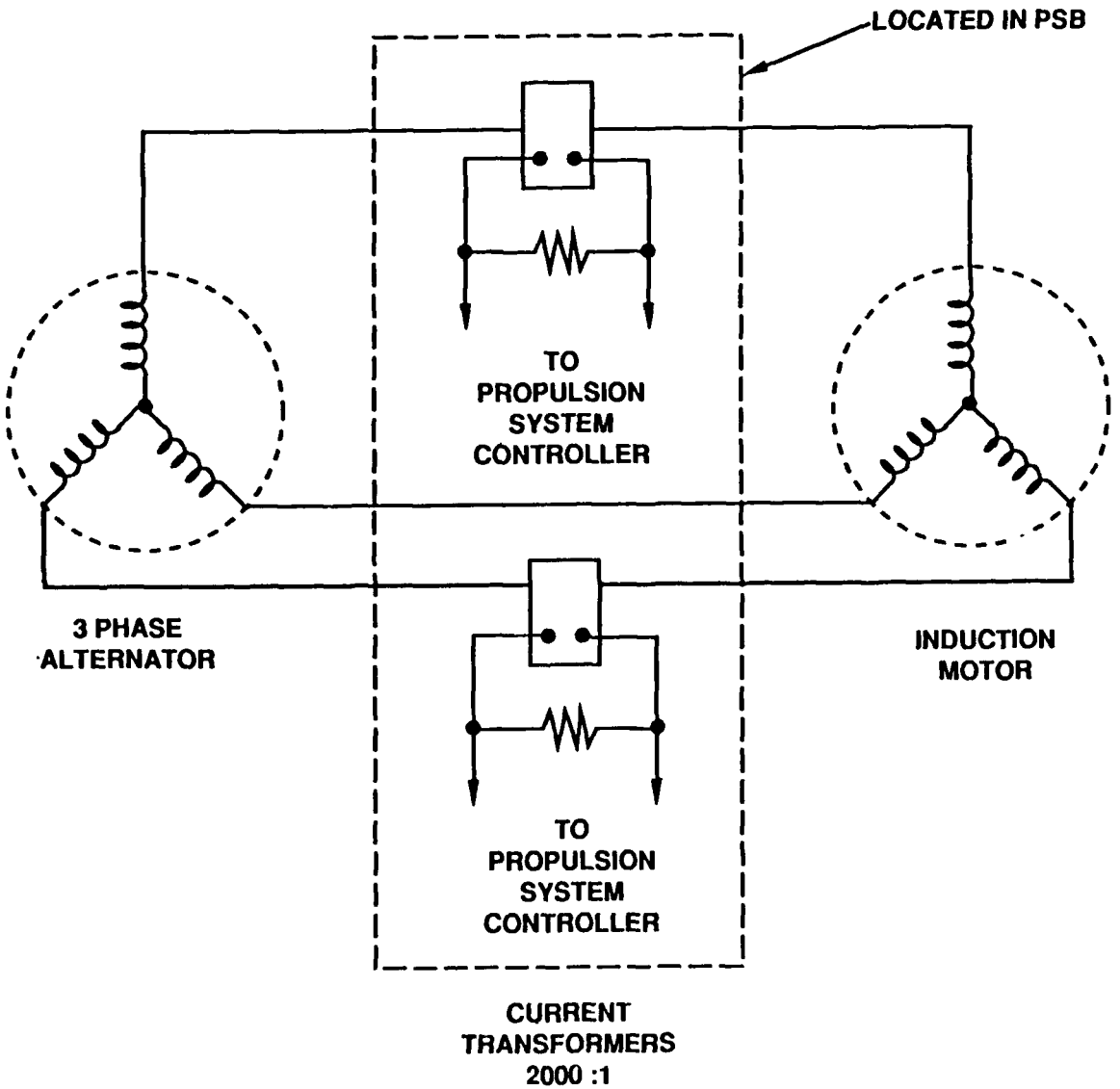

Figure 66. Power Sensing Box (PSB) - Current Sensing

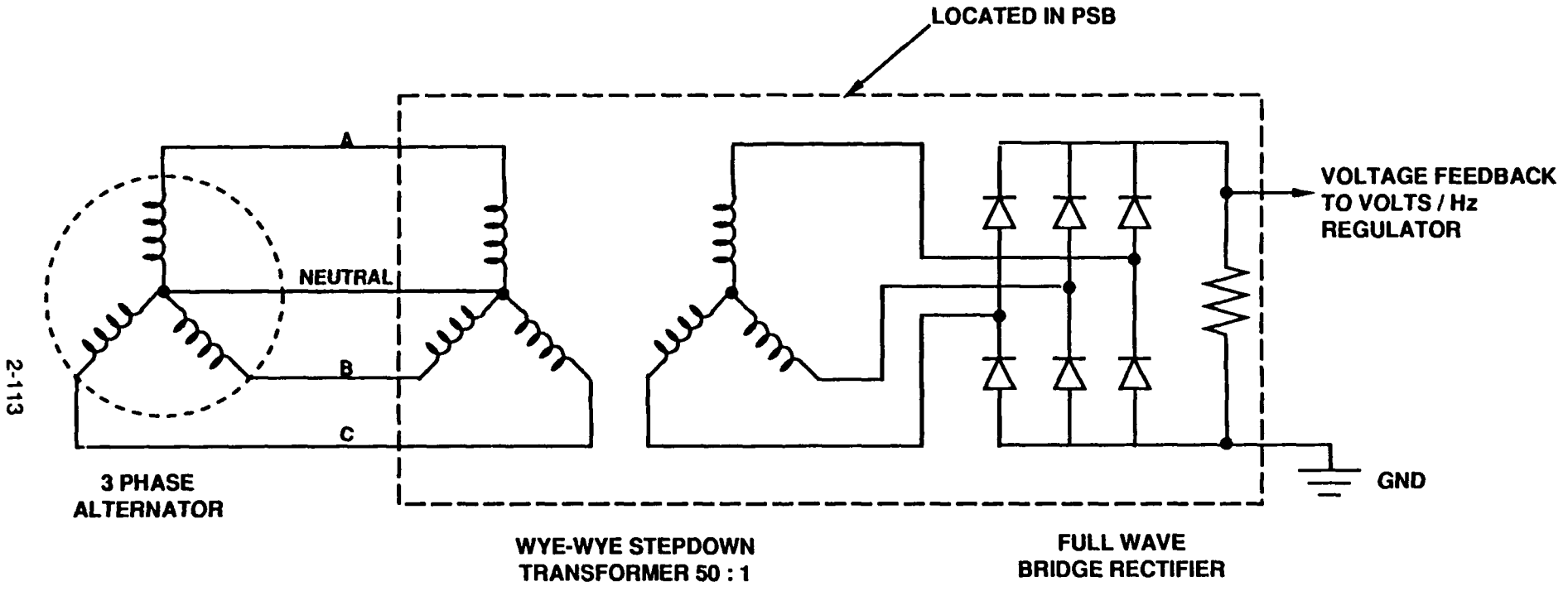

Figure 67. Power Sensing Box (PSB) - Voltage Feedback

2.5.13 PSC External Cable Interconnections

The external cables required for the propulsion system are shown in the cable interconnect diagram Figure 68. The diagram shows the interconnection of power, instrumentation, and vehicle interfaces.

The motor will be connected to the alternator using the 4/0 cable shown in Figure 52, two phases of which are routed through the current transformers located in the power sensing box. The instrumentation cable (W2) from the motor and the instrumentation cables (W5, W4) and the power sense cable (W3) from the alternator are connected to the PSC. Cable W1 connects the vehicle 28 VDC power to the PSC. The console in the vehicle is connected to the PSC via cable W6 and the keyboard and CRT with cable W7. For detailed PSC signal interface description see ICD, Drawing No. E77857.

The criteria for selection of connectors was based on the following specifications:

- Motor connectors and their cable mates must be immersible in sea water to a depth of 20 ft.
- Alternator, power sense box, and propulsion system controller connectors must be moisture resistant.

The motor connectors were selected from the Glenair Geo-Marine Series. These are of a hermetic design and are capable of greater than the design pressure. The other connectors in the system were selected from the military qualified D38999 series. These feature resilient seals between pins/sockets and insulators, which make them impervious to condensing moisture and sea water spray.

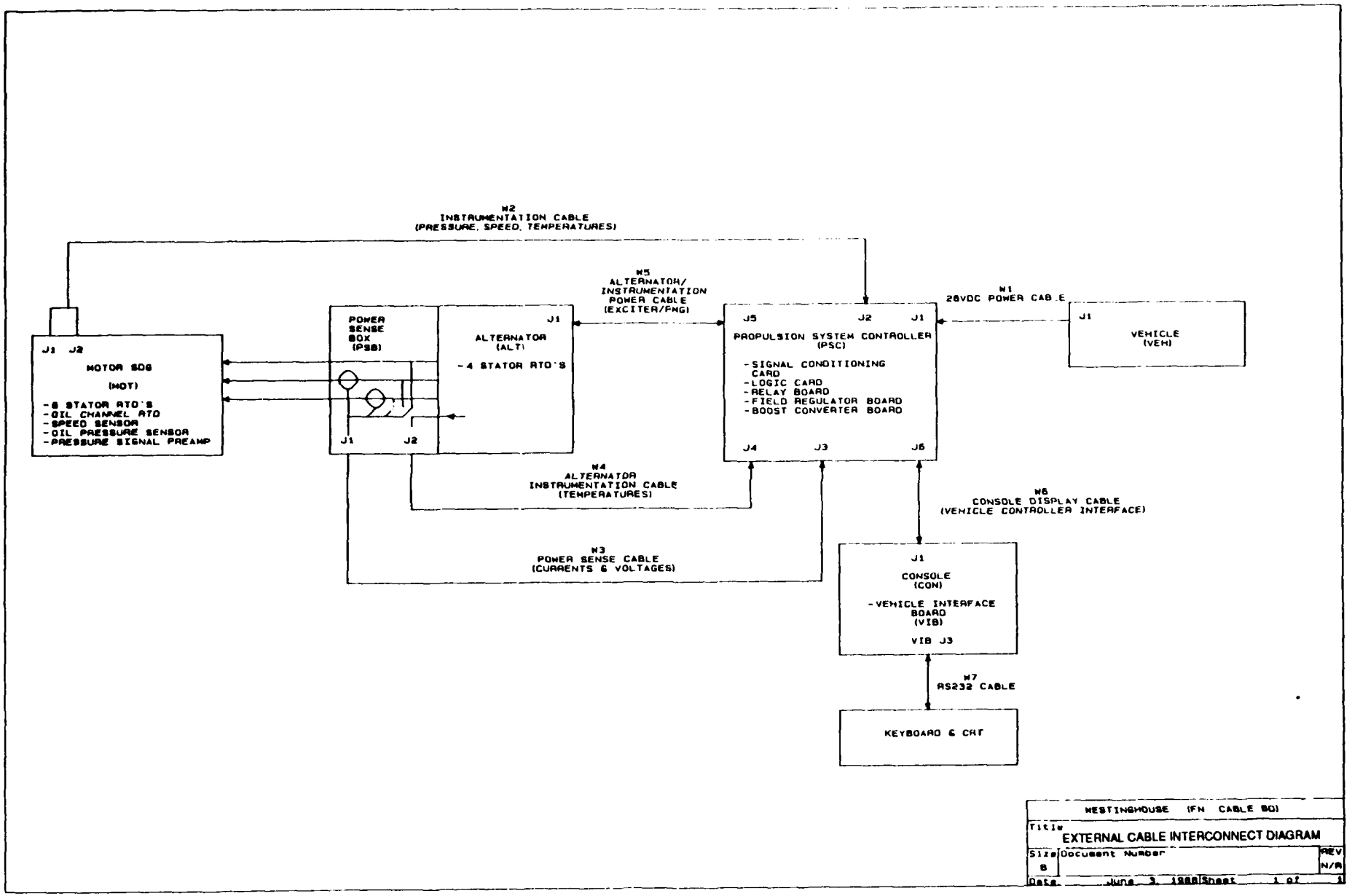

05/204/88/86

Figure 68. Cable Interconnect Diagram

2.6 System Performance Modeling

2.6.1 System Model

The system provides a speed at the load that is directly proportional to the speed of the prime mover for steady-state conditions. The speed of the load is always impelled toward a value that is directly proportional to the speed of the prime mover under dynamic conditions.

Figure 69 shows a general block diagram of the model of the system.

The model represents the characteristics of the actual system hardware with sufficient detail to provide simulation results that accurately predict the steady-state and dynamic behavior of the system.

Each portion or block of the model will be discussed separately in the following, starting from the prime mover and moving through the model to the load.

Prime Mover:

The prime mover is taken to be an ideal mechanical power source. In the model, the prime mover can deliver any needed amount of power at any speed and the speed is not affected by the mechanical load.

Permanent Magnet Generator:

The permanent magnet generator is, in effect, a tachometer that produces an output voltage that is directly proportional to the speed of the prime mover. The output voltage of the permanent magnet generator is the input to the dynamic control system. The terminal voltage of the main alternator is controlled to be directly proportional to the output voltage of the permanent magnet generator.

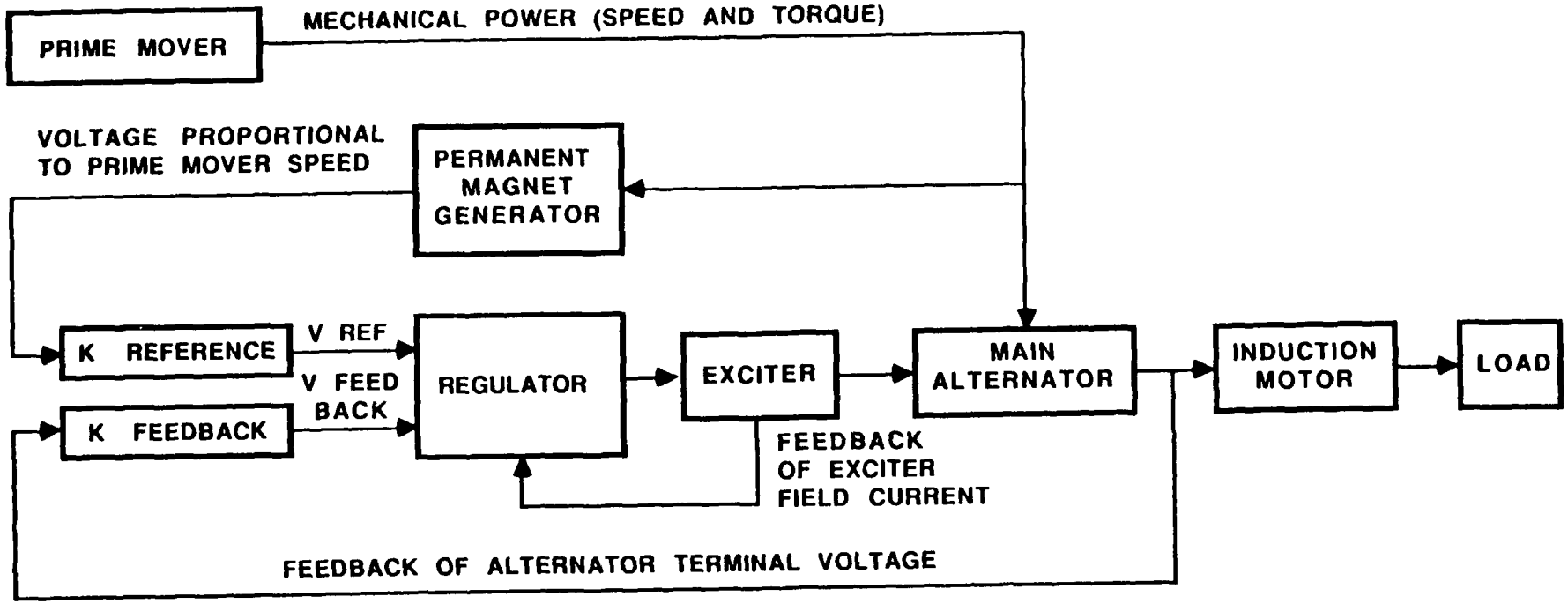

05/204/88/036-F

Figure 69. Block Diagram of System Model

Regulator:

Figure 70 shows a simplified block diagram of the regulator.

In the model, the reference voltage input to the regulator is calculated as a simple constant times the speed of the prime mover. The feedback of the alternator terminal voltage is also calculated by means of a simple constant that takes into account the three phase rectification and attenuation of the system hardware.

The model represents the proportional-integral feedback control method of the regulator, the pulse width modulation drive of the exciter field current, and the inner loop of feedback of the exciter field current that is used to limit the current to the 9 ampere thermal capability of the hardware.

A boost converter is used to obtain 150 volts DC from a 28 volt DC source. The 150 volts is needed to provide sufficient drive with the pulse width modulation to change the exciter field current fast enough to maintain stability during dynamic system variations due to changes of prime mover speed, changes of system load, or combinations of speed and load change.

Exciter:

Figure 71 shows a schematic representation of the exciter model.

The output of the regulator is represented in the model as a voltage input to the terminals of the exciter field winding. This voltage may be - DC bus voltage (-150 volts) or any value within the range of 0 to + DC bus voltage (0 volts to +150 volts). At each time step of the model execution, the differential equation of the exciter field circuit with this input voltage is solved by a fourth order Runge-Kutta numerical procedure to obtain a value for the exciter field current.

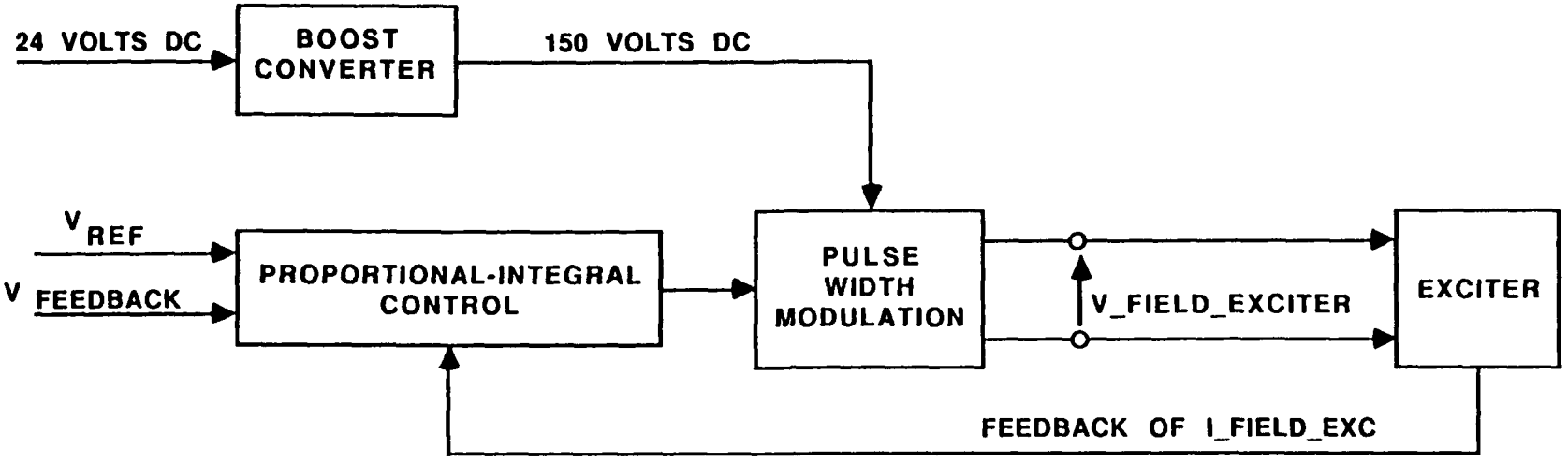

05/204/88/037-F

Figure 70. Regulator Mode!

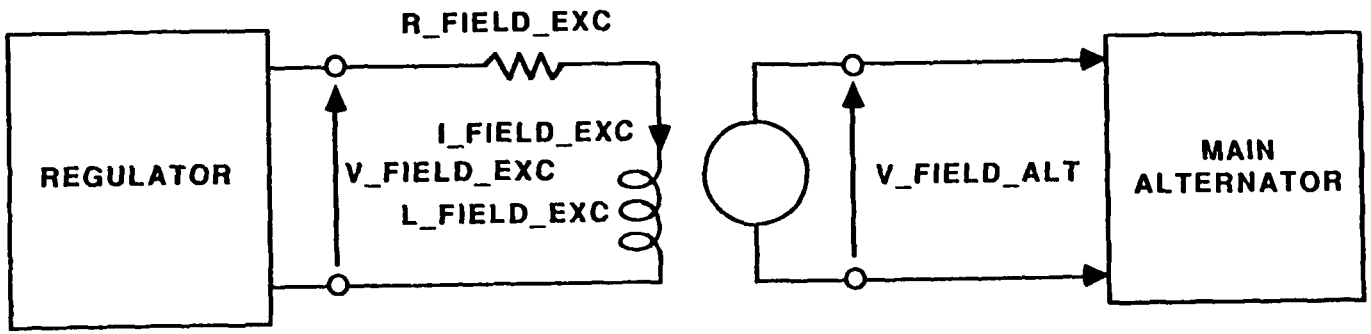

05/204/88/038-F

Figure 71. Exciter Model

The exciter field current is limited to a maximum positive value of 9 amperes. The input voltage to the exciter field is allowed to be equal to negative bus voltage to force the current toward zero, but the field current is not allowed to go negative.

The exciter field current is used as the input to a lookup table that is interpolated to obtain a value for the input voltage to the field of the main alternator. Since the exciter field current is allowed to have only positive values, the input voltage to the field of the main alternator can only have positive values. This simulates the operation of the rectifiers between the exciter output and the main alternator field winding of the actual hardware.

The lookup table has different sets of values for different system operating conditions. A different lookup table is used for each of three equivalent speeds of the prime mover and for the system cold or hot.

The lookup table values have been derived from the transfer curves shown in Figures 72 and 73. The curves show the steady-state relation between the current in the exciter field and the current in the main alternator field with magnetic saturation and machine temperatures taken into account. This information has been translated into curves of DC voltage input to the main alternator field winding versus exciter field current.

Main Alternator:

Figure 74 shows a schematic and block diagram representation of the model of the main alternator.

The calculation of the field current of the main alternator is done in the same way as the calculation of the exciter field current. At each time step of the model execution, the differential equation of the main alternator field circuit is solved by a fourth order Runge-Kutta numerical procedure. The input voltage in this equation is the output voltage of the exciter which is never negative; the main alternator field current can have only positive values and there is no upper limit imposed in the model.

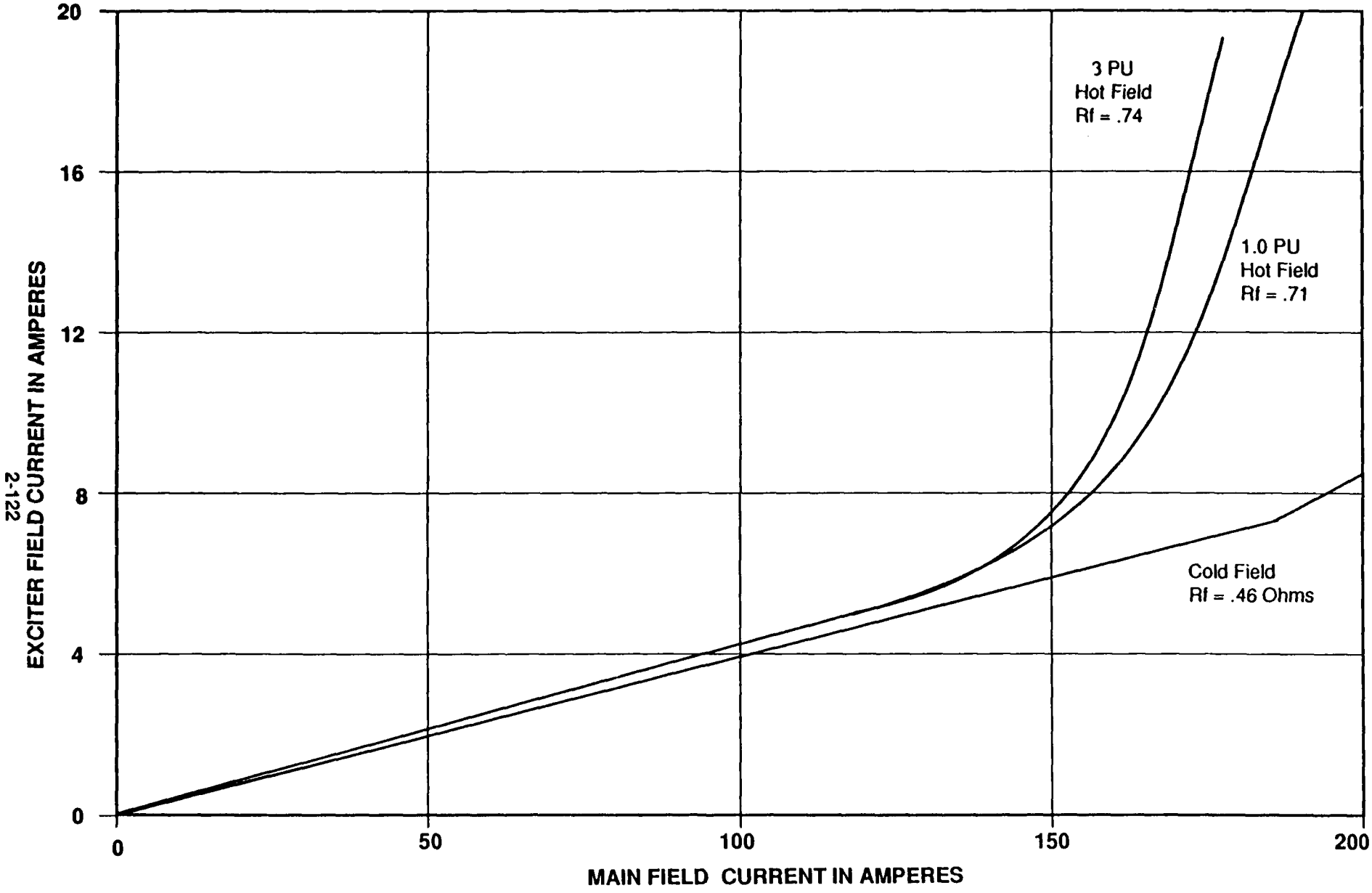

05/204/88/039-A

Figure 72. Exciter Field Current vs. Main Field Current (9000 RPM - Hiperco 50)

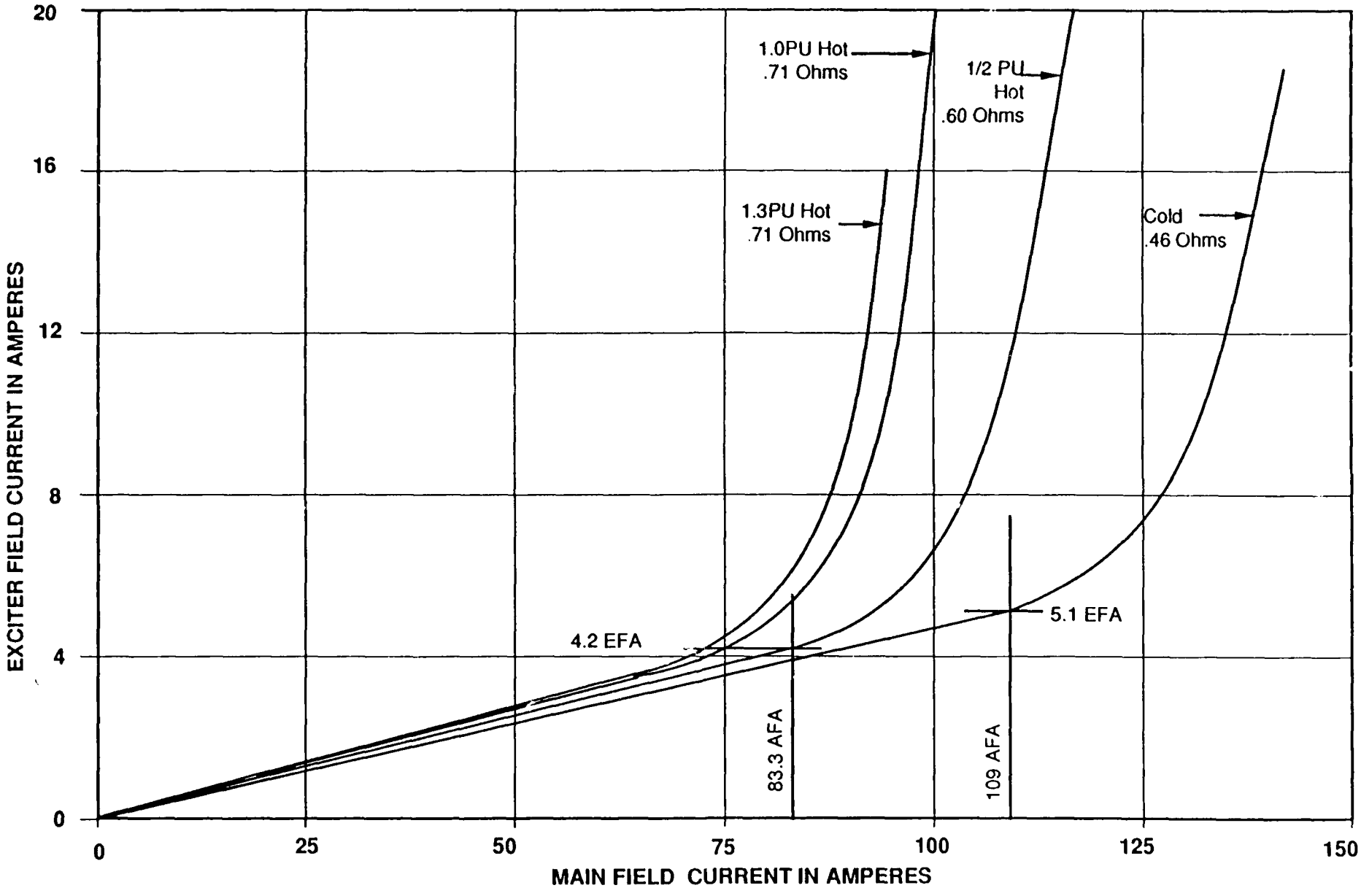

05/204/88/040-A

Figure 73. Exciter Field Current vs. Main Field Current (4306 RPM - Hiperco 50)

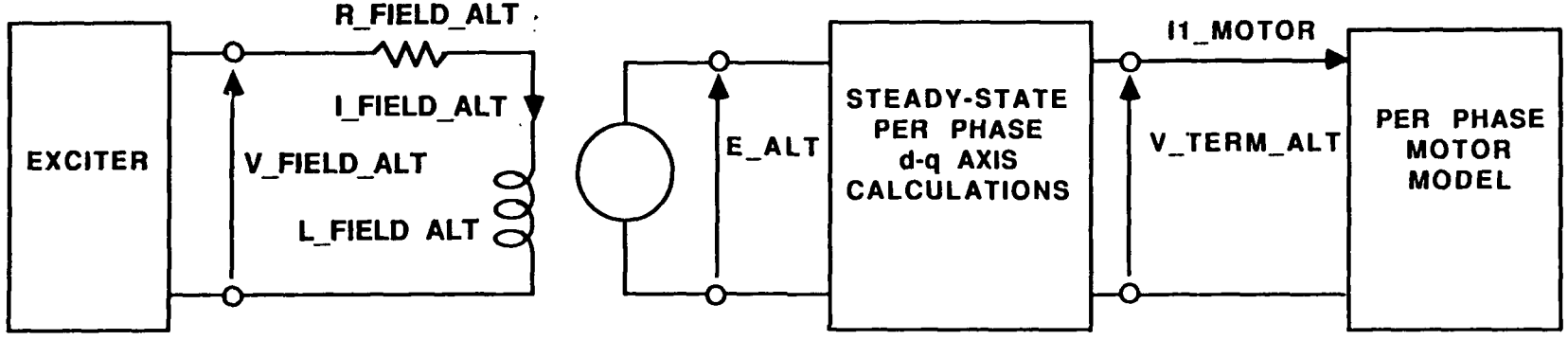

05/204/88/041-F

Figure 74. Main Alternator Model

An "effective" value of field current that is equal to the main alternator field current minus a demagnetizing component of the alternator load current is used as the input to a lookup table that is interpolated to obtain a value for the generated voltage within the main alternator. The lookup table values are multiplied by a constant factor and the prime mover speed to account for the variation of generated voltage with alternator speed. The values used in this lookup table have been derived from the curves shown in Figure 75. The curves show the steady-state relation between the current in the alternator field and the alternator terminal voltage for various load conditions with magnetic saturation and machine temperatures taken into account. This information has been translated into curves of generated voltage versus field current.

A steady-state d-q axis model is used in conjunction with the alternator load current (induction motor input current) to calculate the terminal voltage of the alternator. Figure 76 shows a curve that is used to account for saturation of the leakage inductance of the main alternator versus the load current. This curve is translated into a lookup table that is interpolated in the model. The d-q axis calculations also provide the value of the demagnetizing component of the load current that is subtracted from the field current to obtain the "effective" field current that is used with the lookup table.

Induction Motor:

Figure 77 shows the usual steady-state per phase equivalent circuit representation of the induction motor plus the resistance and inductance of the connecting cable from the main alternator to the induction motor.

The induction motor simulation calculations start from an initial value of motor speed which determines the slip at that moment in time. The voltages and currents in the equivalent circuit of the induction motor are calculated for the particular values of terminal voltage of the main alternator and the motor slip.

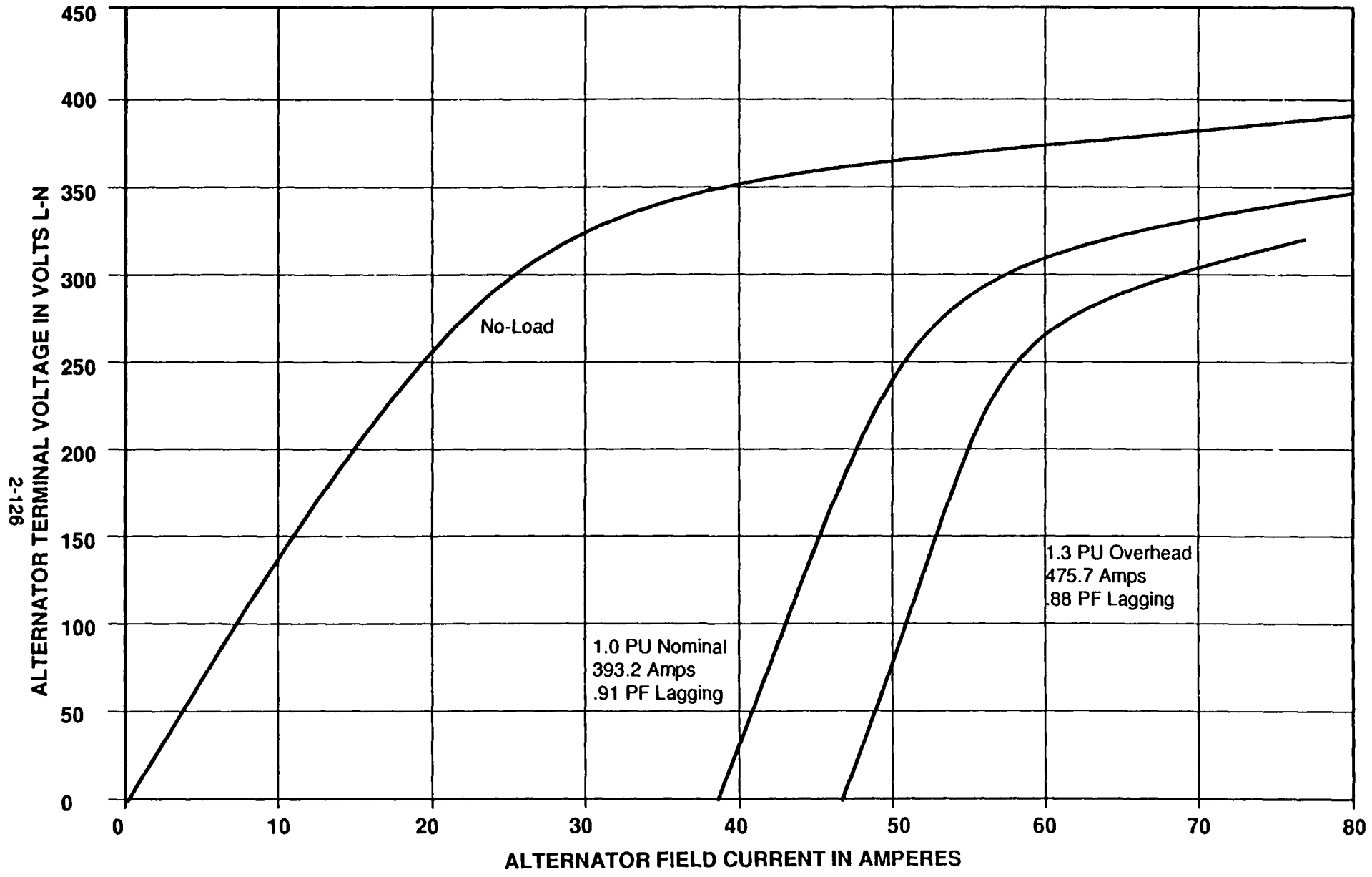

Figure 75. Load Saturation Curves for Main Alternator - - 9000 RPM

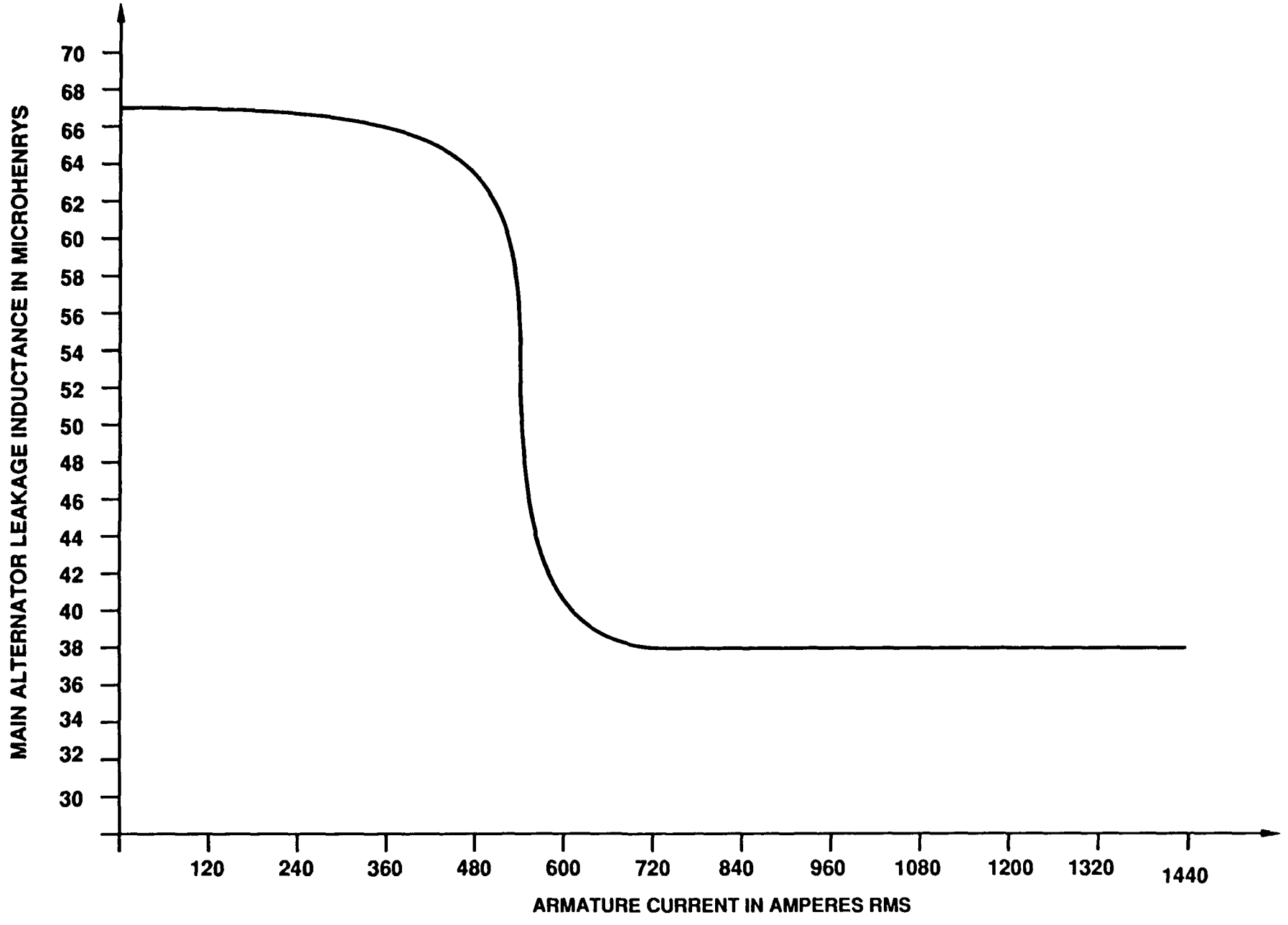

05/204/88/043-A

Figure 76. Main Alternator Leakage Inductance vs. Armature Current

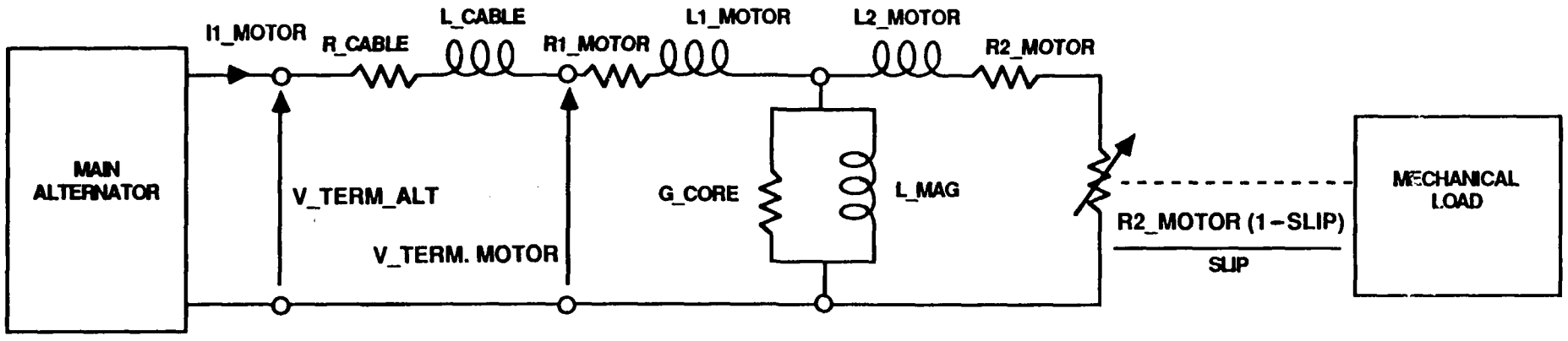

Figure 77. Induction Motor Model

05/204/88/044-F

Figure 78 shows the magnetic saturation of the magnetizing inductance of the motor versus the value of the volts per hertz at an operating point. Figures 79 and 80 show variation of R2_MOTOR and L2_MOTOR versus slip. These curves are used in the model as interpolated lookup tables.

The torque produced in the motor is calculated from the equivalent circuit and is used with the model of the load to calculate the speed of the motor.

Load:

The model of the load is represented by the block diagram of Figure 81 and the torque versus speed curve of Figure 82.

In the model, all load effects are referred to the motor side of the speed reduction gear and the combined equivalent friction and moment of inertia values of the motor, reduction gear, and load are treated as parts of the load. The torque versus speed curve of Figure 82 is represented in the model as torque equals a constant times speed squared. To account for the efficiency of the speed reduction gear, the constant has been chosen so that the nominal steady-state output power of the motor is 310.3 kilowatts (416 horsepower) at an equivalent alternator speed of 9000 rpm.

2.6.2 Results of Simulations Using Non-Linear System Model

2.6.2.1 Starting Simulation

Due to thermal limitations in the alternator, the starting line current must be limited to about 900A for three seconds maximum duration. Figure 83 shows a "cold" start at an ambient temperature of 10 degrees C with all nominal system parameters. The motor started in 2.2 seconds with a peak line current of about 1000A.

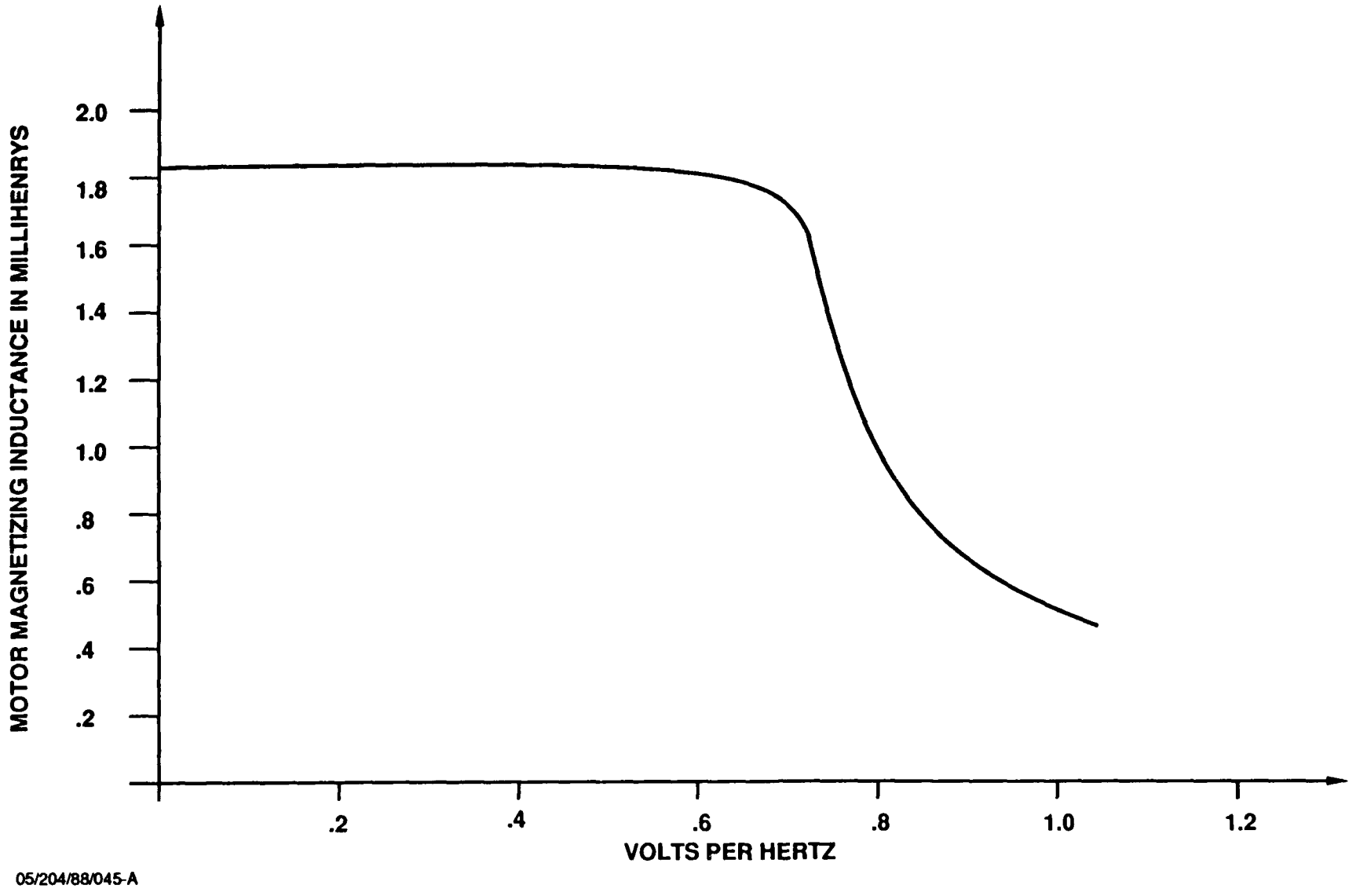

Figure 78. Motor Magnetizing Inductance vs. Volts Per Hertz

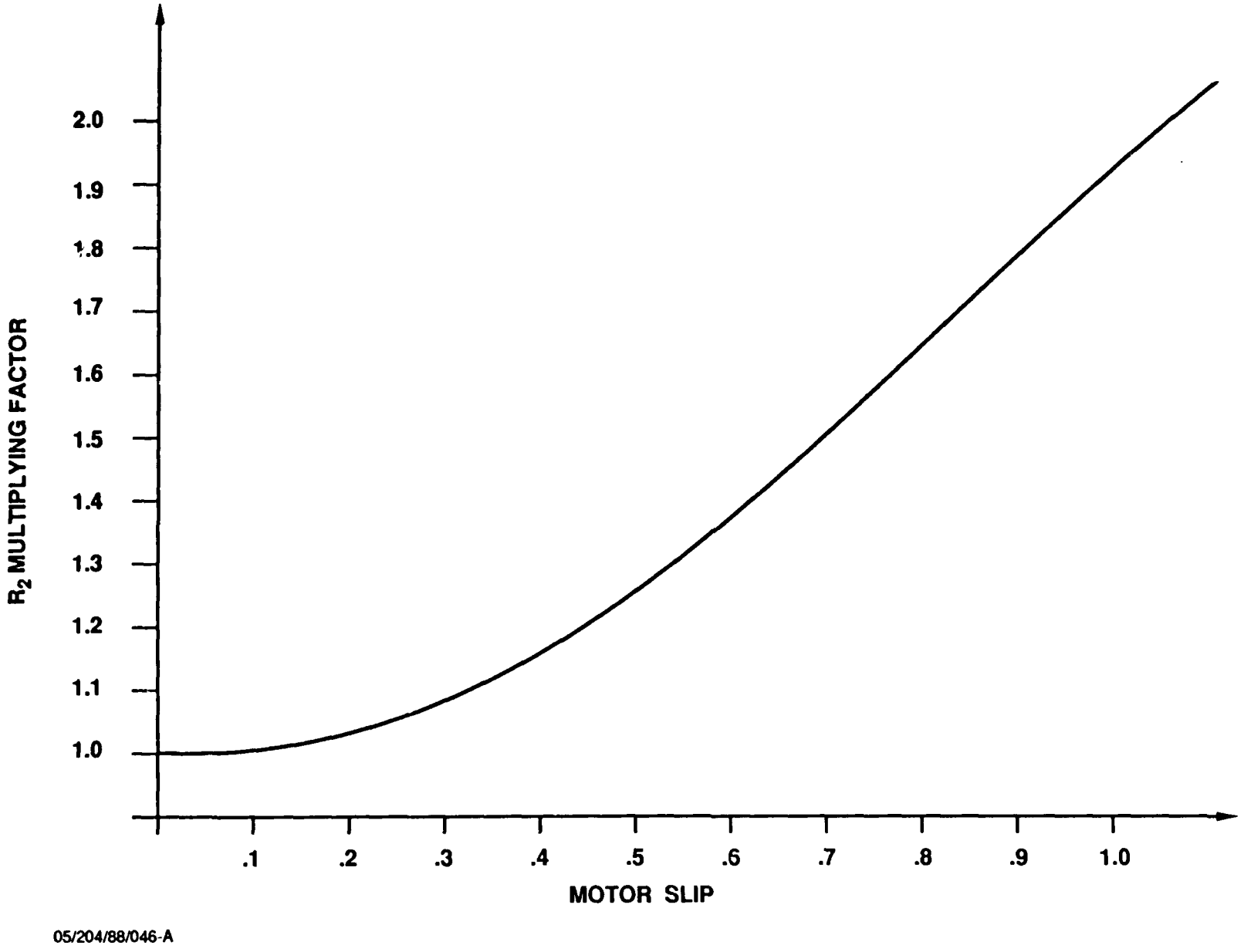

Figure 79. Motor Rotor Resistance Variation with Slip

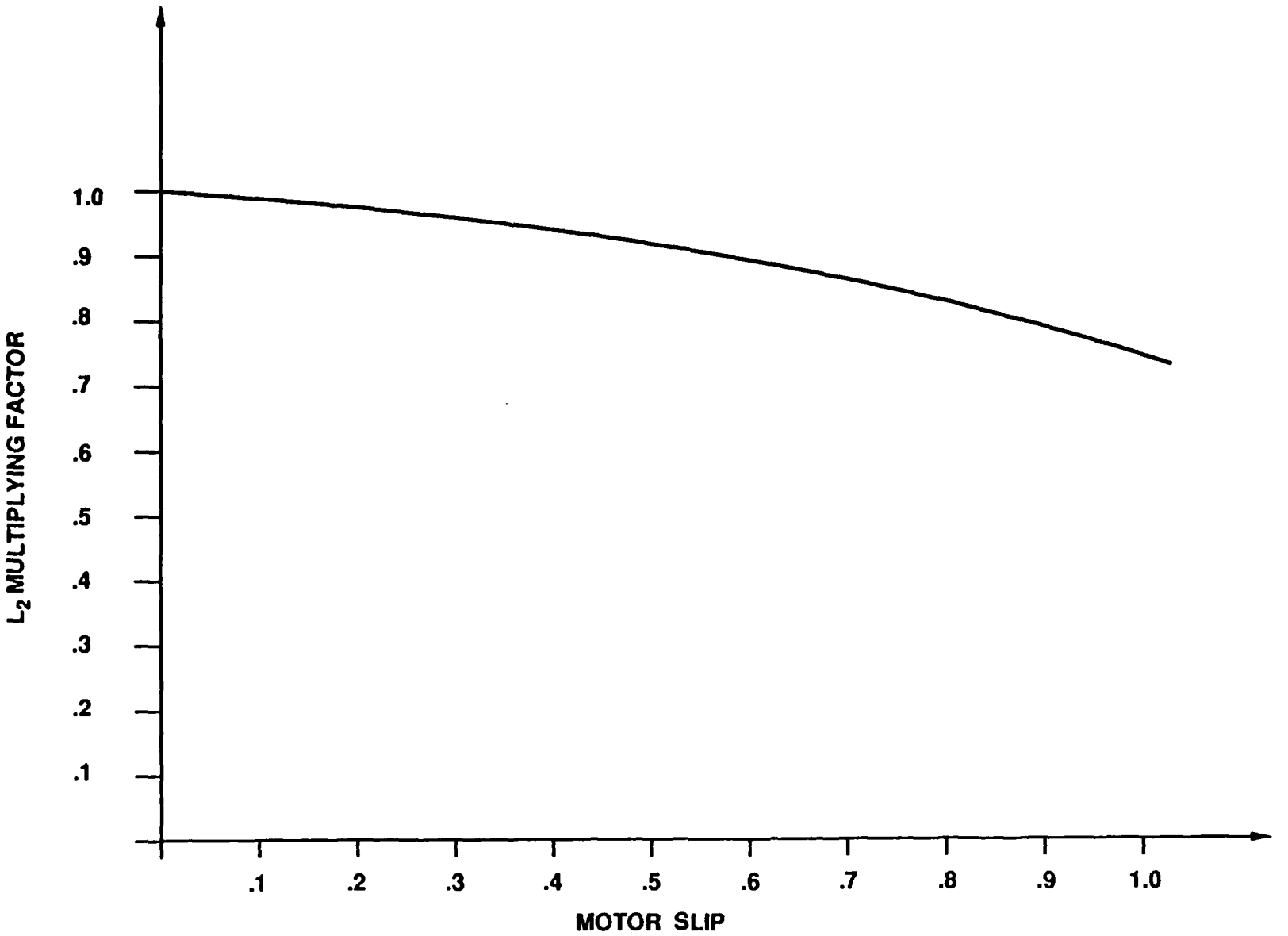

Figure 80. Motor Rotor Inductance Variation with Slip

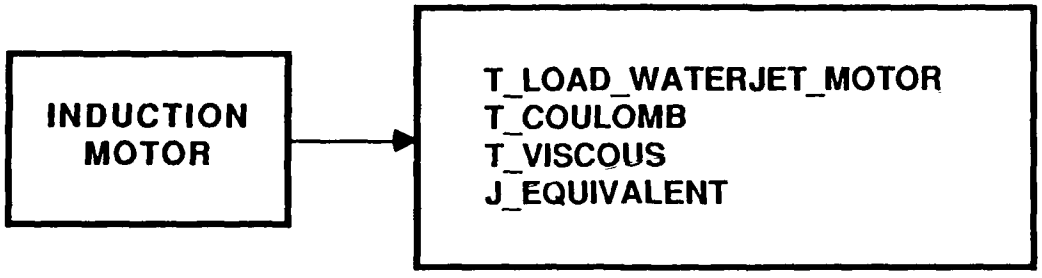

05/204/88/048-F

Figure 81. Load Model

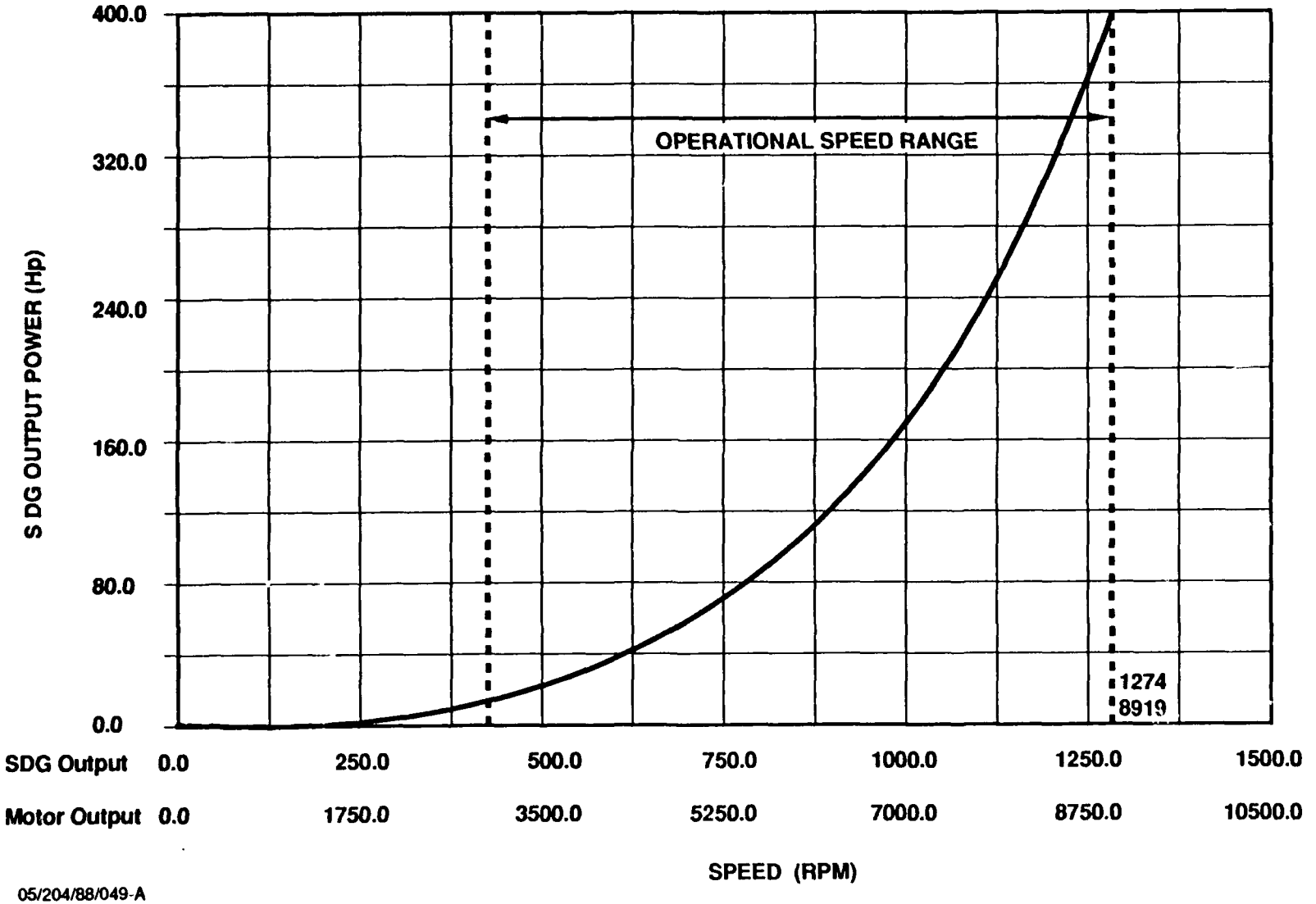

Figure 82. System Power Versus Speed